The interplay between Group A *Streptococcus* virulence factors and a functional antibody response

Jarrod Raymond Lovell

Supervisor: Dr. Reuben McGregor

Co-supervisors: Dr. Nikki Moreland and Dr. Jacelyn Loh

A thesis submitted in fulfilment of the requirements for the degree of Master of Biomedical Science, The University of Auckland, 2023. This thesis is for examination purposes only and is confidential to the examination process

Abstract

Background: Group A *Streptococcus* (GAS) is a serious human pathogen and effective vaccines are lacking. Two major vaccine targets are the M-protein and T-antigen, however there is a gap in understanding as to whether expression of either antigen impacts a protective immune response to the other during infection. This is of particular importance for M-proteins as members of this protein family are capable of interfering with antibody function. Accordingly, the aim of this project was to investigate how M-protein and T-antigen expression levels and functional capabilities influence opsonophagocytosis and killing of GAS in the presence of M-protein and T-antigen specific antisera.

Methods: The project first characterised the rabbit derived antisera using ELISAs to determine the titre of antibodies specific for the antigens of interest. The characterised rabbit sera was then utilised to optimise a flow cytometry protocol to measure M-protein and T-antigen expression on GAS strains that express M proteins with differing immune evasion properties (*emm*1 and *emm*6 strains). Opsonophagocytic killing assays that utilise human neutrophil-like cells (HL-60 cells) were used to investigate the killing capacity of the M- and T-specific antisera alone and in combination against the *emm1* and *emm6* strains.

Results: Serum characterisation established the specificity of the rabbit antisera against the GAS antigens and confirmed the ability for the M1 protein, but not the M6 protein, to non-specifically bind serum antibodies. The flow cytometry showed variation in the expression levels of M-protein and T-antigen on both *emm*1 and *emm*6 strains. The results of the opsonophagocytic killing assays with the rabbit antisera suggested that the level of M-protein expression, as well as the presence of an antibody binding motif within the M-protein, influenced T-antigen specific killing. In particular, a high level of M1 expression was associated with reduced killing by T1 antisera, and the M6/T6 strains were associated with negligible T-antigen expression and opsonophagocytic killing by T-antigen specific antisera.

Conclusion: There is marked differences in opsonophagocytic killing of GAS between strains with different M-protein and T-antigen profiles. This highlights the need for careful consideration of antigen expression and characterisation when selecting strains for vaccine development and assessment.

Acknowledgements

I would like to say a huge thank you to my supervisor Reuben for putting up with me daily, answering incessant questions and supporting me throughout the year. Your constant guidance and chats have been crucial to making this year what it was. To my co-supervisors Nikki and Jace another massive thank you for your support and guidance over the last year. I really appreciate all that you have done for me whether in the lab or out of it. You have both made the undertaking of this thesis an awesome experience and your support was appreciated.

A special thank you to Aimee for taking up an assistant co-supervisor role during my experiments, helping me with OPKAs and solving all the problems I managed to cause in the lab. Another special thank you must go to Ciara who helped proof-read my thesis and was a good friend throughout the year.

A special thank you and shout out to the rest of the Moreland Mob and co who made the year such an amazing experience – Lauren, Alana, Prachi, Francis, Nat, Risa and Tiger – thank you for the yarns, help and incessant question answering throughout the year. I had an amazing time in the lab thanks to all of you!

To Eilidh, Arlo, my Mum Maree, my family, and friends; a huge thank you for supporting me, feeding me, and dealing with me throughout this thesis. Also, shoutout to Luka, Mike and Shaun, my best friends purely because they asked. I love all of you immensely and thank you for everything.

Table of contents

List of Figures

List of Tables

Abbreviations

α	Anti- or Antisera (when talking about serum)
°C	Degrees Celsius
CO_2	Carbon dioxide
A	Active
ARF	Acute rheumatic fever
ARRIVE	Animal Research: Reporting of In Vivo Experiments
ATCC	American type culture collection
AUC	Area under the curve
BRC	Baby rabbit complement
CD46	Cluster of differentiation 46
CFU	Colony forming units
C4BP	C4 Binding Protein
DALYS	Disability-adjusted life years
DMF	N, N-dimethylformamide
Dr	Doctor
ELISA	Enzyme-linked immunosorbent assay
EDTA	Etheylenediaminetetraacetic acid
FACS	Fluorescent Activated Cell Sorting
FBS	Fetal Bovine Serum
FITC	Fluorescein isothiocyanate
GAS	Group A Streptococcus
GRB	Generic Rabbit Block

HCl	Hydrochloric acid
HBSS	Hank's balanced salt solution
HI	Heat inactivated
HRP	Horseradish peroxidase
HVR	Hypervariable region
IgA	Immunoglobulin A
IgG	Immunoglobulin G
KCl	Potassium chloride
KH_2PO_4	Potassium dihydrogen phosphate
MFI	Mean fluorescence intensity
mL	Millilitres
mM	Millimolar
mRNA	messenger Ribonucleic acid
NaCl	Sodium chloride
Na_2CO_3	Sodium carbonate
$NaHCO_3$	Sodium bicarbonate
Na_2HPO_4	Sodium hydrogen phosphate
nm	Nanometres
NSK	Non-specific killing
NZ	New Zealand
OD	Optical density
OPKA	Opsonophagocytic killing assay
OI	Opsonic index
OPS	Opsonisation buffer

PBS	Phosphate-buffered saline
PBS-T	Phosphate-buffered saline-Tween
RHD	Rheumatic heart disease
rpm	Revolutions per minute
S.D	Standard deviation
SEM	Standard error of the mean
THB	Todd-Hewitt broth
THY	Todd-Hewitt broth with yeast
TMB	3,3',5,5'-tetramethylbenzidine
TTC	2, 3, 5-tetraphenyltetrazolium chloride
µg	Microgram
µL	Microlitres
UK	United Kingdom

1 Introduction

1.1 Group A Streptococcus

Group A Streptococcus (GAS) or *Streptococcus pyogenes* are gram positive beta-haemolytic bacteria and obligate human pathogens (1). Colonisation occurs commonly on the skin and throat, with the potential to generate various disease phenotypes. These range from asymptomatic colonisation of the throat (carriage), common skin and throat infections, serious invasive infections, and post-infectious complications. To produce such a wide array of disease manifestations, GAS expresses a plethora of virulence factors at various times during infection (1, 2).

1.2 Transmission and disease burden

The ubiquitous and human-specific nature of GAS has enabled the bacterium to colonise, infect and generate disease in humans globally (1, 2). Although primarily impacting low-income countries, high-income countries also face significant burden, with specific communities disproportionately impacted by GAS disease (2, 3).

1.2.1 Colonisation and transmission

Asymptomatic colonisation acts as a reservoir of infection within the human population, with individuals often termed carriers of GAS. Environmental reservoirs have also been implicated in outbreaks within high-risk settings including hospitals, care homes and day-cares suggesting survival on dry surfaces, but less is known about the fomite transmission of GAS (4). Recently the capability for GAS to spread from asymptomatically colonised children into the air-borne environment was measured in the classroom setting. A spectrum of GAS carrier was observed from asymptomatic "heavy shedders" who shed for several weeks, to transiently colonised individuals within the same environment (5). This colonisation plays a role in propagating GAS infection and disease, but the extent and mechanisms involved are not completely understood (5). The newly developed human challenge model may offer insight into the mechanisms which limit GAS colonisation of the throat to

an asymptomatic state (6). This could benefit GAS study by delineating the host factors involved in various stages of GAS colonisation and disease, although currently limited to infections of the throat. Which in turn helps to understand the impact on GAS's global disease burden (5, 6).

1.2.2 Disease presentation and burden

Common disease presentations from GAS infections stem from skin and throat colonisation which can develop into pyoderma and pharyngitis respectively (1, 7). Globally GAS is responsible for ~100 million annual cases of pyoderma, whilst pharyngitis contributes ~600 million cases (5). Superficial infections by GAS strains possessing streptococcal pyrogenic exotoxins can cause scarlet fever, a highly communicable disease often impacting children that has seen a recent resurgence in case rates, particularly in high-income countries like the United Kingdom (UK) (5, 8, 9). Fortunately, many of these superficial infections and disease presentations are benign, often treated with penicillin which effectively clears GAS infections (10-12). However, superficial infections if untreated can develop into more severe invasive infections or trigger post-infectious complications associated with GAS infection. Invasive GAS infections were estimated to number 663,000 annual cases in 2005 and has been increasing in prevalence over time. A large proportion of these infections result in patient mortality, with mortality rates of approximately 8-23% associated with the first seven days of disease (2, 7, 13). Invasive disease rates in the UK notably are increasing alongside the increase in scarlet fever case rates, with household contacts of scarlet fever cases identified to be at a 20 times greater increased risk of an invasive infection (4). The global burden of disease can be linked to a combination of different host, environmental and virulence factors; one recent example is the increased burden of invasive disease in the UK being directly linked to a dominant M1 strain. This demonstrates the impact a particularly virulent strain has in driving an outbreak (7, 13-15).

Repeated superficial infections with GAS can also develop into post-infectious complications, often due to the development of auto-immune disease. These include acute rheumatic fever (ARF) and rheumatic heart disease (RHD), which is a progression from ARF as well as post-streptococcal glomerulonephritis. Acute rheumatic fever is a systemic auto-immune disease that primarily affects

children. It classically develops following repeated pharyngitis infections but has recently been discovered to also be triggered by skin infections (7, 16-20). ARF as an auto-immune disease causes the stimulation of cross-reactive antibodies and T-cells that target both GAS proteins and host tissue markers (16, 20). These dysregulated immune responses in ARF often target the heart, causing carditis, a severe symptom of ARF. If long-term damage to heart tissues develops the disease progression is classified as rheumatic heart disease (RHD) and if untreated leads to cardiac failure, strokes, and a high patient mortality rate (7, 16-20). A 2005 study estimated the burden of ARF to be roughly 471,000 cases annually with the majority of these in children 5-14, whilst RHD cases totalled 15.6-19.6 million current cases and a conjoined annual death toll of 350,000 people globally (2, 20). More recent estimates for RHD alone calculated 33 million cases that account for 275,000 deaths annually (20, 21). Accurate and timely diagnoses of ARF cases is critical due to the array of clinical symptoms and the consequences for misdiagnosis. If misdiagnosis occurs in healthy children, they are subjected to a rigorous course of unnecessary long-term antibiotic treatment. Whilst if an ARF diagnosis is missed and left untreated, the disease could progress causing heart tissue damage and the development of RHD. Therefore, to enable accurate diagnosis of a first ARF episode, the Jones criteria was developed and has been updated and amended over time (17, 20, 22). The criteria include ascertainment of evidence of a previous GAS infection, often investigating if patient sera displays antibody titres against GAS. In conjunction with a likely history of GAS infection a set of major and minor clinical presentations are outlined. Using these the patient must possess either two major or one major and two minor clinical presentations to qualify for a positive ARF diagnosis (17, 22). There have also been more recent efforts to discover biomarkers of ARF to make diagnosis both easier and more accurate (23-25).

Globally the extent of GAS' disease burden varies massively between countries as does the type of disease manifestation (2, 7). A range of factors contribute to this variation in GAS infections and disease phenotypes between different countries or different communities within a country (7, 13, 14). These include differences between hosts and environments or in the virulence of a regions circulating

strains, all of which can influence the burden of disease. Environmental examples include differences in climate such as winter or tropical conditions. But also include more host factors like poverty and overcrowding, which influence rates of infection. Unfortunately, these factors often directly impact lower-income countries or communities that have a higher proportion of socio-economic and environmental influences on disease (7, 13, 26). Epidemiological data provides direct evidence for the disproportionate impact of GAS on these low-income countries. Particularly with serious disease phenotypes including invasive disease, ARF, RHD and other GAS complications possessing high incidence and mortality rates in these settings (2, 19). Furthermore, circulating strains can vary geographically and temporally, which may further influence disease presentation depending on the virulence of each strain (13, 27). For example, the UK has a very high rate of scarlet fever, and a large proportion of strains circulating that express scarlet fever toxins, whilst in New Zealand (NZ) there are much lower rates of scarlet fever, but higher rates of other GAS disease (3, 5, 8).

1.2.3 New Zealand disease burden

New Zealand has a high burden of GAS disease, exemplified by the high skin infection rates which are double that of other high-income countries like Australia and the Unites States. Māori and Pacific communities are disproportionally impacted by this GAS disease burden (2, 19). Increased rates of skin infections alongside serious diseases such as ARF and RHD are greatly increased within these communities, particularly in children (3, 12, 28). The unacceptable disparity of New Zealand's GAS disease burden is evident when age-standardised mortality rates are compared. ARF and RHD mortality rates for Māori and non-Māori were 9.6 and 2.0 respectively, displaying nearly five times greater mortality in the Māori community, which urgently requires addressing (2). Furthermore, GAS disease causes an enormous economic and health burden in New Zealand, with an estimated annual cost of 29.2 million NZ dollars and 2205 disability adjusted life years (19). The lack of a vaccine is one reason for the higher burden compared to other bacteria like *Streptococcus pneumoniae* (19). Additionally, even though ARF and RHD are rare at the population level they disproportionally

contribute to the cost (36.9% of cost) and the health burden (21.4% of disability-adjusted life years, DALYS) as diseases that primarily impact 5–19-year-olds (19).

1.3 Virulence factors

GAS possesses an arsenal of virulence factors that contribute to its success as a human pathogen. Virulence factors enable colonisation of human tissues, escape from and impairment of the immune system and the ability to survive in and spread through various human tissues (7). A major GAS virulence factor is the M protein, a surface protein involved in adhesion and immune evasion (7). Another is the GAS pili which contributes to binding human tissue enabling colonisation. Each pili consists of adaptor proteins at the tip and base, with T-antigen's polymerising to form the body (Figure 1-1 B) (10, 29-31). Both these virulence factors are major cell surface proteins and provide functional benefits to combat GAS disease; providing a means to classify GAS strains, alongside being potential targets for vaccine development (7, 32-35). Both proteins are focusses for this project due to their key roles in infection, immune evasion, and vaccine development (7, 32-35).

GAS possess a vast array of other cell surface proteins that enable adhesion for tissue colonisation. The extensive arsenal of adhesins enables GAS to colonise and bind to various tissues throughout the human body (30). Tissue binding targets include fibrinogen, fibronectin, plasminogen, collagen, and laminin amongst others, highlighting the diverse opportunities for tissue colonisation (7, 30). These virulence factors involved in adhesion are likely why such variation in initial infection sites and disease presentations are seen globally, due to differences in circulating strains' tissue binding capabilities (7, 13, 34).

1.3.1 M protein

The M protein is a hypervariable surface protein expressed by all GAS which plays a key role in both infection and immune evasion (14, 36, 37). The binding capabilities of M proteins can vary between different GAS M protein strain types often due to structural differences between each protein (14, 32). Structural variation can include differences in the number of repeat regions, which in turn impact the

functional capabilities of the M protein through changes in their potential for protein-protein interactions (Figure 1-1,Figure 1-3) (13, 14, 32). The myriad of differences in M proteins between strains has led to the development of classification methods based on the M protein's sequence, structure, and functional capabilities. Furthermore, if the functional binding capabilities can be understood, insight into how the M protein influences the immune system and thus enables disease progression can be gathered (13-15, 38). This understanding would be crucial for vaccine development, both to identify antigens with potential to generate a protective response and into how strain-based variation in immune evasion capabilities could impact immune protection (Figure 1-4) (32, 39-41).

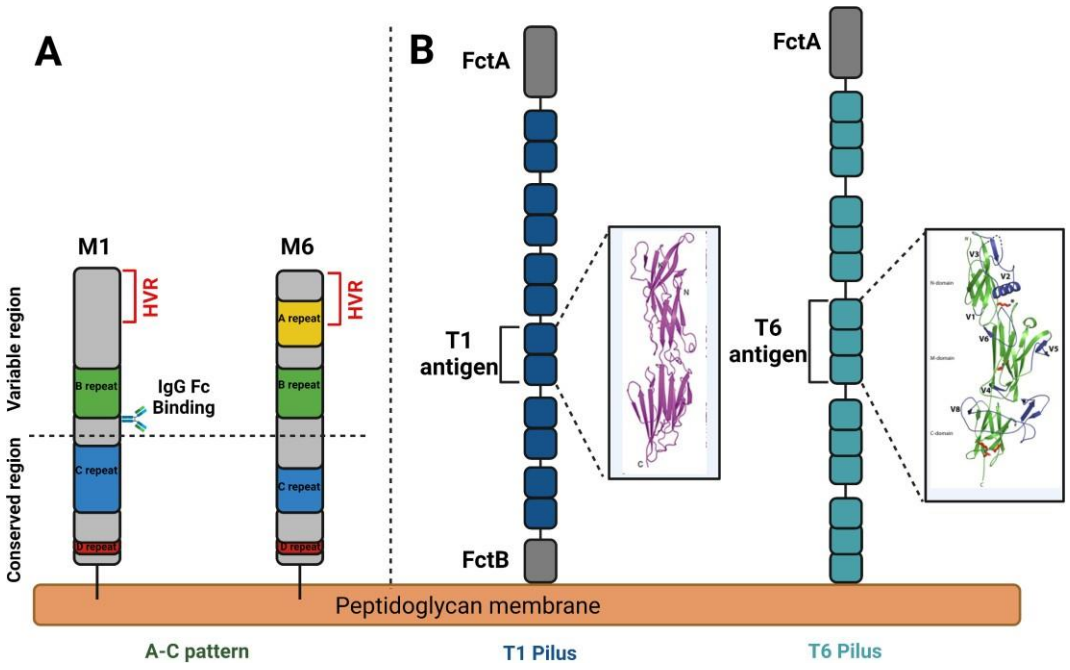

Figure 1-1: The protein structures of the M1, M6, T1 pilus and T6 pilus.

This image is adapted from Raynes *et al.*, 2018 (10). (**A**) The M1 and M6 proteins are displayed with their conserved regions being similar whilst they vary in the variable region with no A repeat region in M1 but present in M6. The Hyper-variable region (HVR) is displayed at the tip of both the M1 and M6 proteins and varies between each. The M1 proteins binding site for the IgG Fc region can also be seen in the variable region of the protein. (**B**) The T1 antigen is a dimer and forms the backbone of the *tee* 1 strains pili which possess an anchoring FctB region and an FctA adhesion region. While the T6 antigen is a trimer forming the backbone of the *tee* 6 strains pili and lacks an anchoring region to the peptidoglycan membrane but possesses an FctA adhesion region. Although both structures are accessible on the bacterial cell surface, the comparably greater size of the pili may makes the T-antigen potentially more antigenically available. This figure was made using BioRender.

1.3.1.1 M protein-based classification

The classification of GAS strains using the M protein has enabled advancement from the previously utilised Lancefield antigen testing, providing more informative classification methods that increased understanding about the impact of strain variation on infection, disease, and immune interaction (1, 2, 4). Importantly classifying the GAS strains based on a primary virulence factor enables a global picture of the strains causing infections and disease, both geographically and temporally including the context of their disease involvement (2, 4). Identifying the circulating strains based on geographical or temporal information can provide strains of interest for developing vaccines for specific regions of the world (5, 6). Whilst understanding strains implicated in specific disease manifestations like ARF and RHD could provide vaccine targets for decreasing the global burden of these specific diseases.

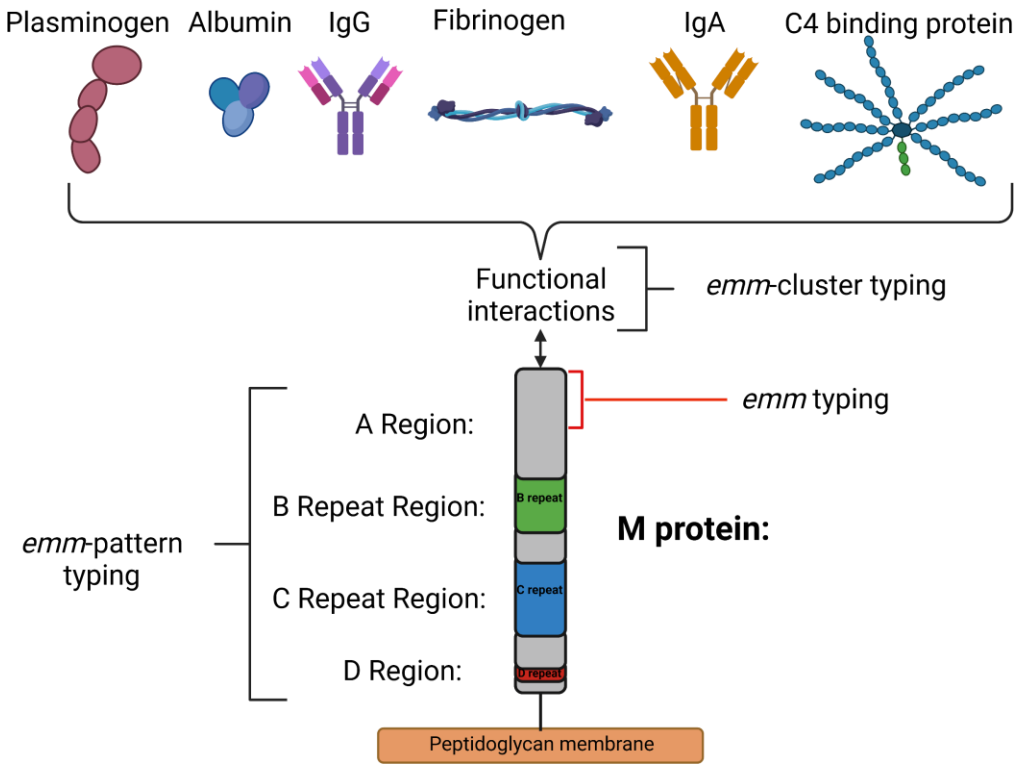

Figure 1-2 The methods of M protein classification.

The M protein is displayed alongside the three methods of GAS characterisation that utilise this protein. *Emm* typing is based on the sequencing of the 5' region of the *emm* gene, which often contributes to the hyper-variable region. Whilst the *emm*-cluster typing utilises the unique binding capabilities of each *emm* type against the proteins displayed to further characterise each strain. Finally,

the *emm* pattern typing uses the *emm* gene's chromosomal structure to characterise the whole protein, considering all four regions of A, B repeat, C repeat and D region. This figure was made using BioRender.

1.3.1.1.1 *Emm* typing:

The *emm* typing method of classifying GAS strains is based on the nucleotide sequencing of the *emm* gene's 5' regions, which is a common source of variation between strains due to it coding for the 'hypervariable region' (HVR) of the M protein (Figure 1-2) (41, 42). *Emm* typing has identified >220 unique *emm* types using the *emm* gene's 5 prime regions (13, 31, 42). This classification can be done on any GAS strain identified from patient swab isolates enabling epidemiological sampling of strain prevalence in different countries and diseases, such as comparing strains causing skin infections to those more likely to cause pharyngitis (12, 18, 43). Overall, *emm* typing has provided an accurate and reproducible means of classifying GAS strains, but it lacked information about the structural and functional character of each M protein (Figure 1-2) (42, 44). Therefore, further classification methods were developed that included the whole *emm* gene sequence alongside the functional characteristics (32, 44).

1.3.1.1.2 Emm-cluster system:

The *emm* typing methodology was used to develop a more informative classification system that accounts for the functional binding capabilities of each M protein, thus producing the *emm*-cluster system (Figure 1-2) (32, 44). This clustering system enabled the 220 *emm* types to be condensed into 48 phylogenetically arranged *emm*-clusters. The unique binding capabilities of each M protein was utilised to classify each *emm* type into functionally similar groups that shared binding properties. The host factors investigated for binding capability were all clinically relevant for M protein adhesion and immune evasion. These were immunoglobulin A and G (IgA and IgG), plasminogen, albumin, and C4 binding protein (C4BP) (Figure 1-2) (32). A direct advantage of *emm*-clustering is the potential to uncover groups of *emm*-clusters possessing similar immune evasion mechanisms and disease

phenotypes (13, 34). An example of this is the division of the X and Y clades within the *emm*-cluster system, which functionally discerns between two large groups of *emm* clusters (32). The X cluster is predominantly associated with the functional binding of immunoglobulins like IgG and IgA, alongside some C4BP binding dependent on the cluster type within the clade, whilst clade Y primarily possesses M proteins capable of binding fibrinogen and one specific cluster that can bind plasminogen (3, 7). Finally, by functionally grouping *emm* types the selection of clinically and geographically relevant strains for vaccine development will be further informed by their *emm*-clusters and potentially provide information about interactions that may influence immunity (32).

1.3.1.1.3 *Emm* pattern:

The investigation into the *emm* gene's chromosomal structure enabled the development of the emm pattern classification method. The M protein was classified using the arrangement of the *emm* and *emm*-like genes to provide an overall classification of the M protein's structure (Figure 1-3) (32, 44, 45). Therefore, each emm type can be classified into one of the five pattern types, A-E. Upon emm pattern typing strains it was identified that emm pattern types correlated with the GAS tissue tropism. Tissue tropisms for each strain patterns were identified with A-C preferentially infecting the throat, D had tropism to the skin and pattern E was identified to be a generalist with equal rates of throat and skin infections (7, 13, 38). This classification method although useful to correlate emm types with tissue tropism lacks information about the emm type's functional capabilities provided by the *emm*-clustering system (32).

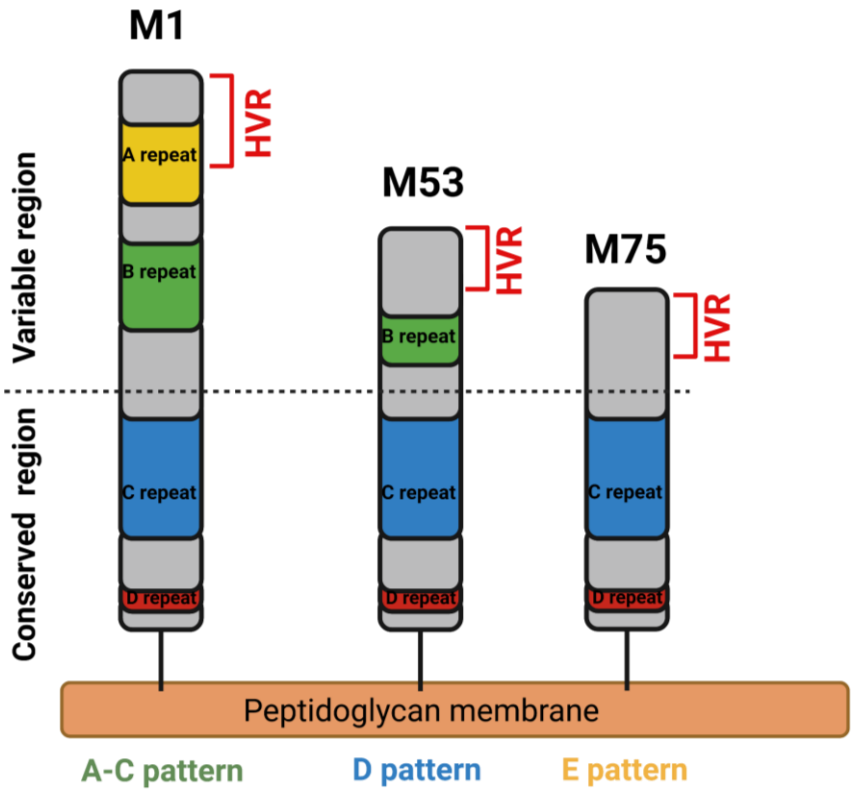

Figure 1-3: Emm pattern type structures

The structures of the three *emm* pattern types are displayed above using the M1, M53 and M75 proteins which are prototypical structures for these *emm* patterns. Most of the structural variation occurs in the variable region with differences in the A and B regions prevalent. The conserved regions particularly the C repeat region and D region are often similar between the *emm* pattern types. Importantly variation between proteins causes differences in length of the M proteins and in binding affinities during infection. This figure was made using BioRender.

1.3.1.2 M protein function

The M protein has an array of functional capabilities especially in relation to immune evasion, however, these can often vary between different strains and M protein types. The *emm*-cluster typing utilises the M protein's variable binding capabilities against host factors including IgG, IgA, C4BP, plasminogen, fibrinogen, and albumin (Figure 1-2) (32, 33). Importantly, each GAS strains' virulence is impacted by the M proteins binding properties, including avoiding opsonophagocytic killing, inhibiting complement cascade activation, or determining potential tissue tropism (7, 32, 46). Furthermore, some M proteins can bind host cell glycoproteins and extra-cellular matrix proteins including fibronectin, whilst others bind specific host cell ligands, including M6 binding CD46 and

M1 binding surface bound glycosaminoglycans (7, 13). Furthermore, the M protein and their respective *emm* pattern types has been determined to be partially responsible for the range of disease phenotypes generated by GAS. An example of this is ARF, which is postulated to be generated through a combination of genetic and phenotypic bacterial characteristics combined with the hosts immune response interaction (43). Another disease implicated is the development of post-streptococcal glomerulonephritis and the over-stimulation of host T-cell responses which varies between infections (7, 41, 46). Therefore, understanding of how host factor binding by the M protein influences the immune response is key. One pathway for understanding this is to investigate how differences in M protein expression and function influences immune evasion against M protein and T-antigen targeted immune responses.

1.3.2 T-antigen

The T-antigen is an important cell surface protein that forms the backbone of the GAS pili, which is essential for adherence and immune evasion during infection. By polymerising up to 100 T-antigen monomers together the backbone is formed, providing the bulk of the pilus structure (Figure 1-1) (10, 29, 31, 35). This expansion via T-antigen polymerisation enables the pili to extend away from the cell wall and increases the potential for binding to host cells during infection (Figure 1-1). However, although this extension increases virulence by extending out past the hyaluronic capsule the immune system has an increased chance of recognising and binding the antigens (10, 29, 35). Structurally, the T-antigen is formed from multiple domains ranging from two to four depending on the strain. The majority are two domains including the T1 antigen on the M1 strains, whereas the T6 antigen possesses three domains (Figure 1-1) (29, 35).

The T-antigen is encoded in the *FCT* region named for its ability to also encode the Fibronectin binding and collagen binding cell surface proteins. This region also contains the coding material for the whole pilus including the assembly sortases required for pilus construction (13, 34). Amongst all GAS strains

there are nine distinct FCT types and within these families of FCT types, further variation is seen between pili, occurring primarily by the encoding of different T-antigen backbones (*tee* types) (34, 47). However, different *emm* types within the same FCT type also display major differences in the sequences of their backbone, base, and tip proteins (48). The T1 and T6 strains utilised in this project belong to the FCT-2 and FCT-6 classes respectively, with differences in their T-antigen structure, sequence and pilus anchoring base proteins (Figure 1-1) (48).

The transcriptional regulation of pili during infection is incompletely understood. The three key transcriptional regulators Nra, RofA and MsmR, vary between strains and may influence expression in via different mechanisms (9, 10). Environmental factors are also thought to modulate expression (9, 11). Temperature based variation in pilus expression has been characterised with lower temperatures. The controlling mechanism was identified as the level of translation able to occur for the *nra* mRNA, which saw increases in translation rates at lower temperatures (11). In contrast to this, upon induction of invasive disease in strains possessing this control mechanism, the increased temperature of human tissue triggered the halting of pilus expression. Unfortunately, the control mechanism appeared restricted to the FCT-3 strains possessing the *nra* gene (9, 11). Other factors influencing expression include pH and it has shown that acidic environments increase pilus expression. Overall, the regulation of pilus expression is extremely multi-faceted varying between extracellular environmental factors and the cells intracellular metabolic activity and genetic regulation (9, 49). Increasing the understanding of how expression is regulated in turn will benefit understanding the impact of expression on the strains virulence and capability for these antigens to be targeted by the immune system.

Originally the typing of T-antigens utilised hyperimmune rabbit serum and investigated the agglutination levels of GAS cells treated with trypsin (13, 50). This developed into typing by sequencing the *tee* gene, which codes for the T-antigen, and this methodology was called *tee* typing (like *emm* typing for M proteins) (13). Upon sequencing and analysing a range of *emm* types for their *tee* types 18 clades and six sub-clades of *tee* types were identified, many being globally and temporally conserved (34). This increased conservation was particularly evident when compared to the *emm*

gene as the *tee* gene was much less variable, likely contributing to why different *emm* types often share *tee* types. This conserved nature provides an opportunity for a vaccine with increased coverage compared to targeting the M protein. However, how the M protein influences a T-antigen targeted immune response is not completely understood and by investigating this interaction we aim to increase understanding of the T-antigen based vaccines potential success (13, 35, 51).

1.4 Vaccine development

Although GAS infections are currently treatable with antibiotics, primarily using penicillin, there is no other preventative measure to combat the large disease burden caused by GAS globally. The development of a clinically approved GAS vaccine is one such route, with research currently ongoing on a range of different vaccines (5, 6). The success of the *Streptococcus pneumoniae* vaccine is an example of the potential for vaccines to decrease the disease and economic burden of infection, suggesting that an effective GAS vaccine is a viable option (19). However, the variation in virulence factors amongst GAS circulating strains means vaccines are required to generate a broader immune response for protection (13). Other challenges facing a GAS vaccine have limited development including the risks of autoimmunity, the incomplete understanding of epidemiologically important strains in different areas worldwide and a lack of understanding about the natural interactions between GAS and the human immune response (40). In response to these challenges multiple pathways for vaccine development are being explored, including the targeting of the two significant type-specific virulence factors, the M protein and T-antigen (Figure 1-4) (29, 39, 52). These routes often try to mimic the natural immune response developed against GAS over time, which has been theorised after studies of adult intravenous immunoglobulin (IVIG) displaying GAS specific antibodies (53, 54). Further targets include conserved GAS surface antigens which are found on all strains of GAS bacteria, which aims to generate a broad protective immune response against all strains (11, 40). These virulence factors include the fibronectin binding protein, group A carbohydrate and serum opacity factor, which

have all been tested for protection in different combinations alongside as single antigen vaccines. However, there has been a lack of clinical trials utilising these vaccine approaches to demonstrate protection in humans (40).

1.4.1 M protein vaccines

As a primary cell surface virulence factor for GAS the M protein has become a significant target for vaccine development. Originally M protein-based vaccines used whole M proteins which showed some evidence of cross-reactive antibodies towards brain and heart tissues, like those targeted in ARF (55, 56). Due to these adverse reactions, vaccine development against GAS using the M protein was halted until the cause for these reactions was identified. The cause was determined to be due to cross-reactivity between specific M protein epitopes and human tissue epitopes triggering auto-immune reactions (11, 55). For GAS vaccine development to continue the M protein epitopes used were carefully selected to avoid adverse reactions, thus creating a new avenue for developing M protein-based vaccines (11, 57, 58). To combat the global disease burden vaccine developers have aimed to provide coverage against as many strains as possible. Hence the improved classification of strain variation with *emm* typing identifying >220 *emm*-type strains and *emm*-clustering producing 48 clusters has provided context for what a successful vaccine will protect against (32). Therefore, M protein-based vaccines have aimed to utilise safe M protein epitopes to avoid cross-reactivity implicated in ARF whilst ensuring maximum strain coverage (10, 11). One approach uses the hyper-variable N terminus from chosen *emm* types and combines carefully selected strains to maximise coverage (Figure 1-4) (52, 57, 58). Utilising this multivalent approach vaccine trials have demonstrated efficacy in both animal models and safety in stage I clinical trials (57, 58). The leading multivalent vaccine candidate is the 30 valent vaccine which targets 30 unique *emm* type hypervariable regions (Figure 1-4) (11, 32, 58). However, this approach remains limited globally due to the diversity of GAS strains with over 220 *emm* types identified worldwide, but it is an approach that has provided opportunities for progress (27, 58). Another approach is the targeting of the conserved region of the M

protein, the C-repeat region, which is shared between *emm* types and is conserved between strains (Figure 1-4). Theoretically, targeting the conserved region of the M protein will generate cross-strain protection (11). The J-8 vaccine uses this mechanism and within early trials has demonstrated safety in humans (Figure 1-4). Animal models have displayed protection against pyoderma and bacteraemia (39, 59, 60). Targeting of epitopes within the C-repeat region is a concern as the accessibility of this region to the immune system is limited, which could impact the potential immunogenicity of the vaccine (39).

1.4.2 T-antigen vaccines

The T-antigen forms the backbone of the GAS pili and previous investigations into GAS infections in humans have indicated the immune response generates T-antigen specific antibodies. This provided evidence for the immunogenicity of the T-antigen and with the advantage of its more conserved nature, when compared to the M protein, made it a prime target for future GAS vaccine research (29, 35). The T-antigen locus possesses 18 *tee*-type genes, which is much fewer when compared to the >220 *emm* types. As a result, the possibility of generating broad-spectrum immune protection is thought to be more feasible when targeting the T-antigen as opposed to the M protein. Therefore, it has been hypothesised that a vaccine developed with epitopes from representatives of all 18 *tee* types could generate global coverage against the majority of GAS strains. Additionally, T-antigens show increased accessibility to the immune system on the bacterial cell surface, due to the large size upon polymerisation (Figure 1-1) (10, 35). One approach to producing a T-antigen targeted vaccine is the multivalent vaccine design which enables the targeting of a range of different strains. One vaccine using this approach is the TeeVax vaccine which consists of proteins generated by fusing immunogenic regions of selected T-antigens into a TeeVax protein (Figure 1-4) (29). The vaccine combined three of these TeeVax proteins and was able to generate antibodies against all 18 *tee* types upon vaccinating rabbits. Furthermore, the TeeVax vaccine demonstrated broad-spectrum protection in mouse models

(29). Importantly, in an invasive GAS mouse model the antibodies generated against the T-antigen displayed immune protection, decreased adhesion, and induced bacterial killing (10, 29, 35).

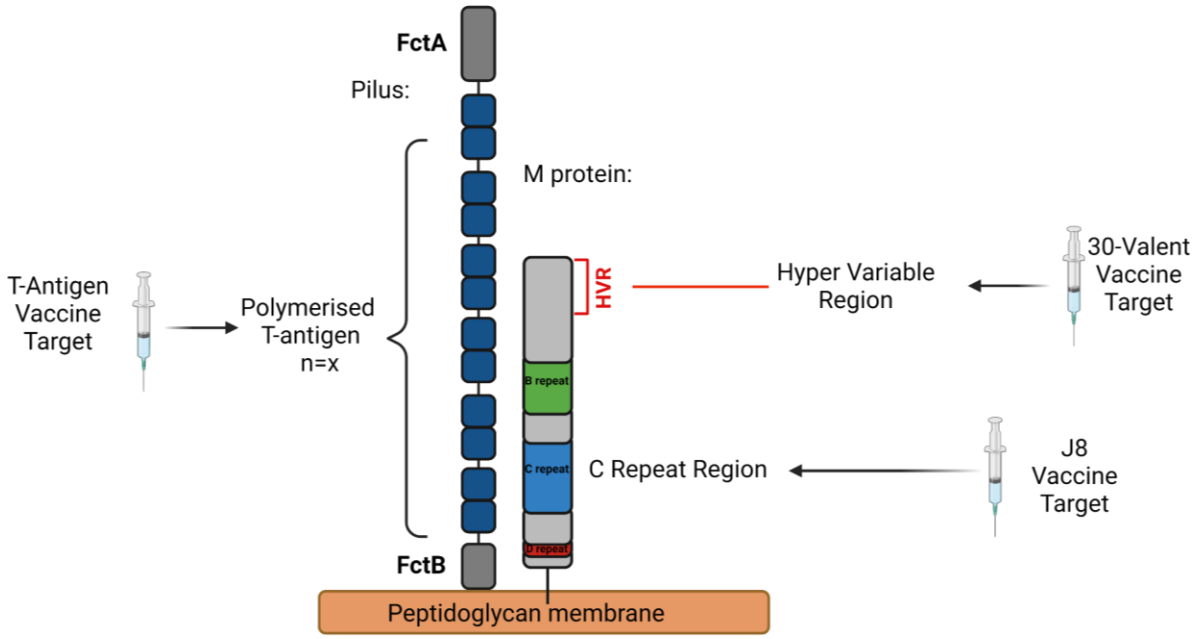

Figure 1-4: Overview of current M protein and T-antigen targeted vaccines in development:

The T-antigen vaccine can be seen targeting the backbone of the pili by generating immune responses to the T-antigens, which is undertaken by creating fusion proteins from a range of *tee* types. Whilst the two M protein targeted vaccines target the hyper variable region (HVR) like the 30-valent vaccine does, by combining 30 unique *emm* type HVR epitopes. Or they target the conserved C repeat region with carefully selected epitopes such as the J8 vaccine, which is a shared epitope between *emm* types that avoids causing any auto-immune cross-reactivity. This figure was made using BioRender.

1.5 Project design

1.5.1 Project rationale

Currently GAS vaccine development is targeted towards virulence factors and cell surface proteins including the M protein and T-antigen. The increased knowledge of the virulence properties, classification and immunogenicity of these proteins has been beneficial to vaccine development as mentioned in section 1.4. Although individually more is known about these proteins, there are

knowledge gaps including their interaction with an immune response, particularly one targeted against the T-antigen. Furthermore, the M proteins can vary both in function and expression, but questions remain with respect to the impact of this biological variation on a vaccine-derived immune response. Therefore, this project was designed to utilise assays that act as correlates for immunity to investigate how the M protein and T-antigen are involved in a targeted immune response.

1.5.2 *Emm* type strain selection

The investigation into the M proteins impact on an immune response including both M protein and T-antigen targeted killing requires the selection of clinically relevant strains that have antisera available that specifically target these antigens (32, 44). Five clinically relevant *emm* types had previously been optimised in established assays and had antisera available for use in the laboratory. Therefore, by comparing their functional characteristics, *emm*-types with variation in their host binding capabilities could be selected (Table 1) (32). This resulted in the selection of *emm* 1 and *emm* 6 as the two *emm* types used for use in this project, with two strains from each *emm* type investigated. The M1 protein (from *emm* 1 strains) displays binding capability to IgG, fibrinogen, and albumin, whilst the M6 protein (from *emm* 6 strains) had no recorded binding capabilities (Table 1) (32, 44). Therefore, by comparing the level of M protein and T-antigen targeted killing between *emm* types the impact of the M proteins host binding capabilities on GAS's immune evasion can be investigated.

Table 1: The typing and binding capabilities of potential Emm type candidates:

Relevant M Proteins:					**Binding Capability to Host Factors:**					
Clade	*Emm* Type	*Tee* Type	Pattern	Cluster	IgG	IgA	Plasminogen	Fibrinogen	Albumin	C4BP
Y	1*	1	A-C	A-C 3						
Y	6*	6	A-C	Single						
Y	12	12	A-C	A-C 4						
Y	53	13	D	D 4						
X	75	25	E	E 6						

The five GAS *Emm* types with established assays are displayed with their classification information and host factor binding capabilities (32). From this information a choice can be made on which *Emm* types to use in the project which are seen with a * in the table (*emm* 1 and 6).

1.5.3 Enzyme-linked immunosorbent assays

Enzyme-linked immunosorbent assays (ELISAs) are a commonly used immunoassay and enable the identification of antibody binding alongside providing a method for quantifying antibody binding titres. The ELISA method utilised in this project is the indirect ELISA which entails coating the antigen of interest directly to the plate. Following this a serum (containing primary antibodies) is screened which, if bound, are detected using a secondary antibody conjugated to an enzyme that will trigger a colour change upon addition of a substrate (61). The indirect ELISA is an accurate measure of antibody binding and provides the ability to measure similar serum types with the same secondary (61). Rabbit antiserum and human antiserum have been used in ELISAs against the M protein since 1976 when an experiment displayed anti-M12 antibodies in both serum types (62).

1.5.4 Flow cytometry

Flow cytometry is a tool that is not commonly used for bacteria, likely due to the range of technical difficulties. The small size creates difficulty in identifying cells from debris alongside potential noise making identifying biological variation within samples using the fluorescence intensity of cells difficult (63). For example, running flow cytometry on GAS strains that can non-specifically bind antibodies, would lead to the misreporting of antibody binding causing inaccurate fluorescent intensities. Fortunately, a protocol developed by Dr. Jacelyn Loh using mice anti-sera provided a basis for which to translate and optimise for rabbit anti-sera (29). This would enable the measurement of M protein and T-antigen expression levels on various GAS strains using anti-M1, anti-T1, anti-M6 and anti-T6 rabbit sera, controlling with pre-immune rabbit sera (Figure 1-5). Comparing the shift in fluorescence between the pre-immune sera control and a protein targeted sera e.g. anti-M1, would enable the relative level of the M1 protein expression to be measured (29). Ascertaining these expression levels will provide insight into the extent to which expression levels of GAS cell surface proteins within an *emm* type affects M protein and T-antigen targeted killing (which will be measured using opsonophagocytic killing assays (OPKA's) outlined in the next section.

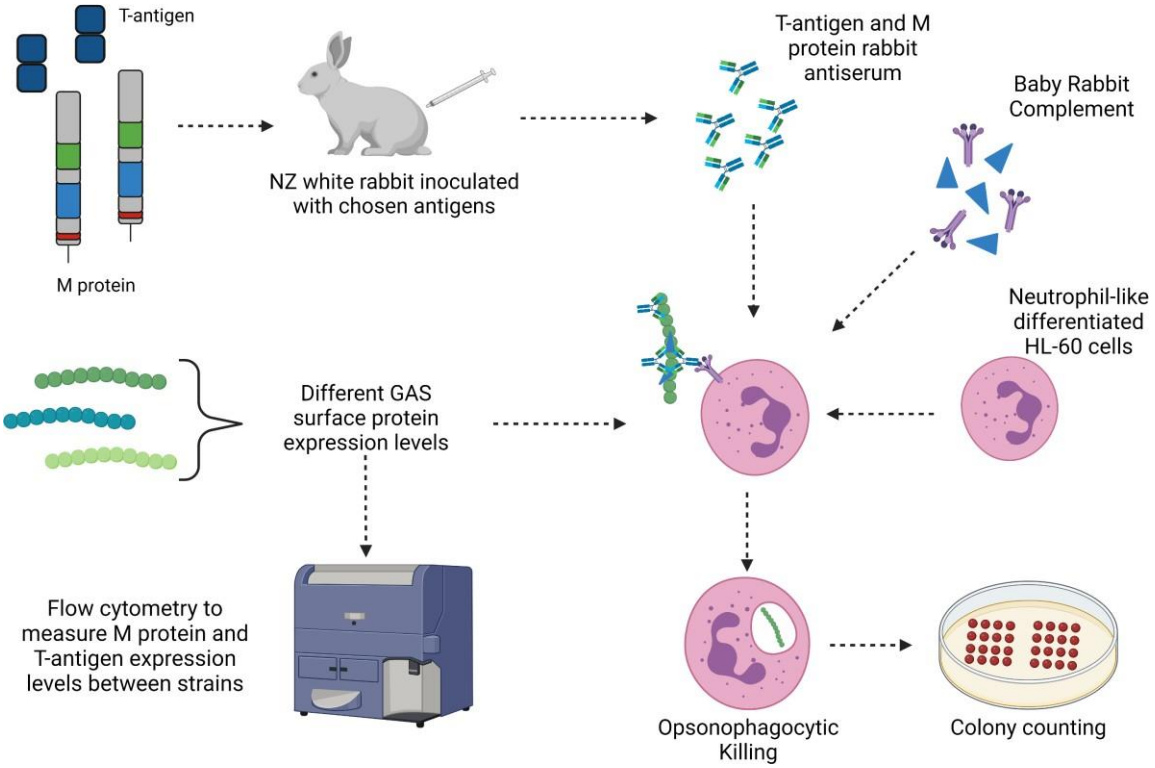

Figure 1-5: An overview of the processes involved in this project

The experimental methods used in this project are displayed within this schematic overview. NZ white rabbits are used to generate antisera to the M1, M6, T1 and T6 antigens. This sera in conjunction with baby rabbit complement and neutrophil-like cells are used in the OPKAs to determine the efficacy of killing on each strain. On top of this, the antisera also provide a means of measuring the GAS protein expression levels with flow cytometry. This figure was made using BioRender.

1.5.5 Opsonophagocytic killing assays

The GAS opsonophagocytic killing assay (OPKA) is a recently developed functional assay that derives from the more classical Lancefield assay. The Lancefield assay utilised antibodies to opsonise the GAS bacteria and trigger leukocytes to phagocytose the bacteria. To achieve this serum from GAS patients was incubated with dilutions of cultured GAS, whilst the complement and leukocytes required for phagocytic killing were provided by donor blood pre-screened to have no GAS antibody reactivity (64). The plating and enumeration of any colonies grown from each of these dilutions would be compared to a control of only GAS to determine if killing had occurred by observing decreased colony forming units (64). This assay displayed high variability resulting from donor's blood and required

consistent screening and collection of fresh blood. Therefore, the OPKA aimed to provide an assay that could measure killing as a potential correlate of immunity by assessing the antibody driven killing whilst being a consistent replicable assay (51, 65). The protocol was optimised and standardized by using the *emm* 1, 6 and 12 strains in the assay, (51, 65). To remove the requirement of fresh donor blood the protocol was adapted to utilize a human cell culture line of HL-60 cells that are capable of differentiating into a neutrophil-like lineage. Additionally, the complement source was controlled by using commercially available baby rabbit complement as opposed to complement sourced from donor blood (Figure 1-5) (51, 65).

1.5.6 Project aims

This project is designed to investigate how the immune evasion properties of GAS virulence factors, particularly the M protein and T-antigen, can influence immune responses targeted towards another virulence factor. How the GAS M protein, which is a multifunctional immune evasion molecule, influences immune responses targeting the T-antigen, which forms the backbone of the GAS pilus. To achieve this the following research questions, aim to be answered:

- Does the level of M protein expression influence the killing capacity of T-antigen targeted antisera?
- How do M proteins from different GAS strains, and with different immune evasion properties, influence the killing capacity of the T protein targeted antisera?

In summary, this project aims to investigate the relationship between the Streptococcal M protein and a T-antigen targeted immune response. Therefore, our use of two GAS strains possessing distinct immune evasion mechanisms will be crucial for this. The M protein and T-antigen expression levels between strains will provide insight into how surface expression levels could influence immune evasion. Thus, the impact of M protein function alongside M protein and T-antigen expression on a T-antigen targeted immune response will be investigated using an opsonophagocytic killing assay (OPKA), as the correlate for immune protection (65).

2 Materials and Methods

2.1.1 Buffers, media, and reagents:

2.1.2 ELISA:

Reagents	Formula	Notes/Methods
Carbonate-bicarbonate coating buffer	• 35mM $NaHCO_3$ • 15mM Na_2CO_3	Adjusted to pH of 9.6 using NaOH or HCL
PBS	• 137mM NaCl • 2.7mM KCL • 10mM Na_2HPO_4 • 2mM KH_2PO_4	Adjusted to pH of 7.4 Can be adjusted to PBS-T by adding 0.1% Tween-20

2.1.3 Bacterial growth and OPKAs:

Reagents	Formula	Notes/Methods
Opsonisation buffer	• 10 % defined foetal bovine serum (Hyclone, Cytiva) • 9% Hanks balanced salt solution (HBSS) (+Ca/Mg) (Thermofisher Scientific) • 0.5% 1% gelatin solution	Heat inactivated. Made up to volume with sterile pyrogen-free water. Prepared on day of assay then discarded.
1% gelatin solution	• 1 % gelatin (Thermo Scientific) • Sterile pyrogen free water	Dissolve gelatin in water and autoclave. Store at RT for up to 2 months.
Todd Hewitt Broth	• 3% Todd Hewitt Broth (BD, Fort Richard Labs) • Distilled water	Volumes adjusted according to requirements. Mix all ingredients in a Duran bottle and autoclave at 121℃ for 20 minutes.

STGG Media:	• 3% Tryptone Soya Broth (BD, Fort Richard Labs; New Jersey, USA) • 0.5% Glucose (Sigma-Aldrich; Missouri, USA) • 10% Glycerol (ECP Limited; Auckland, NZ) • Distilled water	Mix all ingredients in a Duran bottle and autoclave at 121℃ for 20 minutes.
Todd-Hewitt -yeast extract agar (THY) plates:	• 3% Todd-Hewitt Broth (BD, Fort Richard Labs; New Jersey, USA) • 0.5% yeast Extract (Oxoid Ltd, Thermo Fisher Scientific) • 1.5% bacteriological Agar (BD, Fort Richard Labs) • Sterile pyrogen free water	Autoclave and incubate in a water bath at 50℃. Pour 23mL agar into each 100x100mm square plate. Leave to dry on a flat surface for 20 minutes. Invert stacked plates to store at 4℃ for up to 1 month.
TTC stock:	• 2.5% TTC (2, 3, 5-tetraphenyltetrazolium chloride) (Sigma Aldrich) • Sterile pyrogen free water	Dissolve TTC in 40mL water and make up to a final volume of 50mL with the remaining water. Use a 0.22µm filter to sterile filter. Store at 4℃ for up to a month.
Todd-Hewitt yeast extract overlay agar:	• 3% Todd-Hewitt broth (BD, Fort Richard Labs) • 0.5% yeast extract (Oxoid Ltd, Thermo Fisher) • 0.75% bacteriological agar (BD, Fort Richard Labs) • 0.1% TTC stock	Make fresh on day of assay. Autoclave and incubate in a 50℃-water bath until required. TTC prepared as stated above.
Blood Agar Plates:	• Columbia Horse Blood Agar Plates (BD, Fort Richard Labs)	
Baby Rabbit Complement:	• (Pel-Freez Biologicals, AR, USA)	

2.1.4 Flow cytometry:

Reagents	Formula	Notes/Methods
Flow Blocking Buffer:	• PBS • 3% Fetal Bovine Serum (Hyclone, Cytiva) • Etheylenediaminetetraacetic acid (EDTA)	Serum was heat inactivated at 56℃ for 30 minutes
FACS Buffer:	• Phosphate buffered saline (PBS) • 1% Fetal Bovine Serum (Hyclone, Cytiva) • 5mM Etheylenediaminetetraacetic acid (EDTA)	
Flow Blocking Reagent (GRB Block):	• Native Human IgG FC fragment protein (Abcam)	Diluted in FACS buffer to required concentration.
Flow Blocking Reagent (Tru-Stain):	• Human Tru-Stain FcX (Biolegend)	Diluted in FACS buffer to required concentration.
Flow Secondary Antibody Stain:	• Anti-Rabbit Alexafluor 647 (Life Technologies) • Anti-Mouse Alexafluor 647 (AbCam) • Fluorescein isothiocyanate (FITC) (AbCam)	Diluted in FACS buffer to required concentration.

2.2 Full-length M proteins:

The full-length M Proteins were produced prior to this project as described in Jones *et al* (2018) (51). The *emm*1 strain selected to produce M1 protein was SF370 and the *emm*6 strain selected for M6 protein production was MGAS10394. Briefly, these two M proteins were cloned via amplification of genomic DNA using specific primers and Sanger sequencing to confirm the correct sequence. *Escherichia coli* BL21 (DE3) cells were utilised to express recombinant proteins without signal and transmembrane sequences.

2.3 M protein HVR peptides:

The hyper-variable regions of the M proteins were synthesised by GenScript USA Inc. who confirmed their purity to be above 90% by testing the HVR peptides using mass spectrometry. These represent two regions of 50 amino acids, as demonstrated in Table 2 below.

Table 2 : HVR Peptide Amino Acid Sequences.

M Protein Type:	Amino Acid Sequence Represented:
M1	NGDGNPREVIEDLAANNPAIQNIRLRHENKDLKARLENAMEVAGRDFKRA
M6	RVFPRGTVENPDKARELLNKYDVENSMLQANNDKLTTENKNLTDQNKNLT

2.4 Full-length T-antigens:

The full-length T-antigens were generated by Dr Jacelyn Loh prior to this project, in which detailed methodologies are published (Young *et al*., 2019) (Loh *et al*., 2021)(29, 35). The *tee*6 gene was amplified from the MGAS10394 strains genomic DNA, whilst the *tee*1 gene was amplified from the SF370 strain. This process involved the PCR amplification of genes from the sortase motif and signal cleavage site, and the T1 and T6 proteins which were subsequently expressed in *Escherichia coli* BL21 (DE3) cells using recombinant protein expression techniques.

2.5 Rabbit anti-sera:

2.5.1 M protein anti-sera:

M protein anti-sera were produced for a previous study by Jones *et al* (2018) where the M1 and M6 proteins were used to inoculate New Zealand white rabbits emulsified with Incomplete Freund's adjuvant in a 3-dose schedule and then euthanised to enable antisera collection (51). This collection method was approved by The University of Auckland Animal Ethics Committee, and the ARRIVE guidelines were followed.

2.5.2 T-antigen anti-sera:

T-Antigen anti-sera was generated using a similar methodology as the M protein anti-sera. This time it was generated by Dr Jacelyn Loh as part of an earlier study (Loh et al., 2021) (29). New Zealand white rabbits were inoculated with the T1 and T6 antigens emulsified with Incomplete Freund's adjuvant in a 3-dose schedule before collecting the antisera after the rabbits were euthanised.

2.6 GAS strains

Table 3: GAS strain information:

***emm* type:**	**Strain Name:**	**Strain Origin:**	**Project Uses:**
emm 1	SF370	A laboratory adapted strain from ATCC. Originally a wound swab.	Flow cytometry. OPKA.
emm 1	43	Pharyngitis swab isolated from the UK in 2009.	Flow cytometry. OPKA.
emm 1	SF370 M1 Knockout	SF370 strain with the knockout performed by Dr Jacelyn Loh.	Control strain for flow cytometry.
emm 1	SF370 T1 Knockout	SF370 strain with the knockout performed by Dr Jacelyn Loh.	Control strain for flow cytometry.
emm 6	GASOPA6_02 (M6:2)	Pharyngitis swab isolated from the UK in 2009.	Flow cytometry. OPKA.
emm 6	GAS_1070 (M6:1070)	Isolated from an ARF patient in NZ.	Flow cytometry. OPKA.
emm 6	GAS_08308 (M6:09209)	Isolated from an ARF patient in NZ.	Flow cytometry.
emm 6	GAS_09209 (M6:08308)	Isolated from an ARF patient in NZ.	Flow cytometry.

2.7 Enzyme-Linked Immunosorbent Assays (ELISA)

2.7.1 Full-length M protein and T-antigen ELISAs

ELISAs used 96 well plates (ThermoFisher Scientific, Auckland NZ) that were coated with 50µL of either M protein or T-antigen at 5µg/mL in 1x PBS and incubated overnight at 4℃. Plates were then washed 3 times with 300µL of PBS supplemented with 0.1% Tween-20 (PBST) per well followed by blocking with 100µL of 5% milk PBST at 20℃ for one hour. Plates were washed as described above and 50µL of rabbit sera pre-diluted in PBST was added to their respective wells as demonstrated in Figure 2-1. Plates were then incubated at 20℃ for an hour and washed again, before 50µL goat anti-rabbit IgG secondary diluted to 1:10,000 in 5% milk PBS-T was added per well. Following a final 1-hour incubation at 20℃, 50µL of 3,3′,5,5′-Tetramethylbenzidine liquid peroxidase substrate (Sigma; TMB) was added to the wells and incubated for 2.5 minutes at room temperature. The reaction was stopped with 50µL of 1M HCl added to each well, giving the staining effect displayed in Figure 2-1. The absorbance was then measured at 450nm using the EnSight plate reader (PerkinElmer).

2.7.2 HVR peptide ELISAs

HVR peptide ELISAs follow a similar protocol to full-length protein ELISAs but included minor variations. The HVR peptides were coated in Carbonate-Bicarbonate buffer and sealed with an AlumaSeal (MediRay) for 3 hours at 37℃, after which the coated plates were further incubated at 4℃ overnight before use. Furthermore, there was no blocking step for HVR peptide ELISAs, and both primary and secondary antibodies were diluted to 1:10,000 in PBS-T instead of 5% milk PBS-T.

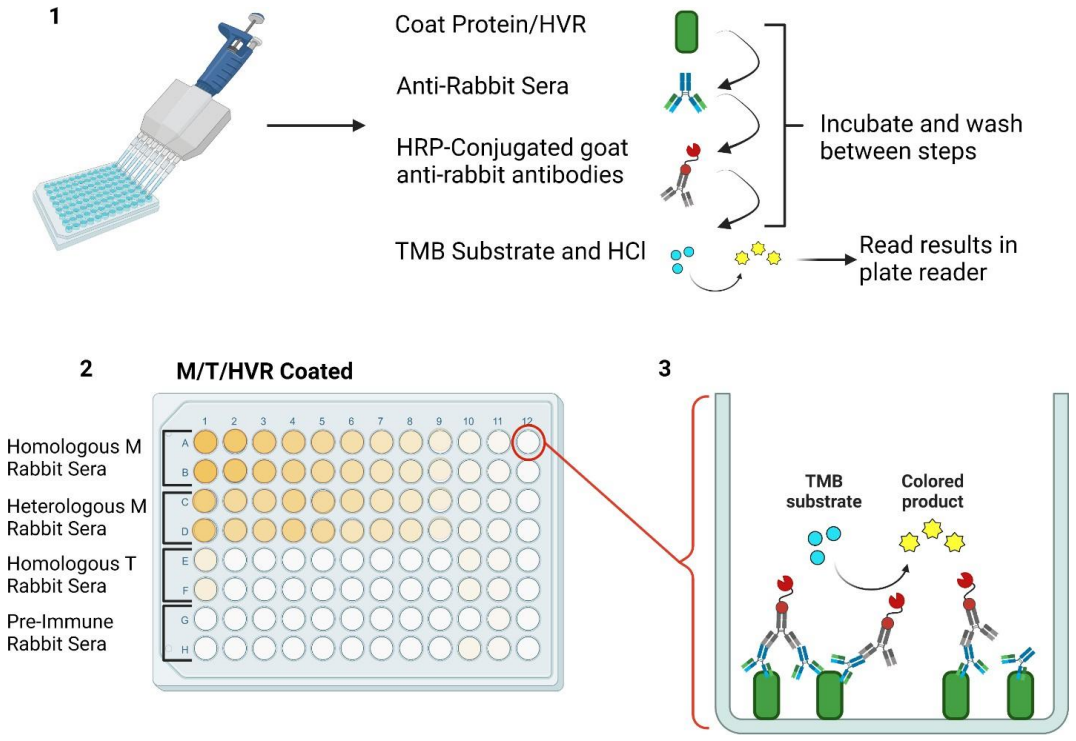

Figure 2-1: Overview of an ELISA protocol, biological interactions, and plate map.

(1) An overview of the ELISA protocol steps. The order in which each component is added and the opportunity for potential binding. The plate is coated with a selected protein or HVR and antibodies from rabbit sera are tested for binding capabilities. The primary antibody is washed off before the secondary antibody binds to any rabbit anti-sera bound to the coated antigen. The secondary antibody is labelled with a horse-radish peroxidase (HRP) that, upon TMB incubation, will react to form a blue-coloured product. HCl stops this reaction and converts it to yellow. (2) The example plate displays a completed ELISA, with the intensity of the colour produced proportional to the antibody concentration bound in the well. This plate would be read at an absorbance of 450nm. (3) An ELISA well with successful binding at all stages is schematically displayed with the outcome of a positive signalling reaction by the TMB and HCl. This figure was made using BioRender.

2.8 Bacterial culturing

2.8.1 Culturing working stocks

The expansion of frozen stocks of *S. pyogenes* to produce working stocks for use in opsonophagocytic assays followed a standard 3-day methodology. The frozen *S. pyogenes* glycerol stocks were removed from the -80°C freezer and kept on dry ice while being streaked onto horse blood agar plates. These were incubated overnight at 37°C, 5% CO_2, to avoid overgrowth and ensure isolated colonies grew. The following day a single colony from each plate was used to seed 10mL of Todd-Hewitt broth which

was incubated overnight at 37℃ in 5% CO_2 without agitation. Finally, on day 3, pre-warmed Todd-Hewitt broth was inoculated with the overnight GAS liquid culture at a 1:10 dilution in a 50mL falcon tube and incubated at 37℃, 5% CO_2 until an optical density (OD) of 0.5-0.7 is reached, after which the growth was stopped by placing it in an ice bath. To create working stocks for freezing, the bacterial suspension was mixed 1:1 with STGG media and vortexed. This mix was made into 500µL aliquots in 1.5mL Eppendorf tubes (Axygen) and frozen at -80℃ until needed.

These working stocks were generated for all strains used in assays throughout the project ensuring batch consistency across all experiments. The M1 strains included M1:SF370, a well-classified laboratory-adapted strain initially isolated from a patient's wound (J Ferretti *et al*, 2001) and the M1:43 strain, a clinical isolate from a throat swab taken from a patient with pharyngitis (51, 66). Furthermore, two knock-out M1:SF370 strains were grown, one with the M protein knocked out and the other with the pilus knocked out, both generated by Dr. Jacelyn Loh, which were used as controls during the flow cytometry. The M6 strains grown included the M6:2 strain, isolated from a throat swab sample in the UK, and the M6:1070 strain, isolated from an acute rheumatic fever patient in NZ using a throat swab. The M6:1070 strain was selected in addition to the M6:2 strain following flow cytometry characterisation described in section 3.2.3.

2.9 Flow cytometry

2.9.1 Optimisation of bacterial fixing mechanism

The bacterial stocks used in the flow required fixing prior to use to ensure biological safety. Therefore, to determine the optimal method for bacterial fixing, an M1:SF370 working stock (0.67 OD) was quick-thawed at 85℃ in a heat-block, centrifuged and re-suspended in blocking buffer at 0.2 OD in preparation for use. Half of the samples were heat fixed at 80℃ for 5 minutes before staining, whilst the others were fixed with 50µL per sample of 4% Paraformaldehyde (Sigma-Aldrich) for 30-minute incubation after staining was completed.

Following resuspension in the blocking buffer, all samples were sonicated, rested on ice, and re-suspended in FACS buffer before 200µL samples were placed into flow tubes. Samples were stained with a primary antibody, either pre-immune, anti-M1 or anti-T1 mouse sera. After washing with 1mL FACS buffer using anti-mouse Alexafluor 647 (AbCam). After being washed and re-suspended in 200µL FACS buffer, samples were run on a BD LSRII flow cytometer (BD Sciences). 10,000 events were collected and analysed using FlowJo.

2.9.2 Determining the optimal anti-rabbit secondary antibody for bacterial flow

The optimal secondary antibody choice and concentration was determined from anti-rabbit Alexafluor 647 (ThermoFisher Scientific) and FITC (AbCam). M1:43 bacteria (OD: 0.534) was diluted in blocking buffer to 0.2 OD and heat-killed. The aliquot was re-suspended in FACS buffer and diluted, ensuring each 200µL sample had less than 1,000,000 cells. Samples were stained with 100µL of either anti-M1, anti-T1 or pre-immune rabbit sera at a 1:50 concentration for 30 minutes on ice. Following a wash, 100µL of secondary was added per sample, which utilised varying dilutions of FITC (1:50-1:200) or Alexafluor 647 (1:50-1:800). Samples were then run on the BD LSRII flow cytometer (BD Sciences), and 10,000 events were collected to be analysed on FlowJo.

2.9.3 Optimising the blocking of M1 Fc binding

The M1:43 strain was used to optimise the blocking of Fc receptor binding by the M1 protein. Frozen M1:43 stocks were quick-thawed, re-suspended in blocking buffer (0.2 OD), and heat-killed. After cooling and sonicating, the bacterial aliquot was re-suspended and diluted in FACS buffer, which gave <1,000,000 cells per 200µl sample. Samples were then blocked with 100µL of either Tru-Stain (BioLegend) at concentrations of 1:10 or 1:20 or Human Fc Receptor (AbCam) at concentrations of 1:10, 1:20 or 1:40. Controls included samples with a FACS buffer block and no-block. All samples underwent a 10-minute blocking incubation at room temperature before being stained with the primary antibodies of either pre-immune or anti-M1 rabbit sera and incubated on ice for 30 minutes. Samples were then washed with FACS buffer and incubated in a 100µL staining volume of anti-rabbit

Alexafluor 647 (1:200) for 30 minutes on ice. After a final wash and resuspension with 200µL FACS buffer, samples were run on the BD LSRII flow cytometer (BD Sciences), collecting 10,000 events, and analysed using FlowJo (Figure 2-2).

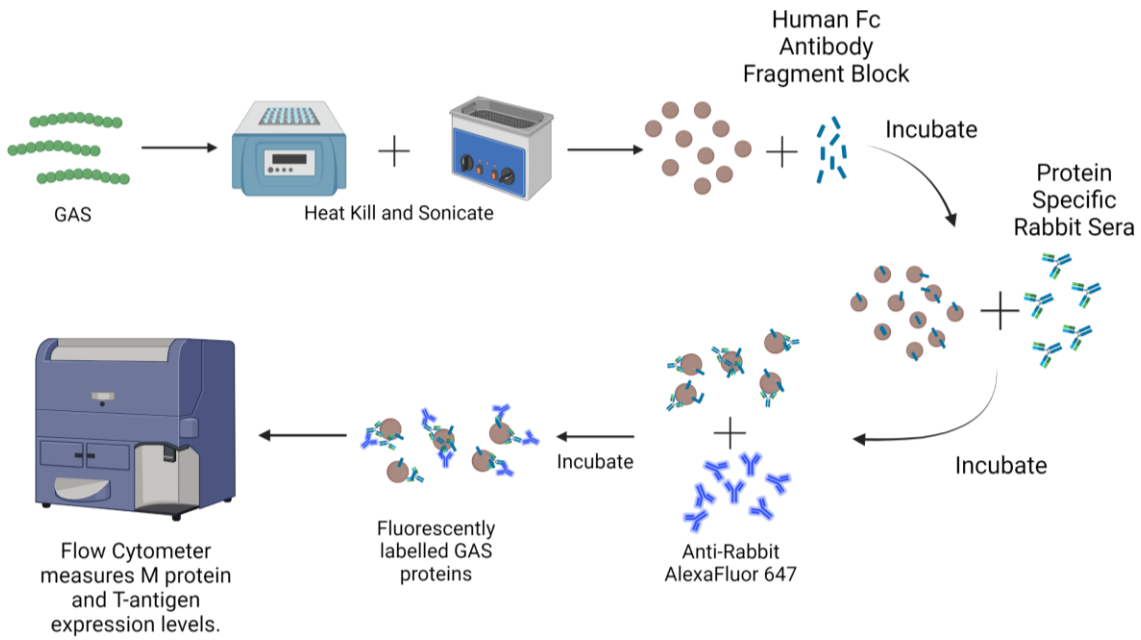

Figure 2-2: Optimised Bacterial Flow Cytometry Protocol.

Bacteria were prepared by heat killing at 80°C for 5 minutes and sonicated for 1 minute. Each sample was diluted to under 1,000,000 cells and blocked with Human Fc Antibody fragment (AbCam) at 1:20 concentration for 10 minutes. Both primary (1:50) and secondary (1:200) antibodies were successively incubated with bacteria on ice for 30 minutes. Samples were run on the BDLSRII cytometer. This figure was made using BioRender.

2.9.4 M1 protein and T1 antigen expression measurement

The optimised bacterial flow cytometry methodology was used to measure the protein expression levels on the M1 strains including the two control knockout strains. All strains were quick-thawed (37°C), re-suspended in blocking buffer (0.2 OD) and heat killed (80°C for 5 minutes) before being cooled on ice. Samples were then sonicated and incubated on ice for 15 minutes before being re-suspended in FACS buffer at <1,000,000 cells per 200µL sample. Half the samples per strain were blocked with 100µL of Human Antibody Fc region (AbCam) (1:20 concentration) for 10 minutes at room temperature. All samples were stained with 100µL of their respective primary antibody of anti-

M1, anti-T1 or Pre-Immune rabbit Sera, all at a 1:50 concentration, and incubated on ice for 30 minutes. A 1 mL FACS buffer wash was completed before staining all samples with 100µL of anti-rabbit Alexafluor 647 for 30 minutes on ice. Samples were washed and re-suspended in 200µL FACS buffer and run on the BD LSRII flow cytometer collecting 30,000 events that were analysed using FlowJo (V 10.8.1).

2.9.5 M6 strain selection and M6/T6 expression measurement

To identify another M6 strain for use in this project, over and above M6:2 that was already shown to behave well in opsonophagocytic assays (Jones et al), the optimised flow cytometry protocol was used (51). All four M6 strains were screened for M6 and T6 expression levels as described in section 2.9.4 using anti-M6, anti-T6 or pre-immune rabbit sera, all at 1:50 concentration. A blocked control sample was run to confirm that no non-specific pre-immune serum binding was occurring. Alongside the samples, a negative control of the M protein knock-out strain was run to ensure serum binding was specific to the M protein. All samples were run using the BD LSRII flow cytometer, collecting 30,000 events, and analysed using FlowJo.

2.9.6 M6 expression analysis at different growth time points

To investigate if the expression profiles of the M6 protein or T6 antigen could be influenced by the bacteria's growth stage, the M6:2 and M6:1070 strains were cultured to generate working stocks from each stage of the bacterial growth curve. Flow cytometry was then completed as described above (section 2.9.5) on the four working stocks per strain staining for M6 and T6, with samples read on the BD LSRII flow cytometer.

2.10 Opsonophagocytic Killing Assays

2.10.1 HL-60 cells

The HL-60 cell lines were cultured, maintained, and differentiated into neutrophil-like cells by Aimee Paterson, a senior research technician in the Moreland laboratory, according to developed protocols

(Jones et al., 2018). Briefly, cells were expanded from frozen stocks and maintained for 2 weeks at a density between $2x10^5$ and $1x10^6$/ml until they were ready for differentiation and use. Differentiation required incubation for 3-4 days at 37℃ in M2 media. On the morning of use cells were centrifuged, washed in HBSS, re-suspended in OPS buffer and viability tested by staining and counting a subset of cells (51, 65).

2.10.2 Optimum dilution assays

These assays determined the correct bacterial and complement dilutions required for each strain's killing assays. Varying concentrations of bacteria were exposed to a range of active complement concentrations (Figure 2-2). The level of non-specific killing was determined using a heat-inactivated complement column at each complement concentration. This experimental protocol was adapted from Jones *et al*. (2018) and McGregor *et al*., (2020)(51, 65). Bacterial dilutions were prepared by first quick thawing a working stock before re-suspending in OPS buffer. In a separate 96-well plate, bacteria were diluted ten-fold in well H1, followed by a five-fold serial dilution up the column (Figure 2-2). From that column, 10µL of bacteria was multi-channel pipetted into each column of the assay plate, producing a vertical gradient of bacterial concentrations.

The assays were completed following the standard OPKA procedure as detailed in section 2.10.3, where the assay plates were first incubated at room temperature for 30 minutes. Active and heat-inactivated complement were diluted in Eppendorf tubes with OPS buffer to dilutions from 1:1 to 1:6. Figure 2-3 displays how the complement was multi-channel pipetted into the assay plate with 10µL added alongside 40 µL of differentiated HL-60 cells into each well. The plate was then incubated at 37℃ for an hour on a 700rpm shaking incubator and set on ice for 15 minutes. Finally, the contents of the wells were plated onto dry THY agar plates spotting 10µL with a multi-channel pipette and immediately tilting, which created horizontal streaks. Each plate fit 3 columns, and once all columns were plated, they were dried at room temperature before THY overlay agar with TTC was poured over the plates. Once the agar solidified, plates were incubated upside down overnight at 37℃. Plates were read the following morning using an automated colony counter. The bacterial and complement

dilutions that produced between 100-200 colony counts while maintaining 10-30% non-specific killing were then selected to be used in the opsonophagocytic killing assays (OPKAs).

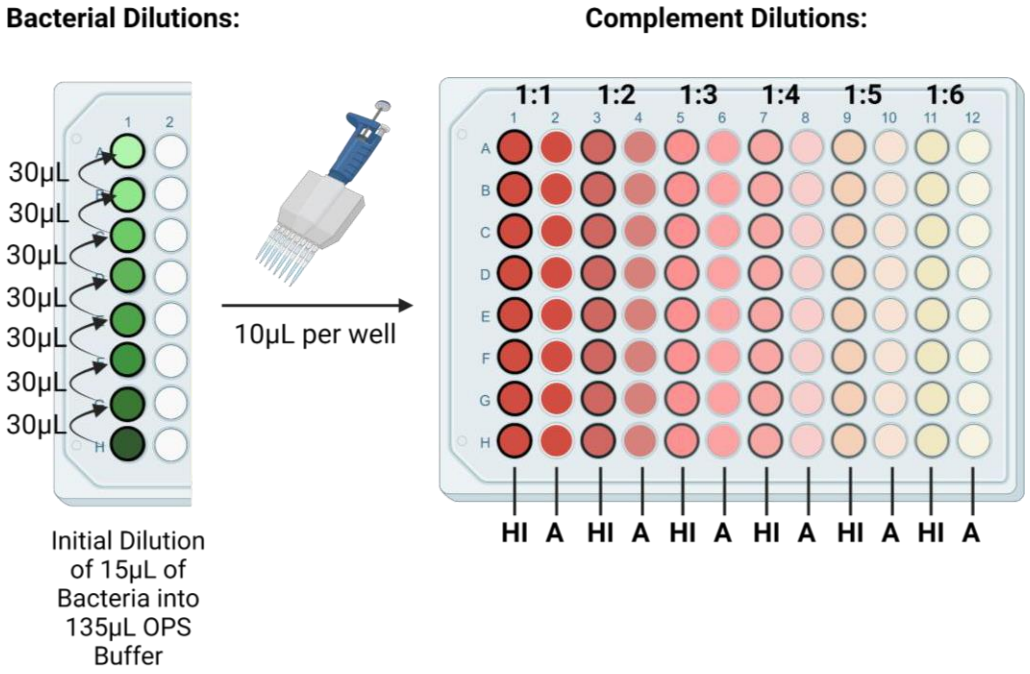

Figure 2-3: Bacterial Dilution Process and Plate Plan for Optimal Dilution Assays.

Bacterial dilutions were prepared in a separate 96-well plate, serially diluting the strain in OPS buffer. Six concentrations of baby rabbit complement were tested using both heat-inactivated and active complement columns (HI and A respectively). Thus, an optimal dilution for bacteria and complement is identified by comparing the killing between the various combinations of bacterial and complement concentrations. This figure was made using BioRender.

2.10.3 OPKAs

The methodology used was originally developed by Professor David Goldblatts laboratory at University College London, London and refined by Dr Reuben McGregor at the University of Auckland (51, 65). The protocol used the bacterial and complement dilutions selected from optimum dilution assays for each strain (section 3.3.1) with the addition of the sera to be tested for killing. An overview of the OPKA is shown in Figure 2-4.

The assay plate was prepared by adding 20µL of OPS buffer to all wells except row H, wells 3-12 of a 96-well round-bottomed plate. 30µL of serum samples pre-diluted in OPS buffer (1:5 unless

otherwise stated) was added into the empty wells of row H, wells 3-12 and serially diluted 3-fold (Figure 2-5). The working stocks were thawed and diluted in OPS to the pre-determined optimal dilution (section 2.10.2) and 10µL of the solution was added to the side of each well. Bacteria were then mixed with sera by tapping plates, ensuring all bacteria entered the wells at a consistent time. Plates were incubated on a shaker for 30 minutes at room temperature, enabling opsonisation of bacteria as per Figure 2-4.

Baby rabbit complement was thawed on ice and a specified volume was heat-inactivated at 56℃/ for 30 minutes. The complement was diluted in OPS buffer to the concentration from the optimal dilution assay (section 2.10.2). Complement was added as per Figure 2-5 with 10µL of heat-inactivated complement added to control column A and 10µL of active complement to the remainder of the wells immediately followed by addition of 40µL differentiated HL-60 (Figure 2-5). The plates were incubated at 37℃/5% CO_2 on a mini-orbital shaker at 700-rpm for an hour, which gave time for complement and HL-60 cells to phagocytose and kill opsonised GAS in the wells. Post-incubation, the plates were put on ice for 20 minutes halting the killing process.

Square THY agar plates were dried at room temperature prior to plating. OPKA plates were mixed gently by vortex and 10µL from each well was transferred to THY agar plates using a multichannel pipette in a column wise fashion (Figure 2-4). Each column was spotted down and immediately tilted, enabling the spot to run horizontally across 1-2cm. This was repeated until three columns were plated to fill one THY plate and repeated until all columns had been plated. The plates were dried at room temperature for 20 minutes. Finally, an overlay of warm liquid THY agar with TTC was added and allowed to solidify. The TTC overlay enabled the visualisation of colonies the following morning, as shown in Figure 2-4**.** The plates were left to incubate upside down overnight at 37℃. Colonies were counted the following morning, after gently wiping the overlay to remove any unwanted bacterial colony spots and then counted using the Protocol 3 automated colony counter's OPKA software (Symbiosis).

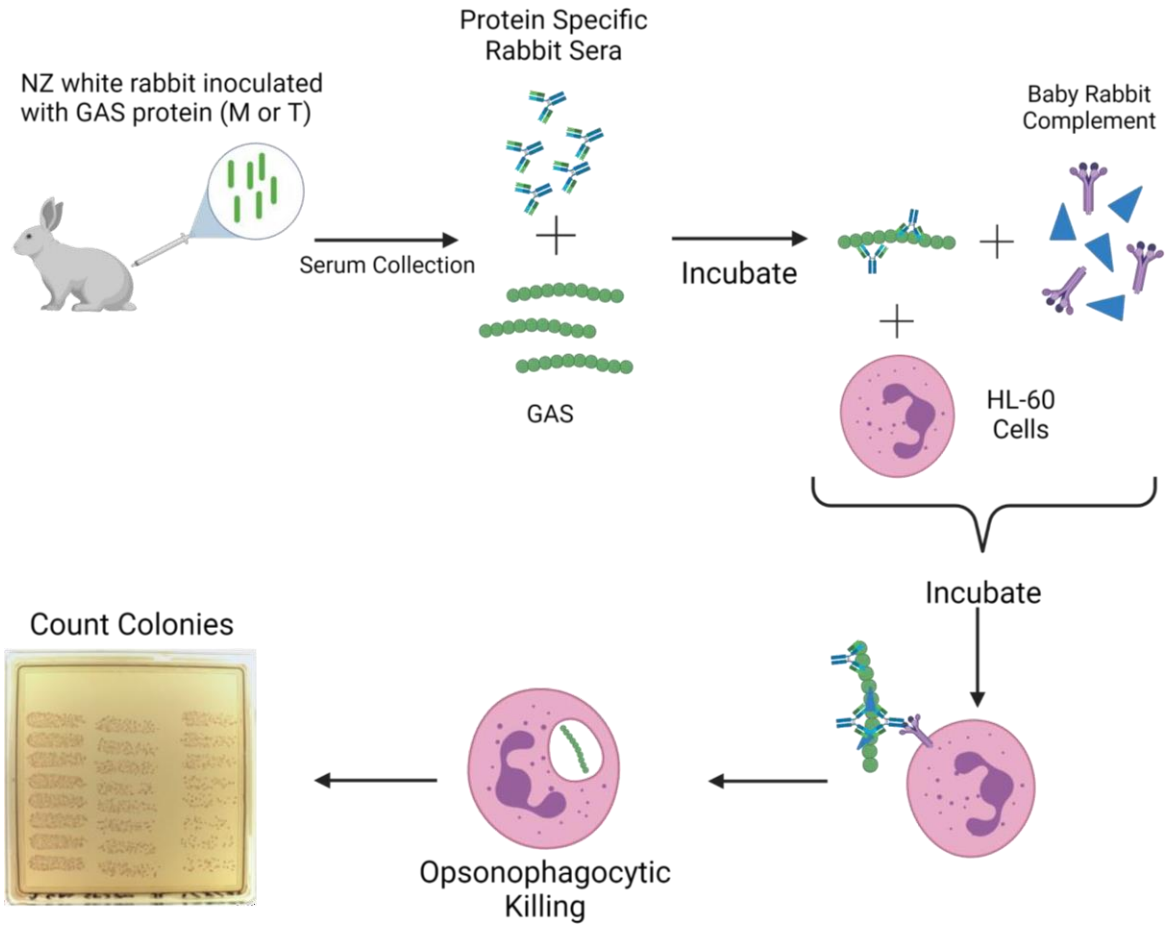

Figure 2-4: Opsonophagocytic Killing Assay Overview - From Serum Generation to Colony Counting.

The protein-specific rabbit sera were incubated with GAS to induce targeted antibody binding. Each well was then incubated with a pre-determined concentration of baby rabbit complement and neutrophil-like HL-60 cells. This induced the killing of GAS via antibody-dependent opsonophagocytosis during the hour of incubation. The killing was stopped by putting the plates on ice. The contents of the wells were then plated onto agar and incubated overnight, which enabled the colonies to be counted and the levels of killing caused by the rabbit anti-serum to be ascertained. This figure was made using BioRender.

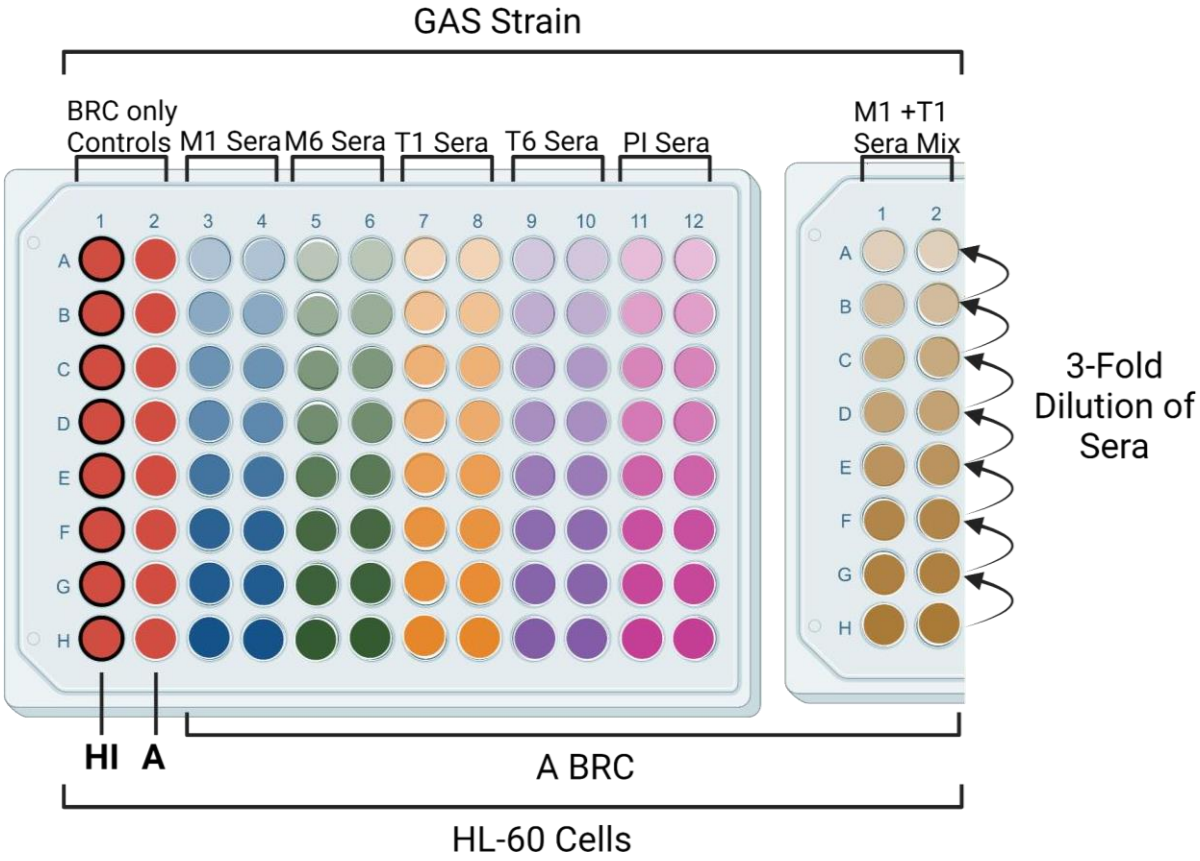

Figure 2-5: Opsonophagocytic Killing Assay Plate Plan:

The plate plan for both M1 and M6 strain killing assay. Both homologous and heterologous M and T Sera were tested alongside pre-immune sera and a mix of homologous M and T sera. All sera were serially diluted 3-fold from row H upward to A, enabling analysis of each serum's killing efficacy at various concentrations. All wells were controlled for non-specific killing using baby rabbit complement (BRC) only wells, from which we could compare the active complement killing activity to heat-inactivated complement. This ensured that killing seen from the sera was specific and not caused by complement activity alone. This figure was made using BioRender.

2.11 Statistical analyses

2.11.1 Area Under the Curve (AUC)

ELISAs were graphed and analysed using GraphPad Prism 8.0.2, as displayed in Figure 2-6. Each point averaged the duplicate absorbance readings at each serum dilution and was plotted with standard error of the mean (SEM) to show any variation in duplicates. To control for background absorbance when calculating the area under the curve (AUC) a negative control was used at the same dilution range as the sera.

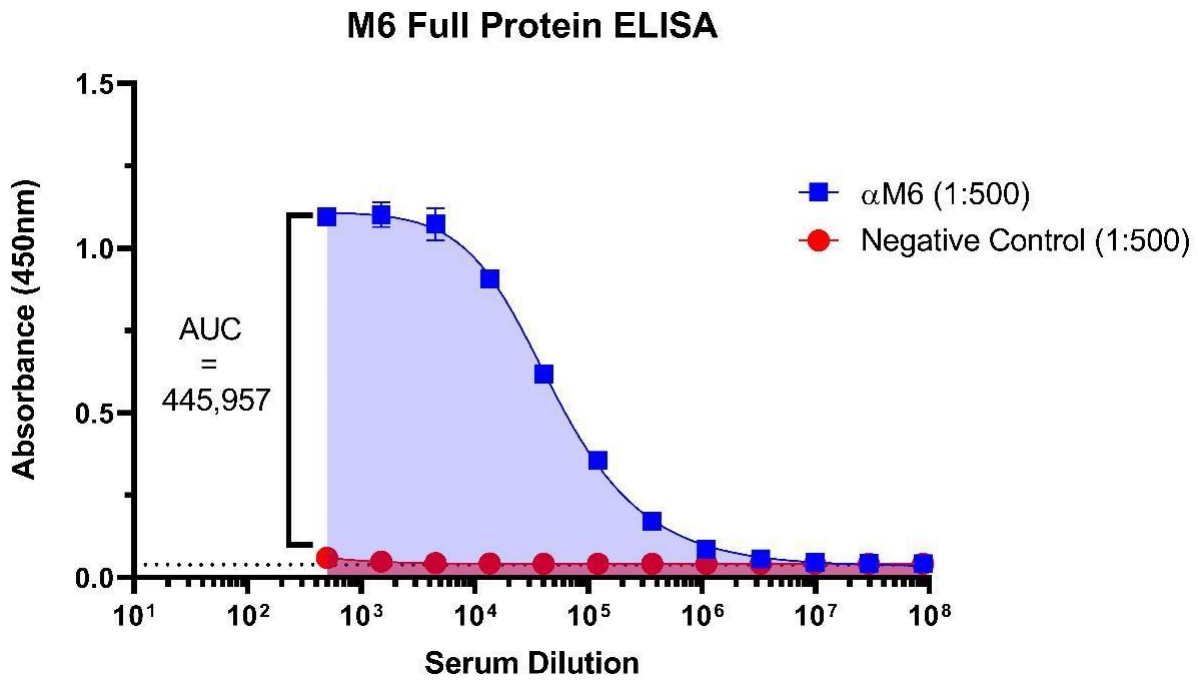

Figure 2-6: Graphical display of the area under the curve calculation.

The ELISA displays binding of the anti-M6 (αM6) rabbit sera and a negative control at a starting dilution of 1:500 against the M6 full-length protein. To generate the area under the curve (AUC), both duplicate sera had a line of best fit attributed to their mean absorbance points along the dilution gradient. This antibody titre AUC is generated for both the sera and negative control, enabling the removal of background binding from the αM6 AUC, giving a final AUC of 445,957.

2.11.2 Staining index

The staining index is an analytical method for flow cytomtery data to enable comparison of positive sample mean fluoresecence intensities (MFIs) whilst incorporating each sample's negative controls to control for spread in fluorescence. The staining index was used to investigate the increase in staining between different protocols relative to a baseline and enabled accurate identification of the optimal method for the flow protocol.

The method of calculating the staining index is displayed in Figure 2-7. The shift in MFI between the M1 stained (positive) and pre-immune stained sample (negative) was divided by twice the standard deviation of the pre-immune stained sample. This gave an index for the experimental methodology that was compared directly to others more accurately than an MFI shift only.

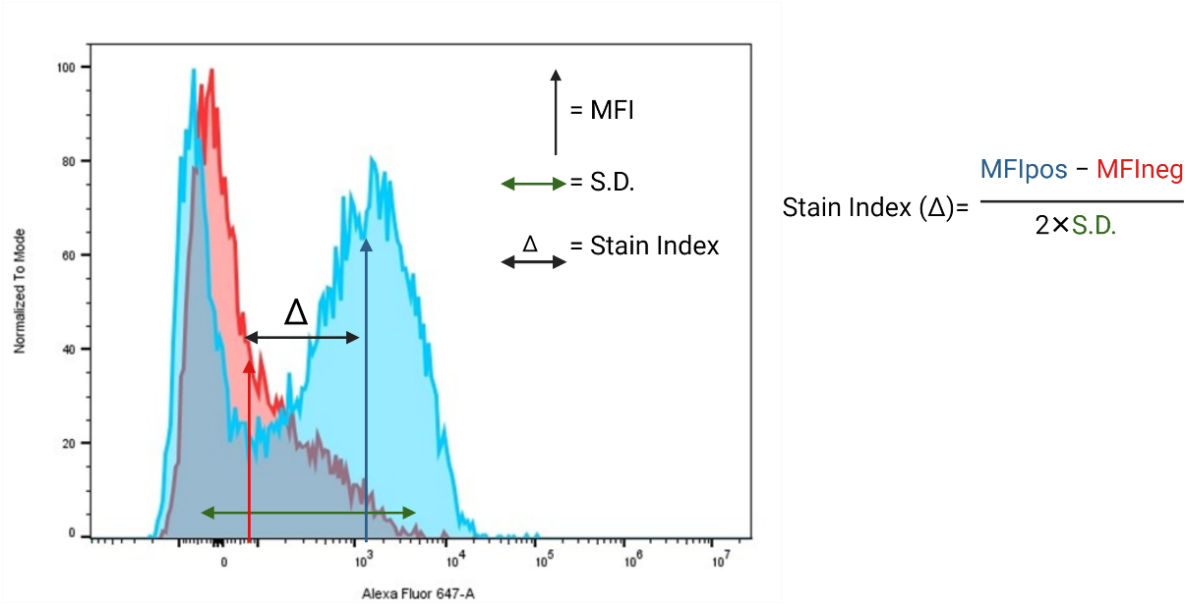

Figure 2-7: Graphical display of staining index calculation using a histogram.

Two sample populations were stained with either a negative primary (red) or a positive primary (blue). Each population's Mean Fluorescence Intensity (MFI) has been identified alongside the negative populations' standard deviation (S.D). These values were plugged into the noted formula and enabled the calculation of the stain index (Δ), providing a read-out that could be compared across samples with differences in staining methodology.

2.11.3 Opsonic Index (OI)

The Opsonic Index (OI) is the read-out used in the OPKAs and quantified the level of killing. OI was calculated using the excel-based Opsotiter software (University of Alabama research foundation Birmingham, AL, USA) which transformed the raw data of colony forming units (CFU) and serum dilutions into OI's as well as quality control metrics such as non-specific killing. Read-outs generated by the Opsotiter software are outlined in Figure 2-8.

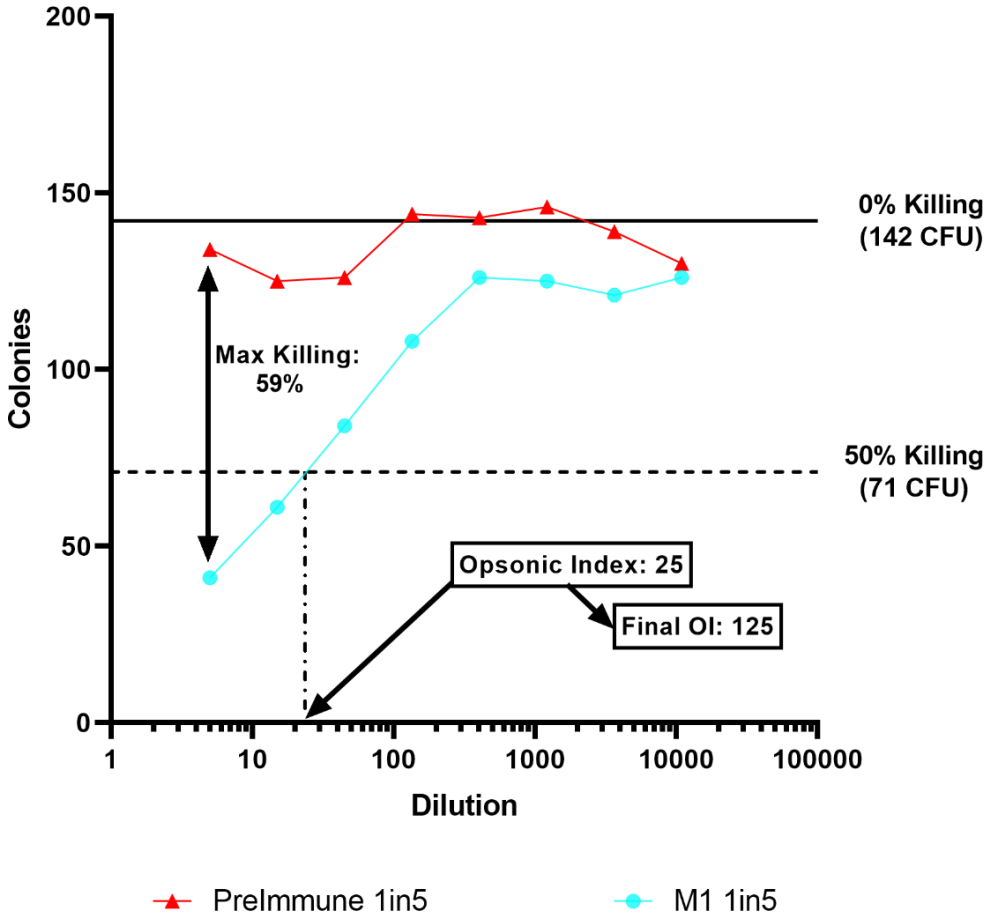

Figure 2-8: Opsonic Index and non-specific killing calculation from an assay graph.

The killing assay results from the negative control of the pre-immune rabbit sera and the αM1 rabbit Sera against SF370 are plotted. The 0% killing threshold was calculated using the active complement control wells, enabling the identification of the colony count at 50% killing. Here the Opsonic index (OI) from the plate was 25. However, the software adapted for the 1:5 initial serum dilution and gave a final OI of 125. The max killing was calculated by taking the lowest colony forming unit (CFU) count from αM1 and the accepted maximum CFU to calculate the percentage difference. In this case, max killing = 1-(58/142)*100= 59%, as is represented in the figure.

3 Results

3.1 Serum characterisation

The overarching aim of this thesis was to test the contribution to opsonophagocytic killing of sera targeting the M protein and/or the T-antigen. To do this, sera targeting M proteins and T-antigens were obtained from rabbits vaccinated with the respective proteins for two representative GAS M-types (section 2.1.1): M1 (expressing M1 and T1) and M6 (expressing M6 and T6). In addition, serum from rabbits was obtained before vaccination occurred producing pre-immune rabbit sera which was used as a control. The sera used in this project are summarised in Table 4.

Characterisation of binding of these rabbit antisera to their homologous antigens as well as any potential cross reactivity between sera in the project was crucial. Antibody binding to the GAS M protein is complex, with multiple domains within each M protein type having varying degrees of conservation with other M-types. Furthermore, some M proteins (particularly M1) are capable of non-specifically binding antibodies via their Fc receptor (section 1.3.1.2). The possible binding profiles are summarised in Figure 3-1**,** using the M1 protein as an example.

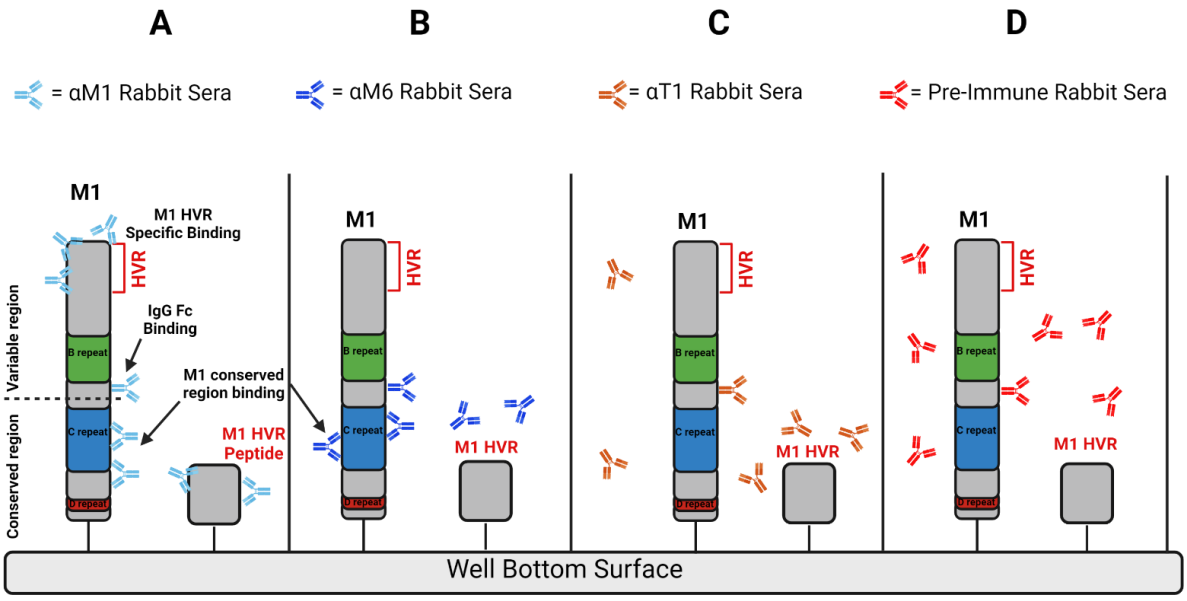

Figure 3-1: M1 protein and HVR serum binding profiles:

This schematic portrays the M1 full-length protein and M1 HVR peptides bound to a plate uniformly. However, during an ELISA, these proteins would be in various orientations as the proteins bind to the wells in various conformations. The different types of protein-antibody binding interactions are modelled using this schematic. (**A**) Anti-M1 sera displays all three types of binding: the HVR region-specific binding, the conserved region-specific binding, and the M1 proteins non-specific binding of IgG via their Fc region. (**B**) The M6 sera, although unable to bind the M1 proteins HVR region, can bind epitopes present in the conserved region of the full-length protein. The M1 protein also displays the capability to bind the M6 antisera's IgG via the Fc region. (**C-D**) Finally, the non-specific binding of the IgG Fc region by full length M1 protein can occur in all sera types, even when no specific binding is present. These binding interactions all contribute to the amount of binding occurring, depending on both the sera type and dilution factor used. This figure was made using BioRender.

3.1.1 Serum dilution optimisation

To determine a consistent dilution range of sera, a set of preliminary ELISAs were run against the respective homologous proteins. Optimum initial dilutions and dilution factors varied between M/T protein and HVR antisera (Table 4), giving a range of absorbance readings (data not shown). Based on these results, the initial dilution was selected to be 1:500, whilst the dilution factor was 3-fold. These parameters enabled ELISAs to be performed for all antigens with the same dilution series; thus, all sera could be run in a single assay and direct comparisons between ELISAs could be made.

Table 4 : Optimal serum dilutions for homologous sera against respective proteins.

	Protein Coated:	Initial Dilution:	Dilution Factor:
Full-Length Proteins:	M1	1:500	2x
	M6	1:500	2x
	T1	1:500	3x
	T6	1:500	3x
HVR Peptides:	M1 HVR	1:100	2x
	M6 HVR	1:100	2x
Final Selection:	**All Proteins**	**1:500**	**3x**

3.1.2 Rabbit antisera characterisation ELISAs

Following ELISA protocol optimisation, binding of all rabbit antisera (Table 4) to each antigen (M1, M6, T1 and T6) was characterised. Briefly, all proteins were coated on plates in individual ELISAs, and binding of their homologous M- and T-antisera, their heterologous protein sera (e.g., M6-antisera against M1 protein) and pre-immune rabbit sera was probed using the optimised dilutions displayed in Table 4. The complete ELISA dilutions are shown (Figure 3-1 Figure 3-4) as well as the respective quantitative AUC calculations in section 2.11.1 (Figure 3-5).

The M1 full-length protein ELISA displayed binding to all four sera with increased binding of M1- and M6-antisera alongside weaker binding of T1-antisera and pre-immune rabbit sera (Figure 3-2**,** A). The observation of binding of pre-immune serum (negative antibody control) at the same level as T1-antisera serum, indicates non-specific binding properties of the M1 protein via the Fc region (Figure 3-1**,** A). To further dissect the ability of the rabbit sera to target different regions of the M1 protein, ELISAs coating only the HVR peptide were also run. The M1 HVR ELISAs showed that only anti-M1 sera bound the M1 HVR peptide (Figure 3-2). Whereas the anti-M6, anti-T1 and pre-immune serum binding was not seen against the M1 HVR region (indicating the HVR region is only targeted by sera specifically generated by the M1 protein) with no cross-reactive epitopes present.

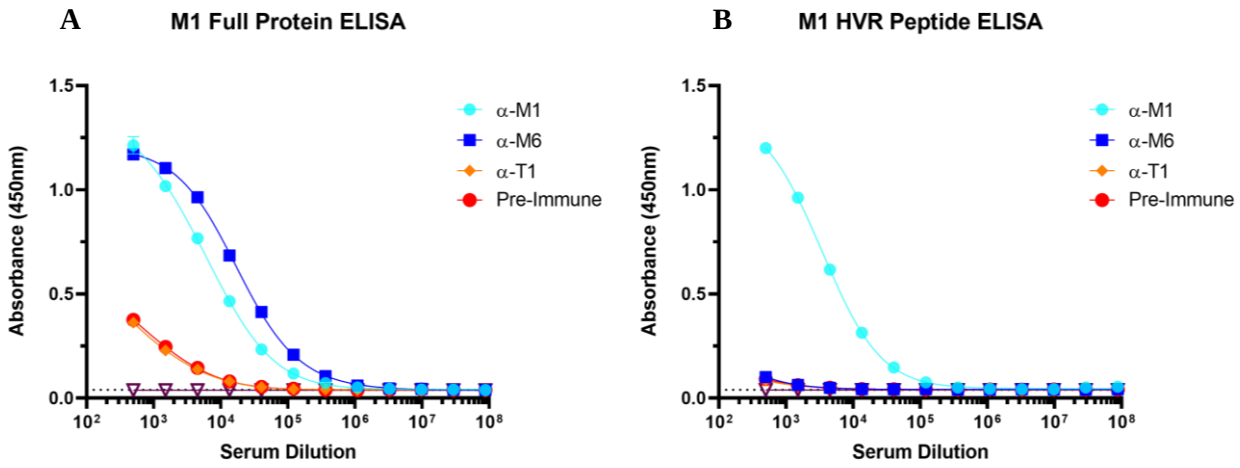

Figure 3-2: M1 full length protein and HVR ELISAs:

Absorbance curves were generated using a plate reader to measure ELISA plates coated with (**A**) M1 full-length protein or (**B**) M1 HVR peptide and incubated with titrated anti-M1, anti-M6, anti-T1 and pre-immune rabbit sera. Anti-rabbit IgG-HRP and TMB substrate were used for detection as they underwent a colour changing reaction from blue to yellow if antibody binding was present (as described in section 2.7). Absorbance values at 450nm were then plotted using GraphPad Prism (V. 8.0.2), with each data point representing the mean absorbance ± standard error of 2 technical replicates. The horizontal dashed line corresponding with the purple triangles indicates background absorbance in absence of serum.

The absorbance curves for the M6 full-length protein showed M6-antisera strongly binding to the full-length M6 protein whilst M1-antisera bound with a slightly weaker absorbance curve (Figure 3-3). The T6-antisera and pre-immune sera displayed no binding to the M6 full-length protein, suggesting that no non-specific binding of IgG occurred against M6. Further investigation into the specificity of these sera's binding capacity used the M6 HVR peptide in an ELISA. The M6-antisera displayed binding activity specifically to the M6 HVR peptide (Figure 3-3, B). However, no binding was seen from the anti-M1, anti-T6 or pre-immune antisera. Therefore, the M6 HVR region was only capable of being targeted by M6 protein specific antisera, whereas full-length M6 protein showed some cross-reactivity with M1 antisera displaying some binding.

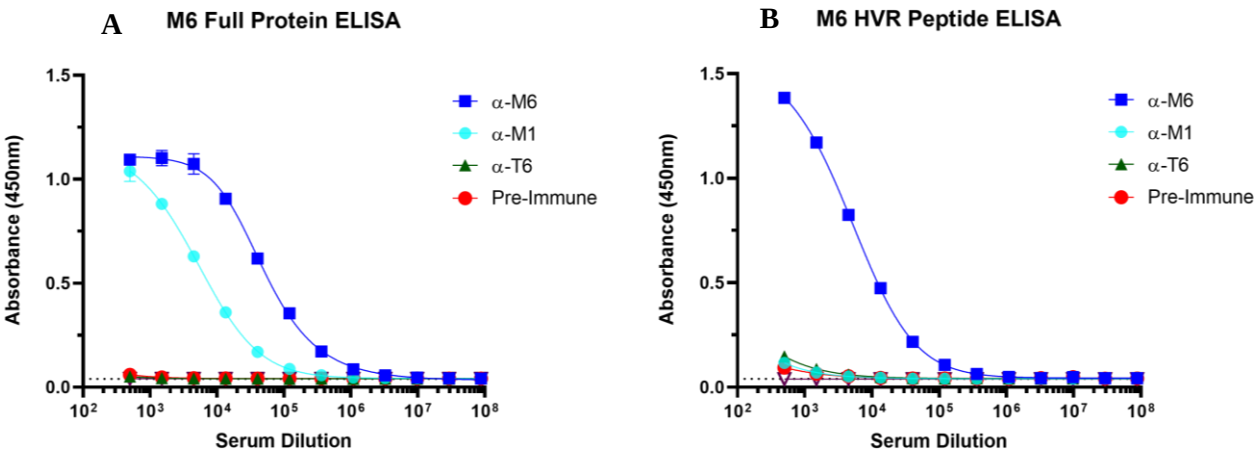

Figure 3-3: M6 full length protein and HVR ELISAs:

These absorbance curves were generated using a Perkin Elmer Ensight plate reader to measure ELISA plates coated with (A) M6 full-length protein or (B) M6 HVR peptide and incubated with titrated anti-M6, anti-M1, anti-T6 and pre-immune rabbit sera. Anti-rabbit IgG-HRP and TMB substrate were used for detection as they underwent a colour changing reaction from blue to yellow if antibody binding was present. Increased colouring was read as increased absorbance at 450nm in the Ensight plate reader, which was then plotted using Prism, with each data point representing the mean absorbance ± standard error of 2 technical replicates. The horizontal dashed line corresponding with the purple triangles indicates background absorbance in absence of serum.

The T-antigen ELISAs characterised the binding of anti-T1, anti-T6, and pre-immune sera to the T1 and T6 full length proteins (Figure 3-4). Alongside these three sera the anti-M1 and anti-M6 sera were ran against T1 and T6 full-length proteins respectively. Therefore, the T-antigens were tested against their specific sera alongside running heterologous anti-T rabbit sera and homologous anti-M protein sera to investigate potential cross-reactivity. Both the T1 and T6 ELISAs only displayed binding against their homologous sera and no other sera showed reactivity against either T-antigen (Figure 3-4).

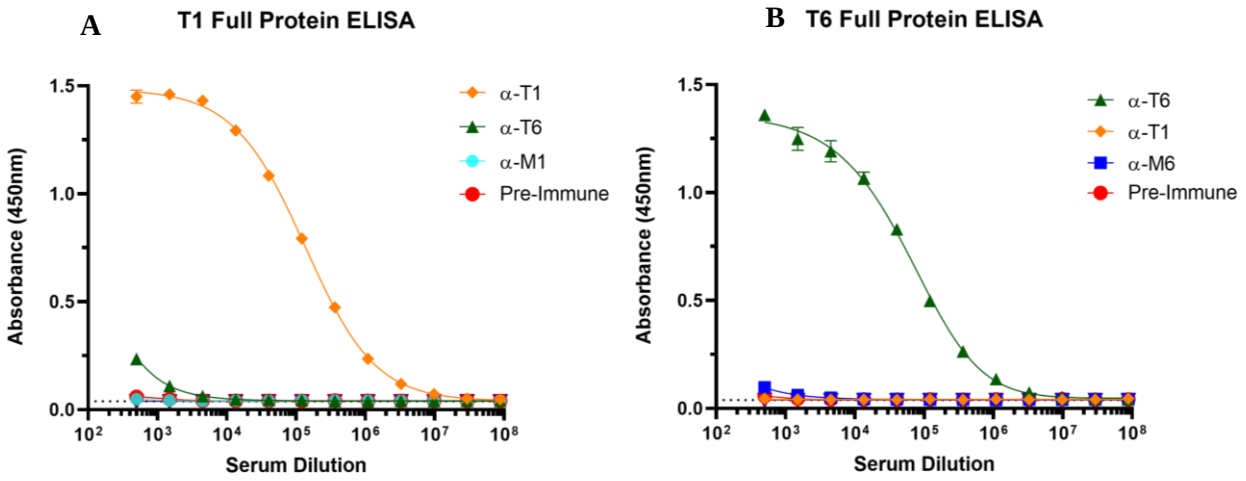

Figure 3-4: T1 and T6 protein ELISA's:

Absorbance curves were generated using a Perkin Elmer Ensight plate reader on ELISA plates coated with the (**A**) T1 and (**B**) T6 full-length proteins. (**A**) The T1 full-length protein was incubated with titrated anti-T1, anti-T6, anti-M1 and pre-immune rabbit sera. (**B**) Whereas the T6 full-length protein was incubated with titrated anti-T6, anti-T1, anti-M6 and pre-immune rabbit sera. Anti-rabbit IgG-HRP and TMB substrate were used for detection as they underwent a colour changing reaction from blue to yellow if antibody binding was present. Increased colouring was read as increased absorbance at 450nm in the Ensight plate reader, which was then plotted using Prism, with each data point representing the mean absorbance ± standard error of 2 technical replicates. The horizontal dashed line corresponding with the purple triangles indicates background absorbance in absence of serum.

Calculating and plotting AUCs as described in Figure 2-6 for each of the ELISA's absorbance curves enabled quantification and a visual comparison of the antibody titres between sera. Binding of all sera (M1-, M6-, T1- and pre-immune antisera) to the full-length M1 protein was observed to varying degrees. However only the M1-antisera bound to the M1 HVR peptide (Figure 3-5, A and B). The M6 full-length protein and HVR ELISA AUCs demonstrated M6- and M1-antisera binding to the full-length protein and only M6-antisera capable of binding the M6 HVR (Figure 3-5, C, D). The anti-T, heterologous anti-M and pre-immune sera were unable to bind the M protein HVRs, with binding only seen by each of the homologous M protein's antisera that possessed specific reactivity to the HVR peptides (Figure 3-5, B, D). Therefore, the binding of anti-T1 and pre-immune sera to the full-length M1 protein is likely due to non-specific Fc region binding (Figure 3-5, A). The M1-antisera AUC against the M1 protein compared with the M1 HVR showed that approximately 50% of the total M1-protein reactivity is directed to the HVR (Figure 3-5, A, C). For the M6-antisera reactivity against the M6 protein, the AUC showed that only

25% of the total M6-protein reactivity was directed to the HVR (Figure 3-5, C-D). However, the AUC's for the overall antibody titres of the M6-antisera is roughly three times greater than the M1-antisera's against their respective homologous full-length proteins (Figure 3-5, A, C). Furthermore, the M6-antisera binding to the M1 full-length protein at a high level (Figure 3-5, A), is likely due to a combination of conserved-region cross-reactivity and the M1-proteins non-specific antibody binding capacity (Figure 3-1, B). Finally, the T1 and T6 protein AUCs showed that only homologous T-antisera could bind the T-antigens, with no cross-reactivity with other serum observed. The AUCs generated from the T1 and T6 ELISAs suggest the anti-T antigen sera is much higher titre than the anti-M protein antisera (Figure 3-5, E-F).

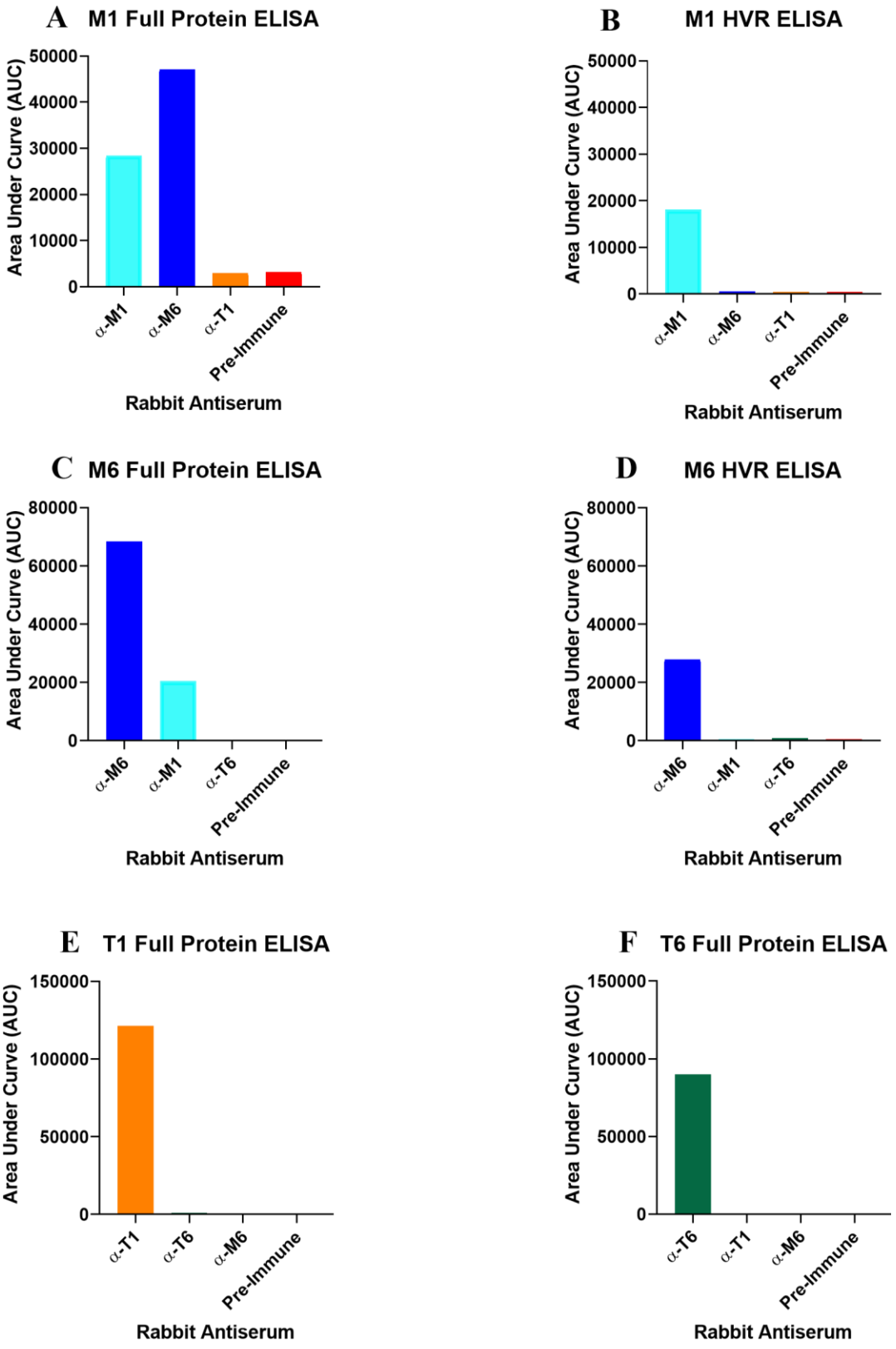

Figure 3-5: Area Under the Curve (AUC) calculations for all ELISAs:

The area under the curves from each ELISA were generated according to section 2.11.1 and plotted using GraphPad Prism (V 8.0.2). The ELISAs were adjusted to only take the first nine dilution points and were base-line corrected, which enabled a more accurate AUC to be determined for each serum titre. Each bar represents the AUC from the corresponding sera in that ELISA, and all bar graphs have standardised axes for easier comparison of the antibody binding levels.

3.1.3 Serum characterisation summary

The rabbit antisera were characterised against the M1, M6, T1 and T6 full-length proteins alongside the M1 and M6 HVR peptides, enabling their binding capabilities to be known for the future experiments. All rabbit antisera bound to their respective antigen targets, alongside some cross reactivity seen between the two full-length M proteins. However, this was lost in ELISAs against the HVR peptide alone and no cross-reactivity was seen between the T-antigens either. Overall, the antibody responses against the T-antigens appeared to possess higher quantities of antibody titres than those against the M protein.

3.2 Flow cytometry

3.2.1 Optimising the protocol for GAS flow cytometry using rabbit antisera

Flow cytometry was used to measure the binding capacity of rabbit antisera to GAS proteins on the bacterial surface, enabling their surface expression levels to be determined for each strain. However, the use of rabbit antisera as the primary antibody required optimisation of the methodology. The fixing method, secondary antibody, and the blocking of non-specific rabbit antisera binding to the M protein (observed in section 2.1.4 required optimisation.

Bacterial fixing was tested using heat and paraformaldehyde which are two methods used in the laboratory to fix the bacteria prior to flow analysis. The M1 strains (M1:SF370 and M1:43) were fixed with both methods and stained with anti-M1, anti-T1 and pre-immune serum as the primary antibodies and histograms of fluorescence were plotted (Figure 3-6). To ensure primary antibodies were binding correctly an M1 knockout M1:SF370 and T1 knockout M1:SF370 strains were also run, these displayed that the sera was binding correctly (results not shown). The heat-killed samples for M1:SF370 and M1:43 generated clear separate positive and negative populations (Figure 3-6 A, C). However, the paraformaldehyde-fixed samples for both strains generated non-distinct populations with

no separation, likely due to the destruction of bacterial cells and protein antigens (Figure 3-6 B, D). Therefore, the optimal fixing method utilised in all future flow cytometry was heat-killing.

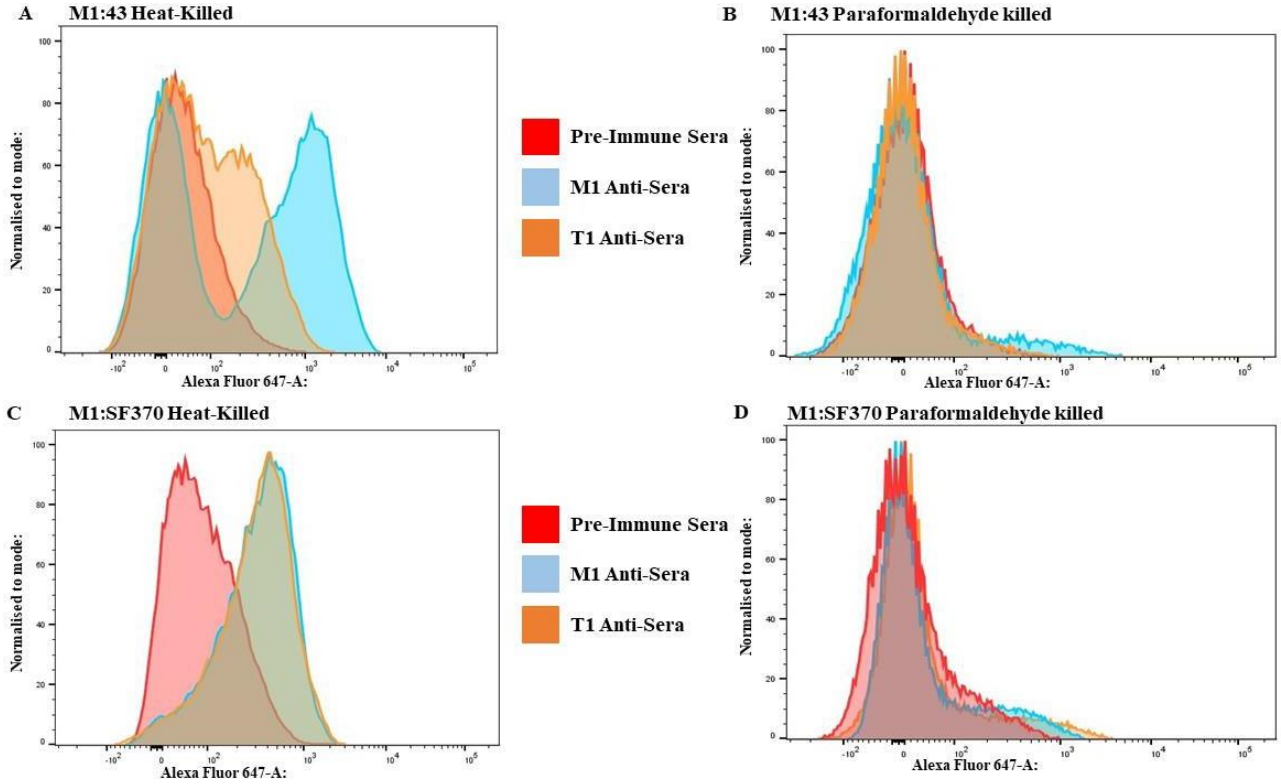

Figure 3-6: Optimisation of bacterial fixing method:

The M1:SF370 and M1:43 strains were run to measure the binding of anti-M1, anti-T1 and pre-immune rabbit sera to heat-killed (80℃ for 5 minutes) and paraformaldehyde-fixed samples. These histograms were plotted using FlowJo analysis software (V 10.8.1) following gating and display the heat-fixed and paraformaldehyde-fixed samples for M1:43 (**A-B**) and M1:SF370 (**C-D**). The histograms display the fluorescence intensity for samples stained with pre-immune (red), anti-M1 (light blue), and anti-T1 (orange) rabbit sera.

In the laboratory, a flow cytometry protocol using polyclonal rabbit antisera had not been optimised and thus, the next optimisation step required for GAS flow cytometry was the identification of a suitable anti-rabbit secondary antibody. Two secondary labels were trialed, FITC and AlexaFluor 647. These secondaries were run against M1:SF370 labelled with anti-M1, anti-T1 and pre-immune antisera at multiple concentrations and from each sample a mean staining index was calculated (Figure 3-7) (section 2.11.2). The samples were controlled against an M1 protein M1:SF370 knockout and a T1-antigen M1:SF370 knockout strain to confirm that primary antibody staining was functioning

properly (results not shown). Comparing the staining indexes between FITC and AlexaFluor 647, the latter produced greater staining signal against the rabbit antisera (Figure 3-7). AlexaFluor 647's optimal staining concentration was determined to be 1:200, meaning future samples were stained with α-rabbit AlexaFluor 647 at a 1:200 concentration.

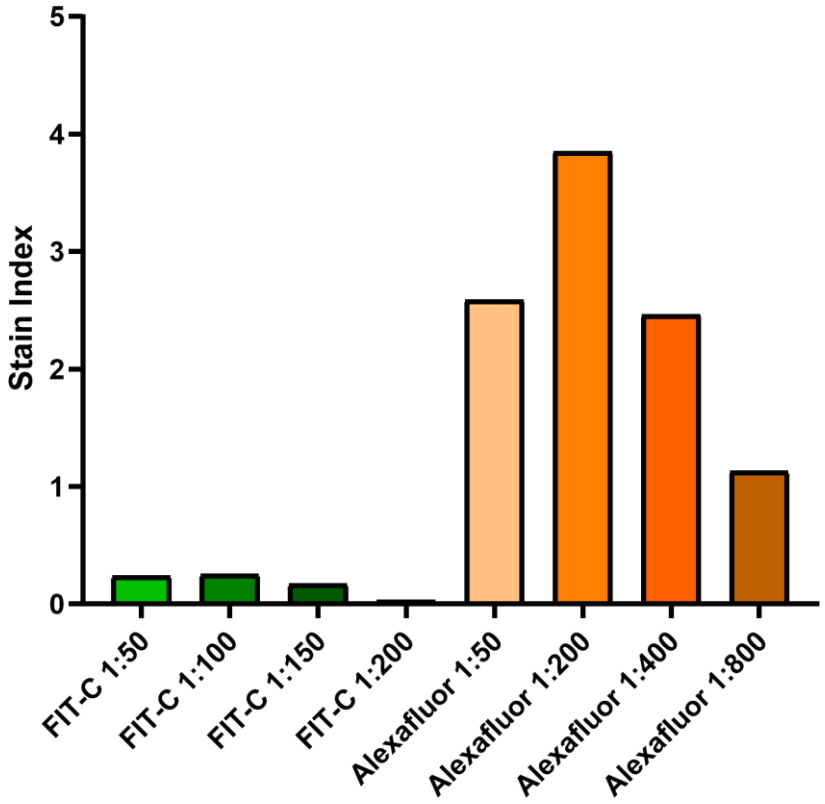

Figure 3-7: Secondary antibody optimisation:

This graph represents the results from the flow cytometry performed on M1:SF370 using pre-immune and anti-M1 rabbit sera with mean fluorescence intensities recorded using FlowJo (V 10.8.1) and then utilised to calculate the staining index (section 2.11.2). Each secondaries' mean staining indexes were plotted as bars using GraphPad Prism (V 8.0.2) for each concentration of the FITC and AlexaFluor 647 anti-rabbit secondaries, enabling comparisons of the potential candidates for use in the optimised flow cytometry protocol.

Previous GAS flow cytometry by Dr Loh used mouse sera as the primary antibody, which through previous experience we know avoids non-specific Fc-binding by the M protein (32). However, the M1 protein was shown to non-specifically bind to rabbit IgG (section 3.1). Therefore, to measure specific protein expression on the surface of GAS, non-specific antibody binding needed to be blocked. Two

blocking solutions were tested at multiple concentrations; a human Fc receptor that was named Generic Rabbit Block (**GRB)** throughout experiments, and the Tru-Stain blocking solution. Two controls were used, the first, a FACs buffer block which controlled any blocking and binding changes occurring as a result of the increased incubation time and sample volume that the primary antibody is added to. The second was a sample that had no blocking solution added to it and thus was a negative control (Figure 3-8). The staining indexes were calculated for each sample identifying the M-specific binding levels while accounting for the non-specific binding of pre-immune rabbit serum. Both blocks increased the staining index compared to the controls, with GRB block producing the highest stain indexes, therefore providing the most effective block for non-specific binding (Figure 3-8). Importantly, the blocking step could prevent the non-specific binding of pre-immune rabbit serum by the M1 protein which was observed in the ELISAs (Figure 3-2). Upon finally selecting the optimal blocking solution, the GRB block produced similar staining indexes at the 1:10 and 1:20 concentrations, therefore, to extend the use of the reagent the 1:20 RB concentration was selected (Figure 3-8).

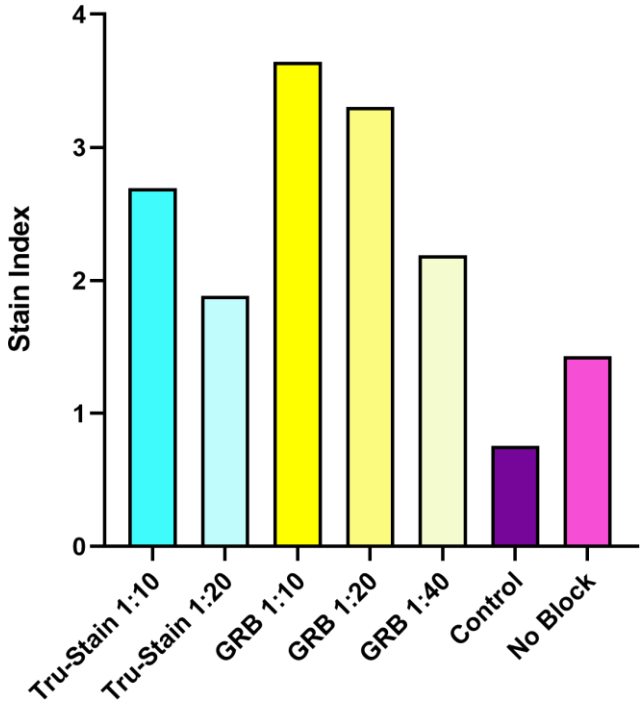

Figure 3-8: Optimising blocking solution against M protein Fc antibody binding:

M1:43 samples were blocked with either Tru-Stain or GRB (Human IgG Fc fragment protein) at varying concentrations and controlled using samples blocked with the FACS flow buffer and the no-block sample had nothing added to the flow samples during the blocking step. These samples were

stained using pre-immune and anti-M1 rabbit sera, with mean fluorescence intensities recorded using FlowJo (V 10.8.1) and then utilised to calculate the staining index (section 2.11.2). Each block's staining index was plotted as a bar using GraphPad Prism and enabled comparisons to be made to determine the most effective blocking solution.

Overall, the optimised flow cytometry protocols were established for the fixing mechanism, blocking solution and anti-rabbit secondary antibody enabling the GAS strains to accurately be run through the flow cytometer. The resulting methodology is displayed below in the schematic outlining the process of selecting the optimised protocol (Figure 3-9).

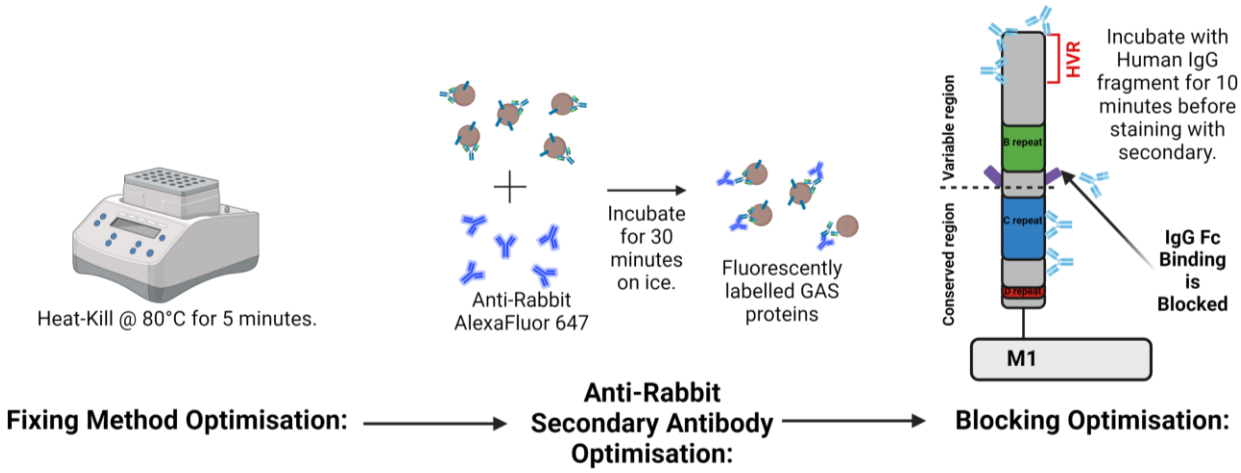

Figure 3-9: Overview of the choices made to optimise the GAS flow cytometry:

The optimised methods chosen for the bacterial fixing, secondary antibody and M1 nonspecific binding blocking are displayed above. These were included into the overall flow cytometry protocol and enabled for reproducible and accurate flow cytometry to be undertaken in the project. To fix the bacteria, a thermo-block at 80°C was used for 5 minutes, killing the bacteria. Furthermore, anti-rabbit Alexafluor 647 at a 1:200 dilution was determined to be the optimal secondary staining antibody for the rabbit sera flow. Finally, to block the non-specific binding of antibodies to the M1 protein the RB block at a 1:20 dilution was identified to maximise the inhibition of unwanted non-specific binding. This figure was made using BioRender.

3.2.2 Measuring the M1 strains protein expression and non-specific antibody binding

The now optimised flow cytometry protocol (Figure 3-9) was used to measure the expression of M and T proteins on two M1 strains, M1:SF370 and M1:43 (Figure 3-10 B, D). An unblocked control was

also included to enable the measurement of non-specific binding (Figure 3-10 A, C). The anti-M1 and anti-T1 MFIs for blocked samples were used to represent M1 and T1 protein expression (Figure 3-11). By internally controlling background staining with the pre-immune sera, the M1 protein to T1 antigen expression levels can be compared across the two strains. To confirm primary antibodies were binding correctly these stains were controlled using an M1 protein M1:SF370 knockout and a T1-antigen M1:SF370 knockout strain (results not shown).

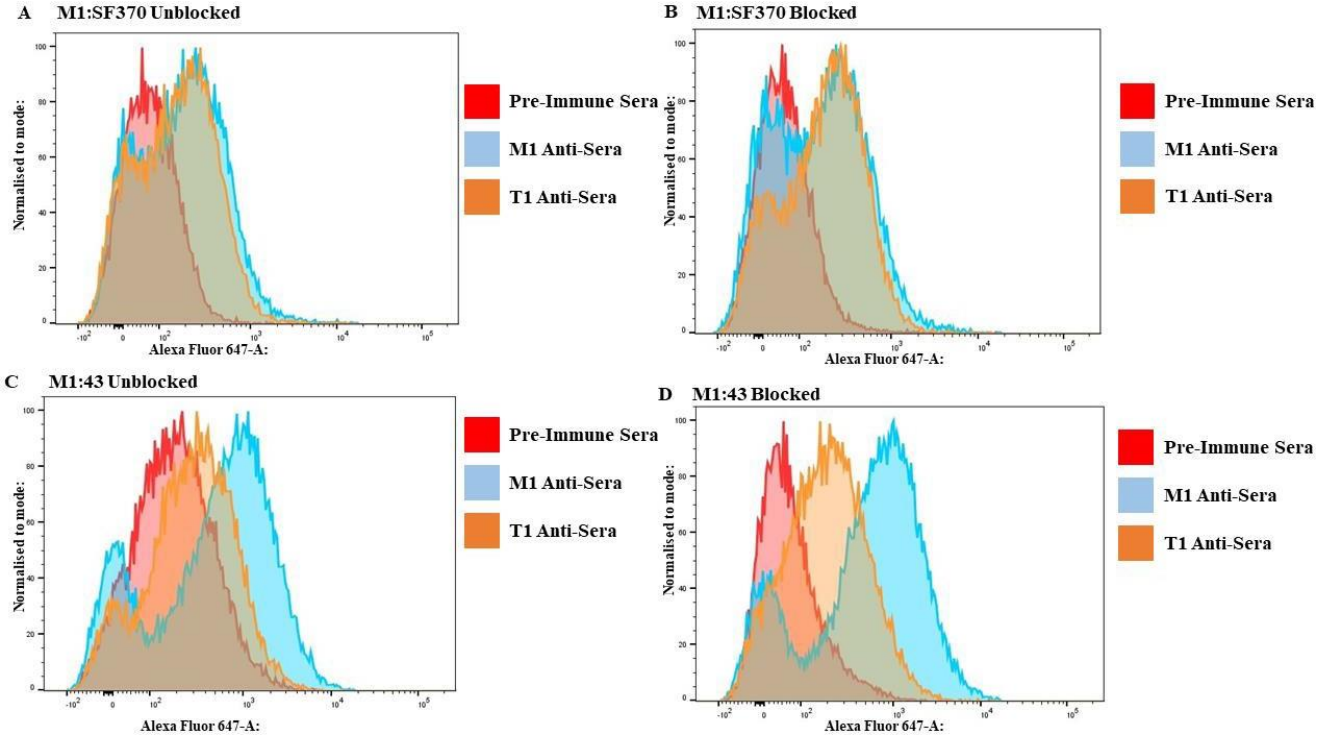

Figure 3-10: M1 strain characterisation histograms:

The M1:SF370 and M1:43 strains were ran once using the optimised flow cytometry protocol to measure the binding of anti-M1, anti-T1 and pre-immune rabbit sera to blocked and unblocked samples. These histograms were plotted using FlowJo analysis software (V 10.8.1) following gating and display the blocked and unblocked samples for M1:SF370 (**A-B**) and M1:43 (**C-D**). The histograms display the fluorescence intensity for samples stained with pre-immune (red), anti-M1 (light blue), and anti-T1 (orange) rabbit sera.

The M1 expression profiles differed between M1:SF370 and M1:43 strains, with M1:43 expressing three times higher levels of the M1 protein (Figure 3-11). The T1 expression profiles for both strains were similar. SF370 expressed the M1 protein and T1 antigen at equal levels as illustrated in the

histograms, although a proportion of SF370 cells appear to not express M1 or T1 (Figure 3-10 B and Figure 3-11). M1:43 differed by expressing three times greater M1 protein than T1 antigen in the blocked stained samples (Figure 3-11). Next, non-specific serum binding was investigated by comparing the staining populations of pre-immune in blocked and un-blocked samples (Figure 3-10). The pre-immune stained populations varied between the blocked and un-blocked samples with clear negative shifts produced upon blocking (Figure 3-10). Plotting the pre-immune MFIs for both strains demonstrated a minor increase in M1:SF370 when unblocked, whereas M1:43 generated a major MFI increase in the unblocked sample (Figure 3-12). The large proportion of non-specific binding by the pre-immune sera on the M1:43 strain likely reflects its higher M1-protein expression. As these assays were only completed once, repeating these experiments would enable the confirmation of the binding profiles displayed in these results.

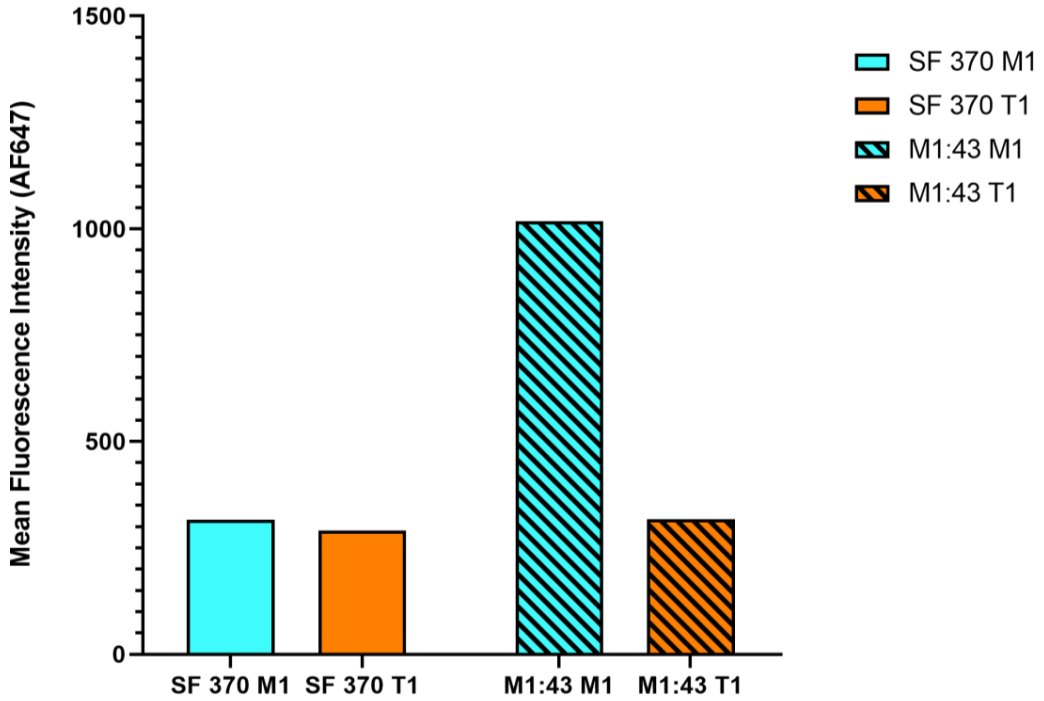

Figure 3-11: The M1 and T1 protein expression levels for the M1:SF370 and M1:43 strains:

The histograms for the blocked M1:SF370 and M1:43 samples were analysed using FlowJo (V 10.8.1) and graphed using GraphPad Prism (V 8.0.2), with each bar representing the mean fluorescence intensity (MFI) for either the M1 protein (light blue) or T1 antigen (orange). The MFI was used to directly represent the level of expression for either M1 or T1 on each strain. Therefore, M1:43 expressed much higher levels of M1 protein than SF370, whereas the T1 expression profiles were similar between the two strains.

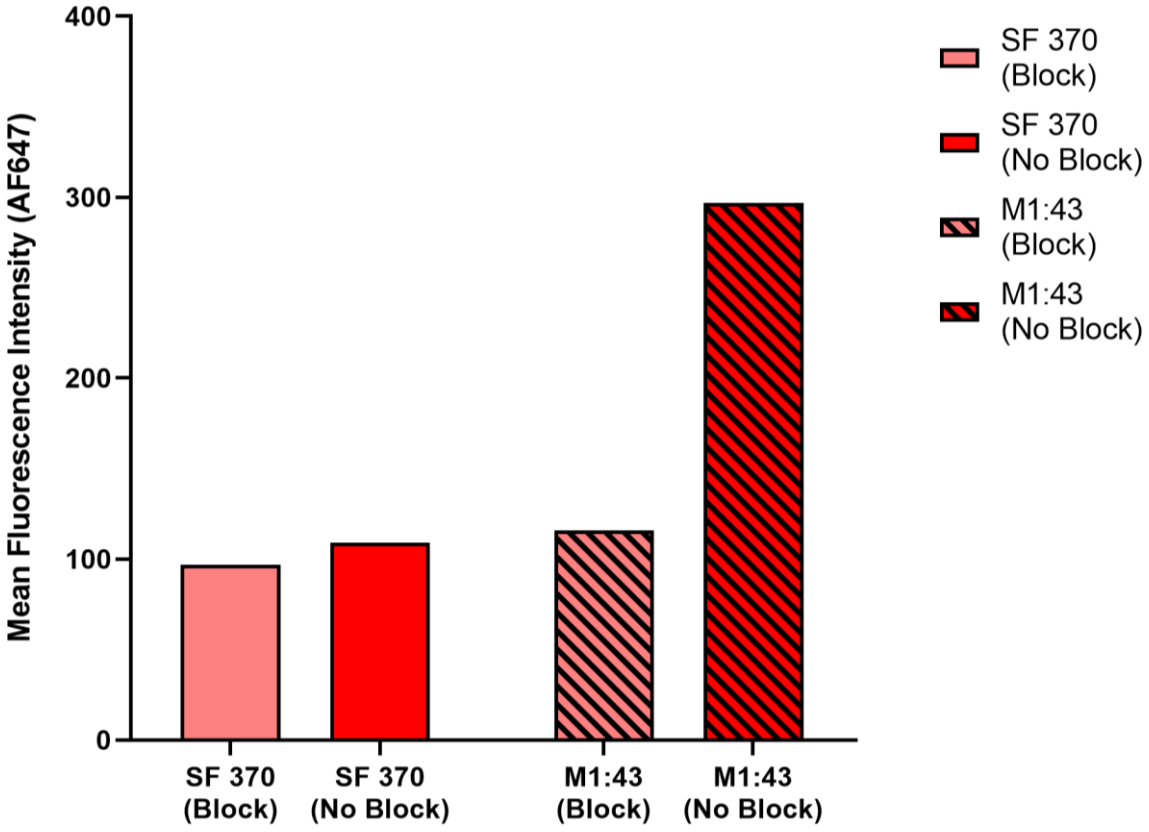

Figure 3-12: M1 strains mean fluorescent intensity when treated with pre-immune rabbit sera when blocked and unblocked.

The two M1 strains M1:SF370 and M1:43 were measured using pre-immune rabbit sera against blocked and un-blocked bacterial samples and the mean fluorescence intensities were analysed using FlowJo (V 10.8.1). The MFIs were plotted using GraphPad Prism (V 8.0.2) and the difference between blocked and unblocked samples represented the amount of non-specific binding occurring between the M1 protein and pre-immune antisera. Both strains when unblocked displayed increases in the MFI of pre-immune sera-stained samples. This increase was more prevalent in the M1:43 strain which increased to a greater extent than SF370.

3.2.3 M6 Strain selection and characterisation

The M6:2 strain selected for this project had previously been well characterised in opsonophagocytic killing assays (OPKAs) in the laboratory (51). However, a second comparative M6 strain required selection from those available in our stocks: M6:1070, M6:08308 and M6:09209. Flow cytometry using pre-immune, anti-M6 and anti-T6 sera on blocked samples enabled the measurement of each strain's M6 and T6 expression (Figure 3-13). The expression levels for each strain were internally controlled for background fluorescence by the pre-immune staining population. Therefore,

comparisons could be made between the strains' MFIs to identify the second M6 strain for study (Figure 3-14).

All four strains consistently expressed the M6 protein, with M6:1070 expressing the highest levels of M6 (Figure 3-14). The M6:2 and M6:1070 histograms generated single staining populations for anti-M6 sera staining. Whilst the M6:08308 and M6:09209 strains saw the anti-M6 stained population generating two peaks, one positive and one negative for M6 expression (Figure 3-13). This could be the results of technical issues in which anti-M6 failed to completely stain the samples, although this seems unlikely as the M6:2 and M6:1070 strains stained correctly. Another possibility is differences in the regulation of protein expression. Furthermore, when stained with anti-T6 sera all four strains showed low expression of the T6 antigen, especially in comparison to the pre-immune background MFIs (Figure 3-14). In comparison to T1 expression in SF370 and M1:43, all M6 strains expressed T6 at much lower levels on average (Figure 3-11 and Figure 3-15). Overall, the four M6 strains had poor T6 expression levels and displayed no discernible differences between strains. Therefore, due to the differential M6 expression by M6:1070, this strain was selected to investigate the functional impact on increased M protein expression. The chosen M6:2 and M6:1070 strains were subsequently stained with pre-immune sera against blocked and un-blocked samples. This confirmed a lack of non-specific antibody binding by the M6 protein, as observed in ELISAs (Figure 3-3 and Figure 3-15).

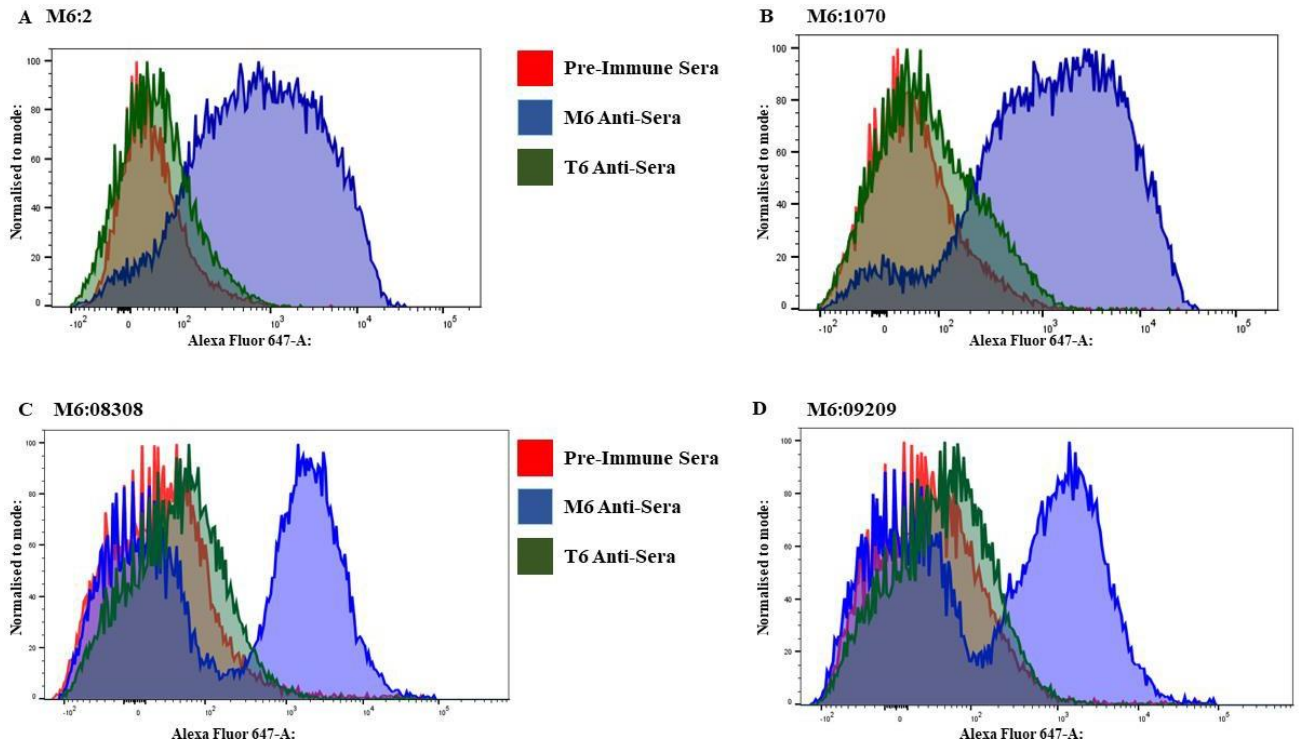

Figure 3-13: Histograms from the flow cytometry screening the M6 strains.

The histograms for the M6:2 (**A**), M6:1070 (**B**), M6:09209 (**C**) and M6:08308 (**D**) were generated using FlowJo (V 10.8.1). These display the expression profiles of the M6 protein and T6 antigen for each strain with the pre-immune sera as a negative control of background binding and fluorescence from a single assay each. All four strains display similar expression profiles, with limited T6 antigen expression seen and the M6 protein expression also remaining consistent. The M6 protein staining was much cleaner in the M6:2 and M6:1070 strains (**A-B**) as one prominent peak was seen as opposed to the double peaks generated in the M6:08308 and M6:09209 strains' histograms (**C-D**).

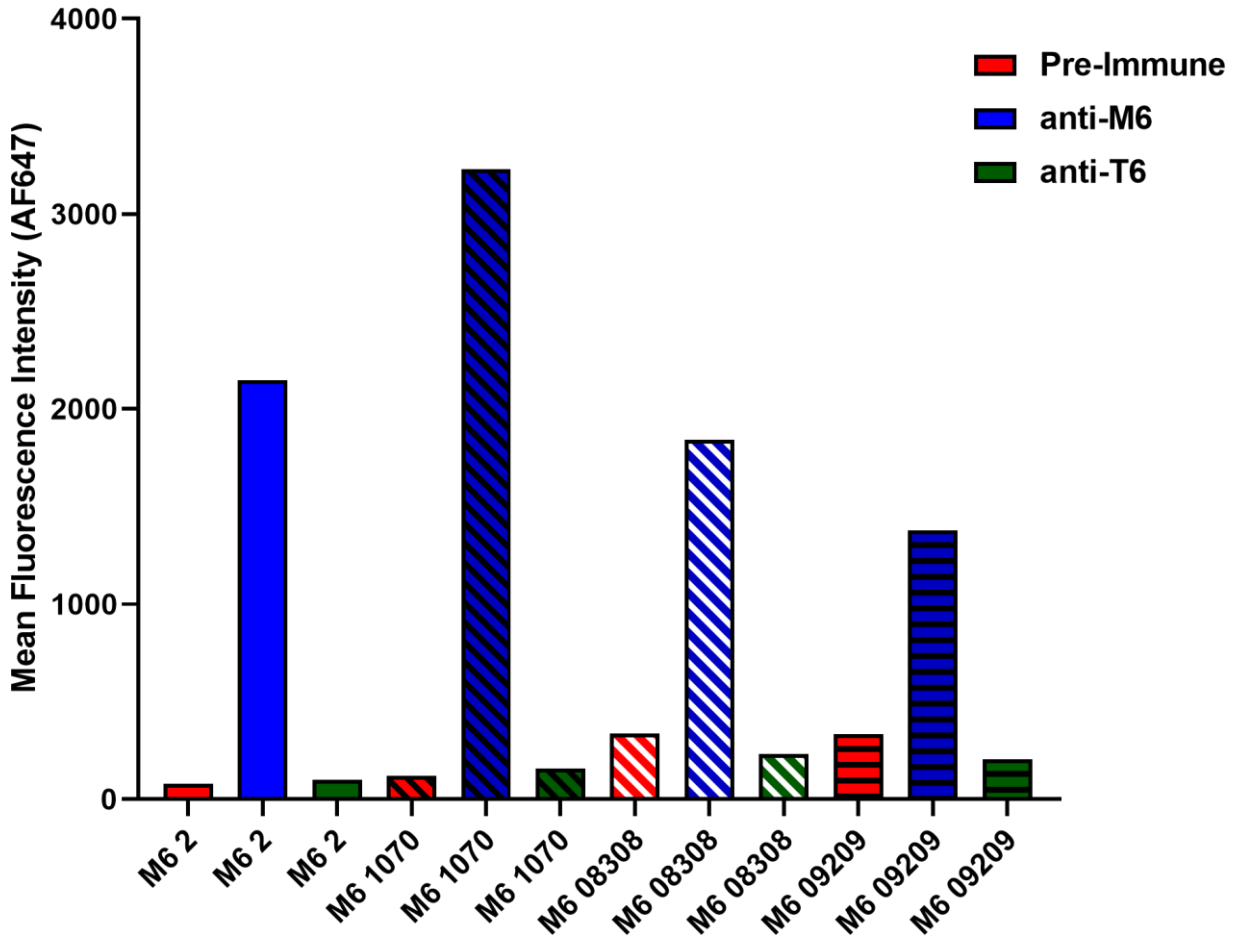

Figure 3-14: Screening the protein expression profiles for available M6 strains.

The M6:2, M6:1070, M6:08308 and M6:09209 strains were screened using the optimised flow methodology to measure the MFIs for the pre-immune, M6 and T6 antisera binding as a representation of their protein expression. Each bar is the mean fluorescence intensity for each serum bound to the bacteria, with the background MFI controlled using the pre-immune sera's binding. With anti-M6 (dark blue), anti-T6 (green) and pre-immune sera (red), and each strain's bars demarcated differently. Therefore, by comparing the M6 and T6 MFI levels to the strain's background the M6 and T6 expression level can be discerned. M6:2 and M6:1070 displayed positive T6 expression with slightly higher than background MFIs recorded for anti-T6 sera, whilst the M6:08308 and M6:09209 both generated T6 MFIs lower than the pre-immune serum background MFI. All four strains displayed high levels of M6 expression, with M6:1070 possessing the highest expression levels and the most different to the M6:2 strain.

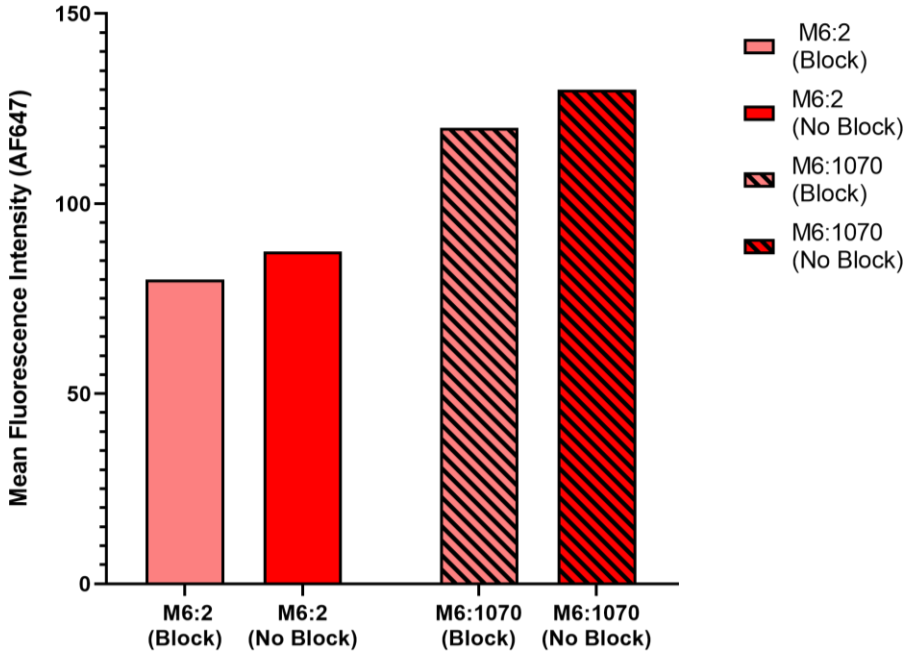

Figure 3-15: Pre-immune serum binding on the M6 strains.

The chosen M6 strains M6:2 and M6:1070 were ran blocked and unblocked against pre-immune rabbit sera to confirm that no non-specific binding was occurring between the M6 protein and IgG like that seen in the M1 protein. Each bar is the mean fluorescence intensity from the histograms generated using FlowJo (V 10.8.1) and enabled comparisons between each strains blocked and unblocked samples. The difference between the blocked and unblocked pre-immune sera MFIs for each strain is representative of non-specific binding, and the two M6 strains displayed no clear difference between the blocked and unblocked samples' MFIs. Hence, no non-specific binding was occurring between the M6 protein and rabbit antisera.

3.2.4 Growth stage impact on M6 and T6 expression

The original aim was to investigate the functional impact of M6 and T6 expression levels on immune targeting and immune evasion, in particular the ratio of M6 protein expression against T6 antigen expression. Unfortunately, unlike the two M1 strains chosen with varying M protein and T-antigen expression levels, both the M6 strains were phenotypically similar and had low T6 expression. Therefore, the impact of the different growth stages on protein expression was investigated to generate an M6 strain with increased T6 expression or a lower M6 to T6 expression ratio. Previous studies suggested a range of mechanisms that could alter GAS surface protein expression, with one potential mechanism being growth stage. Therefore, the impact of the growth curve and different growth stages on protein expression was investigated. The M6:2 and M6:1070

strains were grown with sampling from each stage of the growth curve (Figure 3-16) prior to antibody labelling for flow cytometry analysis. Background fluorescence levels were internally controlled between the samples by staining with pre-immune sera alongside the anti-M6 and anti-T6 sera (Figure 3-17). T-antigen expression remained consistent in both strains throughout all four growth stage samples (Figure 3-17). However, the lower MFI values compared to the pre-immune sera raise concerns about the staining of T6 in these experiments. This might suggest that neither strain expressed any T-antigen in this experiment or that the anti-T6 staining of T6 antigens failed for an unknown reason. Regardless, the M6 protein expression was constant throughout the experiment, except for the highest optical density (OD) samples taken from the overnight cultures which demonstrated elevated M protein expression (Figure 3-17). This death phase result could be due to a change in regulation under the stress of bacterial death in the micro-environment. Overall, for the M6 strains (2 and 1070), there was no clear variation in protein expression observed when measured at different growth stages, thus it was decided to proceed to OPKA using standard log-phase bacteria.

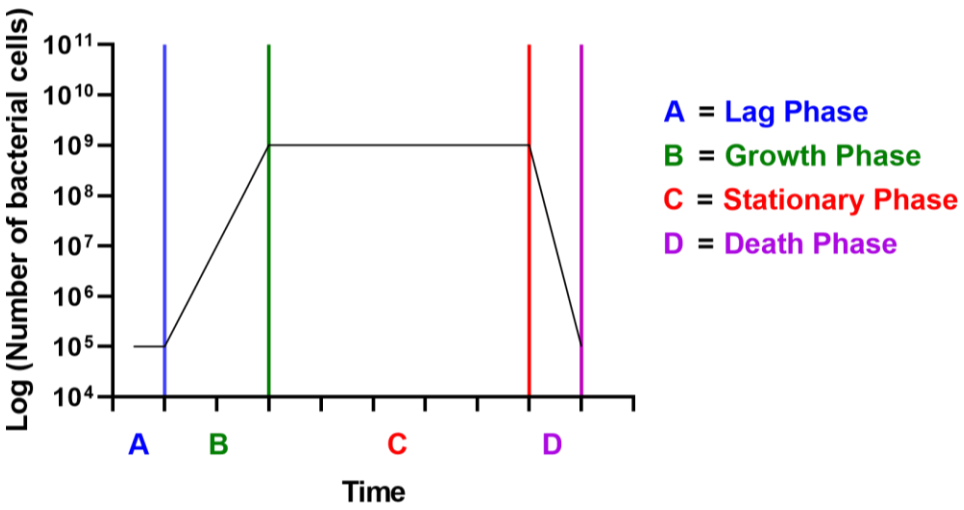

Figure 3-16: Bacterial Growth Curve:

This demonstrates the known progression of bacterial growth by displaying the Log number of cells present in the liquid culture media over incubation time. Each growth phase is attributed to a specific optical density (OD.) range and that enables for bacterial growth to be measured. (A) The lag phase is attributed to 0.0-0.2 OD, (B) the growth phase is attributed to be between 0.2–0.5 OD, the stationary phase is between 0.5–0.7 OD, and (D) the death phase of greater than 0.7 OD.

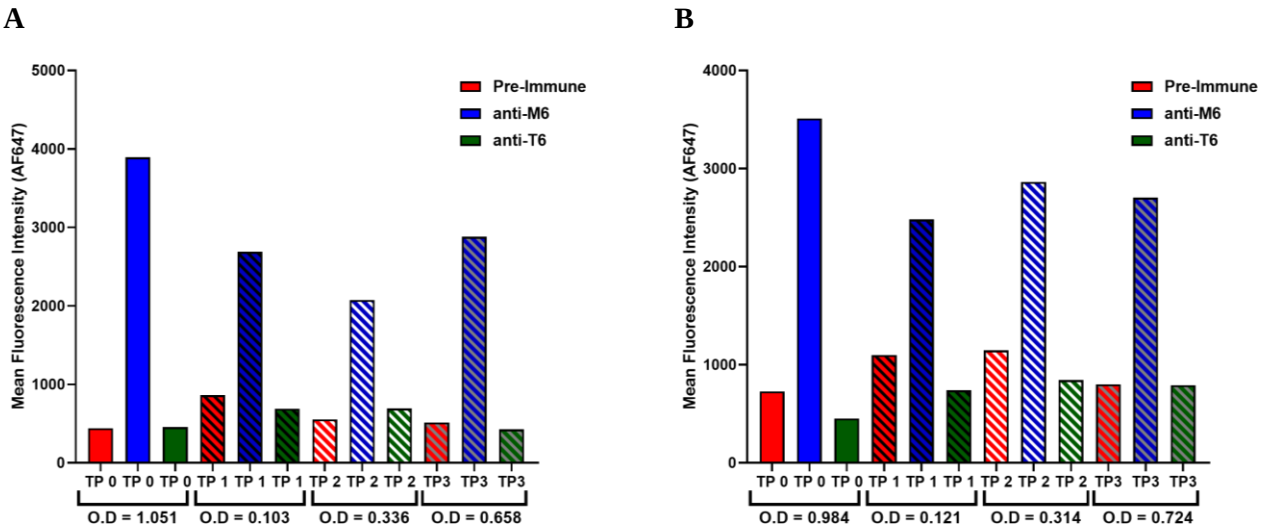

Figure 3-17: M6:2 (A) and M6:1070 (B) protein expression profiles expressed by MFI across the four growth stages.

After growing each strain to multiple optical densities (OD) the optimised flow cytometry protocol was used to measure staining of the anti-M6 and anti-T6 sera (section 2.9.6). The MFIs for the M6 and T6 sera binding were measured alongside the pre-immune serum readings which provided a background measurement for each time point and acted as an internal control for the samples. The graphs portray each strains expression profiles at the various time points by representing each MFI as a bar. Both strains demonstrated that varying the growth stage had no impact on the T-antigen expression levels and only small changes in the M protein expression level except when grown to an OD of 1.051 or 0.984 which was generated by measuring directly from an overnight culture (**A, B**).

3.2.5 Flow cytometry summary

The flow cytometry protocol was optimised for GAS by identifying heat-killing as the optimal fixing method. Whilst the anti-rabbit Alexafluor 647 and human IgG Fc fragment (GRB) were chosen as the optimal secondary antibody and blocking solution respectively. Subsequently protein expression on the M1 strains M1:SF370 and M1:43 was measured. Equal levels of T-antigen expression were seen, whilst the M1:43 strain expressed twice the M1 protein as M1:SF370. All M1 strains displayed non-specific binding, seemingly correlating with the M1 proteins expression level. Furthermore, the M6 strains M6:2, M61070, M6:08308 and M6:09209 all were measured for M6 and T6 expression, with low levels of T6 expression seen on all four strains. The M6 expression profiles varied between strains,

with M6:1070 possessing the highest levels with M6:2 next. With no M6 proteins displaying non-specific binding.

3.3 Opsonophagocytic Killing Assays (OPKA)

3.3.1 Optimum dilution assays

The opsonophagocytic killing assays (OPKAs) aim to provide a functional correlate for antibody mediated immune protection against GAS by measuring the opsonisation and antibody-dependent phagocytosis induced by each serum. To fulfil these immune interactions, baby rabbit complement is required as part of the opsonisation process (section 2.10.2). As complement can also non-specifically kill some bacteria, complement dilutions are standardised between experiments to provide enough complement for the phagocytic process whilst minimising non-specific complement-mediated killing (Figure 3-18). Optimal dilution assays are completed before the killing assays to identify the required complement concentration per strain. This needs to be completed for each batch of assay stock as they will be grown to slightly different OD (although all within log phase of growth) each time (Figure 3-18). By optimising and controlling these variables in the killing assays the impact of the sera can be more accurately determined. The optimised dilutions calculated with stocks used in this project are similar for the three clinical strains, whilst the laboratory adapted M1:SF370 required higher dilutions for both complement and bacteria (Table 3). The increased dilutions required for M1:SF370 is likely due to this being a laboratory adapted strain and thus, less virulent.

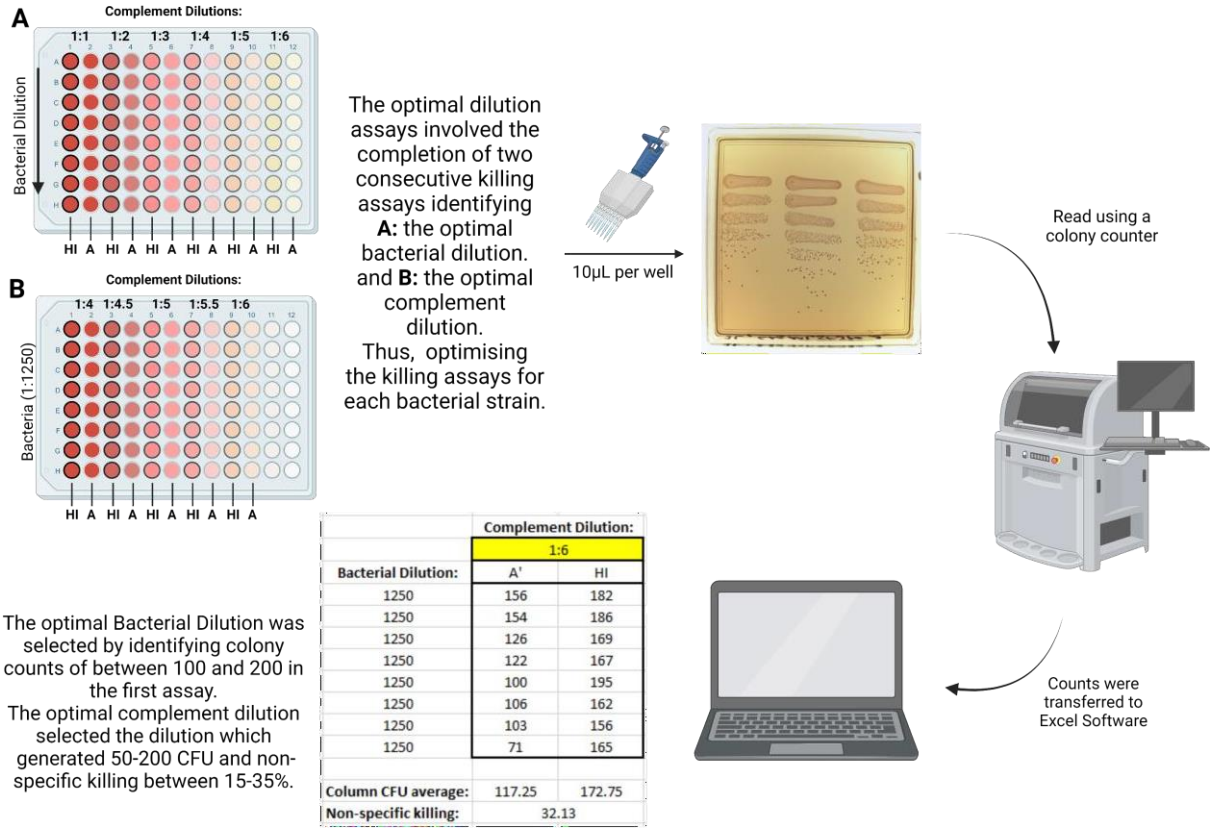

Figure 3-18: Overview of the optimum dilution assays.

Each strain of bacteria is optimised to determine the bacterial and complement dilutions that would generate the most accurate data in the killing assays. At each complement concentration both heat-inactivated (HI) and active (A) complement were compared (**A**) (**B**). After completing each assay and recording Colony Forming Units (CFU) counts using the Synbiosis protocol3 counter, an excel software formatted the assays. This enabled the analysis of each dilution to determine if the criteria set upon the development of these assays was met. The bacterial dilution required a CFU of between 100 and 200 and the complement dilution needed a CFU of between 50 and 200. Furthermore, the non-specific killing (NSK) was calculated from the colony counts of the active and heat-inactivated complement-only wells and for a reliable assay was required to be between 15 and 35%. This figure was made using BioRender.

Table 5: Optimal dilutions identified for each strain.

	Strain:	**Bacterial Dilution:**	**Complement Dilution:**
M1:	SF370	1:1500	1:6
	43	1:500	1:2.5
M6:	2	1:500	1:2
	1070	1:400	1:2.5

Each strains' optimal dilution results were collated to provide insight into any major variations between each strains requirements for the killing assays to work.

3.3.2 Opsonophagocytic killing assays

All strains were tested in the optimised OPKA using anti-M1, anti-M6, anti-T1, anti-T6 and pre-immune sera, along with a mix of the homologous M and T antisera (section 2.10.3). All assays generated a killing curve which provides trends of killing and enables the calculation of the total killing and opsonic indexes (OI).

3.3.3 M1:SF370 OPKAs

M1:SF370 is a laboratory adapted M1 strain and is well established in these protocols with many cases of previous use in OPKA experiments (51, 65). A representative killing curve shows increase colonies (reduced killing) along the titration curve for the anti-M1, anti-T1 and mixed anti-M1/anti-T1 serum (Figure 3-19 A). A lack of killing is evident for the anti-M6, anti-T6 and pre-immune sera which saw stable CFU numbers across the titration curve. The anti-M1/anti-T1 serum mix's killing curve overlaps that of the anti-T1's, suggesting that the addition of anti-M1 sera did not improve the killing by anti-T1. If synergistic killing was present between the two sera, upon addition of the anti-M1 sera the mixed sera would kill at higher dilutions and generate a higher opsonic index than the anti-T1 sera alone. Using the killing curves from three replicate assays, each sera's opsonic indexes were generated, plotted, and statistically analysed using a one-way ANOVA (Figure 3-19 B). The killing capacity of the anti-M1, anti-T1 and anti-M1/anti-T1 mixed sera were all significantly greater than the baseline readouts seen from anti-M6, anti-T6 and pre-immune sera ($p<0.001$) (Figure 3-19 B). Killing by the anti-T1 sera was demonstrated to be the most potent, with an average opsonic index of 4557 being the highest and significantly higher than the anti-M1 ($p<0.05$). The addition of anti-M1 sera to the anti-T1 sera was shown to not significantly impact the killing capacity. Finally, although the M1:SF370 killing appeared primarily to be by the anti-T1 sera, the anti-M1 sera was also capable of killing but had an opsonic index 12 times lower than the anti-T1 (Figure 3-19 B).

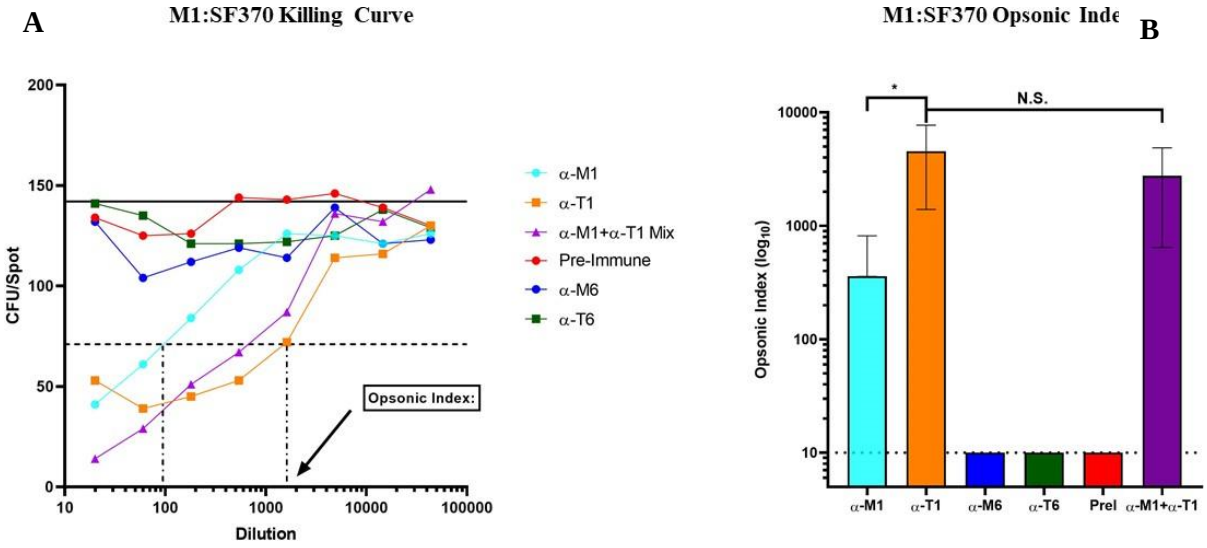

Figure 3-19: M1 SF370 representative OPKA and opsonic indexes.

The M1:SF370 OPKAs were run as biological triplicates of three independent assays, but a singular killing assay was chosen as a representative graph for the antisera's (α-) killing capabilities and trends (**A**). Only the anti-M1, anti- T1 sera and anti-M1/anti-T1 mixed sera killed the M1:SF370, generating opsonic index (OI) read-outs that provide a quantitative measure of bacterial killing. Each sera's opsonic index was averaged over the three replicate assays and displayed as a bar on the right with the standard deviation denoted by error bars, enabling each serum's killing capacity to be compared (**B**). Statistical analyses were performed using a one-way ANOVA on the OI values. Which displayed a significant difference in killing between the anti-T1 sera compared to anti-M1 ($p<0.05$), whereas the anti-M1/anti-T1 serum mix was not significantly different to the anti-T1 sera alone.

3.3.4 M1:43 OPKAs

The anti-M1 and anti-M1/anti-T1 mixed sera generated curves that demonstrated killing along the titration curves against M1:43 at similar dilutions (Figure 3-20 A). All other sera tested were unable to cause any killing against M1:43. The overlap in killing curves between anti-M1/anti-T1 mixed sera and anti-M1 suggests that the addition of anti-T1 sera did not improve killing by the anti-M1 sera. Using the killing curves from three assays, each sera's opsonic indexes were generated, plotted, and statistically analysed (Figure 3-20 B). The anti-M1 and anti-M1/anti-T1 mixed sera showed significant killing compared to the other sera ($p<0.0001$). However, no significant difference between anti-M1 and anti-M1/anti-T1 mixed sera killing was displayed in the Opsonic Indexes (OI), confirming that anti-T1 sera addition does not improve killing. This was expected as anti-T1 sera alone displayed no ability to kill the M1:43 bacteria unlike the M1:SF370 OPKA results, where anti-T1 sera

generated killing (Figure 3-19 B). Both strains possess similar levels of T1 antigen expression, therefore, it is likely that the M1:43 strains' increased level of M1 protein expression is influencing the anti-T1 sera's ability to kill. Therefore, M1:43 killing was only driven by the anti-M1 sera, and OIs were greater than those seen against M1:SF370.

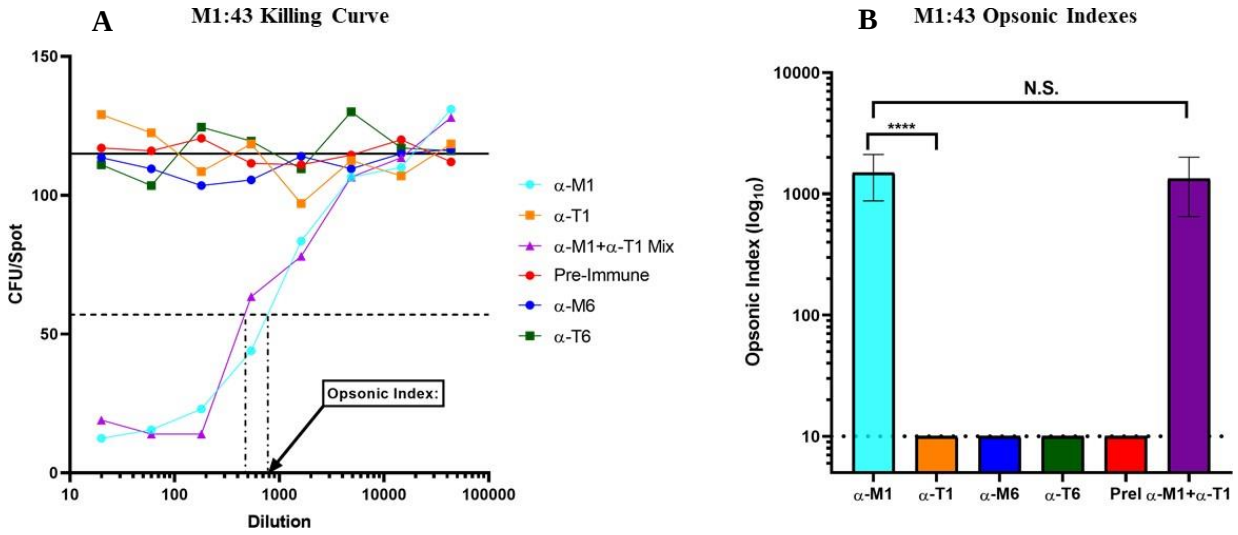

Figure 3-20: M1 43 representative killing assay and opsonic indexes:

The M1:43 OPKAs were run as biological triplicates of three independent assays, but a singular killing assay was chosen as a representative graph for the antisera's (α-) killing capabilities and trends (**A**). Only the anti-M1 and anti-M1/anti-T1 mixed sera killed the M1:43, generating opsonic index (OI) read-outs that provide a quantitative measure of bacterial killing. Each sera's opsonic index was averaged over the three replicate assays and displayed as a bar on the right with the standard deviation denoted by error bars, enabling each serum's killing capacity to be compared (**B**). Statistical analyses were performed using a one-way ANOVA on the OI values. Which displayed significant killing by the anti-M1 and anti- M1/anti-T1 mixed sera when compared to the remaining serum tested which all gave baseline OI readings (**B**).

3.3.5 M6:2 OPKAs

The M6:2 strain killing curves trends follows similar trends to that of the M1:43; only the homologous M sera and the mixed sera caused killing along the titration curve (Figure 3-21 A). The anti-T6, anti-M1, anti-T1 and pre-immune sera all showed no killing capabilities against the M6:2 bacteria. The anti-M6 and anti-M6/anti-T6 mixed sera generated similar killing curves, likely demonstrating that

adding anti-T6 sera did not improve the killing by the anti-M6 sera. Especially as anti-T6 alone demonstrated no ability to kill M6:2. The killing curves from three triplicate assays enabled the calculation of each sera's opsonic indexes which were plotted and statistically analysed (Figure 3-21 B). The OIs for the anti-M6 and anti-M6/anti-T6 mix displayed significant killing of the M6:2 bacteria compared to the negative controls ($p<0.0001$). The OIs reinforced the lack of improvement in killing seen when anti-T6 was added to anti-M6 with no significant difference between the anti-M6 and mixed sera. Against the M6:2 strain, it appeared that only the anti-M6 could kill the bacteria and no anti-T6 serum or cross-reactive activity was seen.

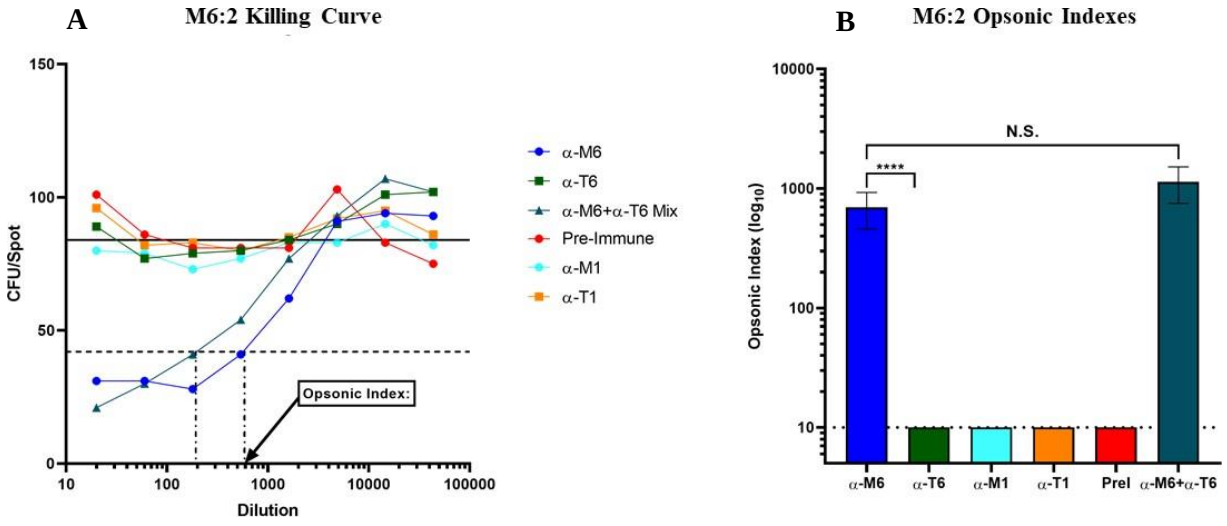

Figure 3-21: M6 2 representative OPKA and opsonic indexes:

The M6:2 OPKAs were run as biological triplicates of three independent assays, but a singular killing assay was chosen as a representative graph for the antisera's (α-) killing capabilities and trends (**A**). Only the anti-M6 and anti-M6/anti-T6 mixed sera killed the M6:2, generating opsonic index (OI) read-outs that provide a quantitative measure of bacterial killing. Each sera's opsonic index was averaged over the three replicate assays and displayed as a bar on the right with the standard deviation denoted by error bars, enabling each serum's killing capacity to be compared (**B**). Statistical analyses were performed using a one-way ANOVA on the OI values. Significant differences were seen between the anti-M6 sera and the anti-M6/anti-T6 mixed sera compared to all other sera tested ($p<0.0001$). However, no significance was seen between the anti-M6 and mixed sera. (**B**).

3.3.6 M6:1070 OPKAs

M6:1070 generated similar killing curves to M6:2 with only anti-M6 and the mix αM6/anti-T6 sera causing killing (Figure 3-21 A and Figure 3-22 A). However, in comparison with M6:2 killing curves, the M6:1070 appeared to be killed by the anti-M6 and αM6/anti-T6 mixed sera at higher dilutions (Figure 3-21 B and Figure 3-22 B). Against M6:1070, the killing curves for the anti-T6, anti-M1, anti-T1 and pre-immune sera all demonstrated an inability to kill (Figure 3-22 A**)**. Furthermore, the killing curves generated by the anti-M6 and anti-M6/anti-T6 mixed sera were similar, and as anti-T6 sera alone was unable to produce killing, it is likely that the addition of the anti-T6 sera did not augment killing by the anti-M6 sera. Three assays were completed and the OIs from each assay's killing curves were averaged, plotted, and analysed (Figure 3-22 B). As expected, the OIs for the anti-M6 and anti-M6/anti-T6 mix were significantly greater than the other sera, which generated baseline readouts of no killing ($p<0.0001$). There is no significant difference in OIs between the anti-M6 and anti-M6/anti-T6 mix. Therefore, the anti-M6 sera was the only sera capable of killing the M6:1070 strain, which is in line with the M6:2 OPKAs.

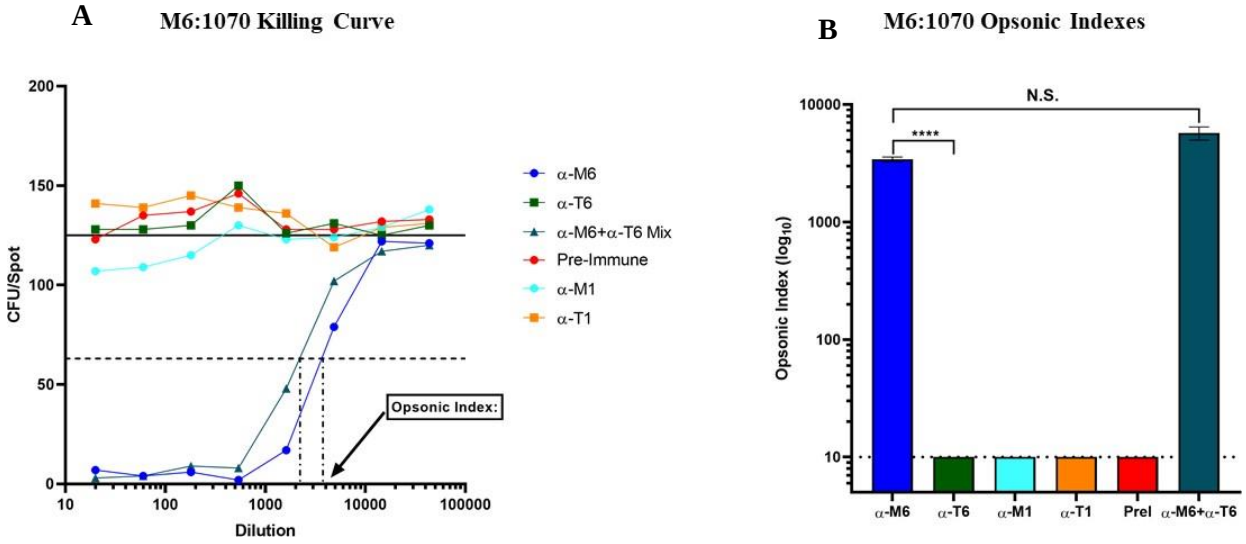

Figure 3-22: M6 1070 representative OPKA and opsonic indexes:

The M6:1070 OPKAs were run as biological triplicates of three independent assays, but a singular killing assay was chosen as a representative graph for the antisera's (α-) killing capabilities and trends (**A**). Only the anti-M6 and anti-M6/anti-T6 mixed sera killed the M6:1070, generating opsonic index (OI) read-outs that provide

a quantitative measure of bacterial killing. Each sera's opsonic index was averaged over the three replicate assays and displayed as a bar on the right with the standard deviation denoted by error bars, enabling each serum's killing capacity to be compared (**B**). Statistical analyses were performed using a one-way ANOVA on the OI values which displayed significant killing by the anti-M6 and anti-M6/anti-T6 mix sera compared to all other sera tested ($p<0.0001$), whilst no significance was seen between the anti-M6 and anti-M6/anti-T6 mix (**B**).

3.3.6.1 OPKA Summary

In summary the OPKAs showed α-M sera mediated killing in all four strains tested, but α-T sera killing in only the M1:SF370. Furthermore, mixing the α-M and α-T sera was unable to increase the killing against any of the strains above what a singular serum could achieve. Finally, no cross-reactive serum activity was seen in the OPKAs as the heterologous α-M and α-T sera was ineffective at killing any of the strains.

4 Discussion

This project aimed to investigate the interaction of two key GAS virulence factors, the M protein and T antigen, with a functional antibody response. Both antigens are major vaccine targets, thus understanding their relationship with each other and the immune response is important (29, 40, 58). To achieve this the project was divided into three main parts. The key reagent used in this project was rabbit sera generated to these antigens. Thus, the first part of this project was using ELISA to quantify titres of antibodies to the M proteins and T antigens to inform downstream experiments and result interpretation. The second part of the project utilised the rabbit sera in flow cytometry to probe the expression of virulence factors on whole GAS bacterium. The third and final part of the project used opsonophagocytic killing assays (OPKAs) to determine how the expression and function of M proteins and T-antigens on GAS influenced antisera driven opsonophagocytic killing. Overall, the project sought to inform the understanding of effective M protein and T-antigen based vaccines.

4.1 Serum characterisation

The characterisation of the rabbit sera using ELISAs enables the measurement of each serum's antibody titre and their binding specificity. The immunogenicity and binding capabilities of sera targeting the M protein and T-antigen are well characterised in the literature (29, 51). However, it was crucial to characterise the binding specificities of each serum before use in functional assays so when used in downstream experiments, we have confidence in the serum's specificity and titre. Moreover, a large component of the natural immune response to GAS is the generation of protective antibodies (29, 58). Vaccine development efforts have focussed on the M protein and T-antigen, by mimicking natural immunity, with adults thought to develop an effective natural immune response to GAS (7, 40, 54). Studies have characterised these natural responses and often focus on the intravenous immunoglobulin (IVIG) in which GAS specific antibodies are seen (29, 40). The interaction of these antisera with key virulence factors on live GAS in this project are important as they have been shown to play a role in immune protection (29, 40, 51). ELISAs provide the foundation for understanding this basic binding

of sera to their GAS targets. As such, ELISAs are frequently used in current vaccine studies to investigate the immunogenicity and specificity of vaccines in animal models and human trials by measuring antibody titres against specific antigens (29, 58).

4.1.1 M protein specific rabbit antisera binding

The ELISAs confirmed the binding of the anti-M1, anti-M6, anti-T1 and anti-T6 rabbit antisera to their homologous proteins (section 3.1). The anti-M1 and anti-M6 sera contained antibodies to the hyper-variable region (HVR) of their respective M proteins. The HVR forms the basis of the 30-valent vaccine (52, 58) reinforcing the idea of the HVR being a target for immune responses. However, in this study the majority of the antibodies in the rabbit sera targeted other epitopes outside the HVR along the full-length protein showing that other regions of the M protein are also immunogenic. The cross-reactivity of anti-M1 sera to M6 protein and vice-versa, suggests that a proportion of antibody titres are specific to epitopes in the conserved region that are shared by both the M1 and M6 proteins. This cross-reactive immune response to conserved M protein epitopes has also been explored as a mechanism for vaccine development. Currently, a GAS vaccine is being developed targeting a specific conserved M protein epitope (J8) that has demonstrated some protective capabilities (59). However, during the opsonophagocytic killing assays in this project the cross-reactive binding of the rabbit sera was unable to induce killing to any *emm*1 or *emm*6 strains (section 3.3). This suggests the rabbit sera, whilst capable of binding, as shown by ELISA, is unable to stimulate opsonophagocytic killing of heterologous M-types, and that type specific immunity is the major mechanisms for OPKA in the M-type specific sera.

4.1.1.1 M protein conserved region targeting by rabbit antisera

The lack of cross-reactive killing by the M protein rabbit sera suggests that the conserved or cross-reactive epitopes did not trigger opsonophagocytic killing. This highlights a potential need to target specific protective epitopes in the conserved region when designing a vaccine based on this portion of the M protein. The J8 vaccine exemplifies this approach by targeting a very specific epitope in the

conserved region, generating antibodies that can bind the epitope on different *emm* types and subsequently induce immune killing (39, 59). It is possible that the lack of cross-reactive killing by M protein sera in this project is because antibodies specific to the conserved region represented in the J8 vaccine are not present (32). The difficulty in generating a potent immune response to the conserved region of the M protein is even more accentuated when the risks of cross-reactive epitopes and triggering of auto-immune disease is factored in (55, 56). However, unlike the inoculation of the full-length M protein, which was done to generate sera for this project, the J8 vaccine was designed specifically to avoid potentially cross-reactive epitopes in the conserved region (39, 59).

4.1.2 M protein driven non-specific serum binding

Previous studies identified the functional capacity of M proteins to bind a myriad of host factor proteins, including immunoglobulin G (IgG) and A (IgA) (7, 32, 36). Using functional experiments and genetic analysis of the M proteins, the IgG binding region and the predicted sequence was identified (32, 33). Using this information, the M1 protein was determined to bind the IgG Fc region whilst the M6 protein lacked this binding ability (32, 33). The serum characterisation in this project confirmed the M1 protein's ability to bind rabbit antisera non-specifically, as shown by the binding of the anti-T sera and pre-immune sera (Figure 3-5) (32). This in turn informed optimisation of flow cytometry where rabbit antisera were used to measure *emm*1 strains protein expression. As non-specific binding was observed against the M1 protein, blocking of these Fc binding sites on the M protein was required (section 3.1 and 3.2) to enable quantification of the M1-specific antibodies in sera, which bound M protein via the Fab portion of the antibody molecules. In contrast to M1, the M6 antigens are not reported to contain an IgG Fc binding motif and this was supported by the lack of pre-immune or anti-T1 sera binding to M6 full-length protein (Figure 3-3) (32).

4.1.3 T-antigen specific rabbit antisera binding

Characterising the anti-T1 and anti-T6 rabbit antisera revealed there was no cross-reactive antibody binding between the two T-antigens (section3.1.2). This suggests that despite the T-antigen being more

conserved than the M protein, the structural and sequence differences between these two T-antigens are such that they contain no shared epitopes (34, 35, 48). This is in keeping with the T-antigen based vaccine (TeeVax) in which both T1 and T6 antigens were included to ensure immune coverage against both strains and their respective FCT-2 and FCT-6 strain families (29, 48).

During the development and testing of Teevax, five two domain T-antigens (one FCT-2, one FCT-3 and three FCT-4) were used to make the Teevax1 protein which was inoculated into rabbits. This elicited a cross-reactive serum response and ELISA characterisation determined cross- reactivity to fifteen other two domain T-antigens, including T-antigens from FCT-5 and FCT-6. This suggests that cross-reactivity in sera responses between T-antigens is reliant on structural similarities (29, 48). Providing an explanation as to why no cross-reactive binding of sera between the two-domain T1 antigen and three-domain T6 antigen was seen in this project (Figure 3-4).

Interestingly, the anti-T1 and anti-T6 rabbit antisera displayed much higher antibody titres than the anti-M1 and anti-M6 sera (Figure 3-5), suggesting the T-antigens maybe more immunogenic than the M proteins. During natural infection the polymerisation of T-antigens in the pilus backbone may influence this increased immune response, as there are more antigens present during the inoculation, however this is unlikely to impact the immune response during vaccination with T-antigen only in this project (10). Furthermore, the sera were generated at different times, and natural variation between rabbits also could have influenced the antibody titres potentially leading to this increased reactivity in the anti-T sera (section 2.1.2) (29, 51).

4.2 Measuring GAS protein expression profiles

Measuring differences in expression of M protein and T-antigen within and between *emm* types is important for understanding the variation of GAS surface protein expression as it impacts strain virulence, immune evasion, disease burden and, in turn, how an effective vaccine can be developed (18, 40). The selection of two *emm* types (*emm*1 and *emm*6), and multiple clinically relevant strains

from each *emm* type were used for this purpose, the two *emm*1 strains M1:SF370 and M1:43, alongside the *emm*6 strains M6:2, M6:1070, M6:08308 and M6:09209.

The optimisation of a flow cytometry protocol to measure the M protein and T-antigen expression on whole GAS in this project has also informed other research in the Moreland laboratory over the last year. This protocol has now been utilised on a range of other *emm* types (*emm*12, *emm*53, and *emm*75) in the laboratory to measure M protein expression levels to understand their targetability in killing assays for related projects.

4.3 The impact of varying M protein expression on opsonophagocytic killing

To investigate the influence of M protein and T-antigen expression levels on antibody mediated killing, results from opsonophagocytic killing assays (OPKA) were compared within the *emm*1 and *emm*6 strains. The M1:SF370 and M1:43 displayed phenotypic differences, with M1:43 expressing approximately three times more M1 protein than M1:SF370, yet both strains expressed similar levels of the T-antigen. OPKA results showed effective killing of both strains using anti-M1 sera, however, the M1:43 was approximately three times more susceptible to anti-M1 targeted killing than M1:SF370 (Figure 3-19 and Figure 3-20). This suggests a positive correlation between the anti-M1 targeted killing and M1 protein expression on the bacterial cell surface, likely due to an increased availability of the M1 protein for targeted binding of anti-M1 rabbit sera and thus triggering opsonophagocytic killing.

In contrast to the M1 expression, the T1-antigen expression levels on *emm*1 strains were similar (Figure 3-11). The anti-T1 sera was more effective at killing M1:SF370 than the anti-M1 sera (Figure 3-19 and Figure 3-20). However, anti-T1 sera was unable to kill M1:43, despite equal expression levels of the T1-antigen on both strains.

4.3.1 The impact of M1 expression on the killing of *emm*1 strains

A key aim of this project was to investigate the impact of M protein expression on T-antigen targeted immune responses, as the T-antigen based vaccines are currently under development (10, 29). Previous T-antigen vaccine research primarily used SF:370 in killing assays, which displayed effective killing,

similar to results seen here (Figure 3-19) (29). However, an effective vaccine will need to be able to induce killing of all strains within an *emm* type, such that the lack of killing of the M1:43 in this project requires further investigation. Two potential mechanisms could be inhibiting the anti-T sera killing of M1:43. One is that the M1:43's high level of non-specific IgG Fc binding may inhibit anti-T sera from binding to the T-antigen, thus preventing opsonophagocytic killing from occurring (Figure 3-12). The second possibility is that increased M protein expression is sufficiently high to mask the T-antigen binding sites on the GAS cell surface. However, the latter is unlikely since the anti-T1 antisera bound the M1:43 strain as detected by flow cytometry.

Future work will be necessary to completely clarify the mechanism causing inhibition of T1-targeted killing on M1:43. One possible approach would be to utilise specificity assays which are an adaptation of OPKAs that include a pre-incubation step of the serum and chosen antigens. This pre-incubation depletes antibodies to specific antigens and thus will block the antibodies from being able to induce opsonophagocytosis. For this research specificity assays would pre-incubate M1:43 with the Generic rabbit block (GRB) to remove non-specific binding as it did during flow cytometry (section 2.9.3). Doing so would help determine if the inhibition of M1:43's non-specific IgG binding would make it susceptible to a T1 targeted immune response, as seen in M1:SF370.

4.3.2 The impact of M6 expression on the killing of *emm*6 GAS strains

In order to identify M6/T6 strains for this project a screening process was undertaken using four *emm*6 strains, M6:2, M6:1070, M6:08308 and M6:09209. M6 protein expression levels varied among all four strains, but the T6 expression remained consistently low (Figure 3-14). For the two strains selected for OPKA, the anti-T6 sera showed no killing against M6:2 and M6:1070 (Figure 3-21 and Figure 3-22). This suggests that the *emm*6 strains tested in this project did not express sufficient levels of T-antigen to be targeted for opsonophagocytic killing. It is known that environmental factors and growth stage may influence T-antigen expression and so attempts were made to manipulate the M6:2 and M6:1070 T-antigen expression levels (67). This involved measuring T6 expression throughout the growth cycle, but unfortunately, this experimental procedure proved ineffective using the *tee*6 strains (Figure 3-17).

Overall, this lack of T6-antigen expression maybe due to the laboratory culture conditions utilised, which maybe in line with conditions to a blood-stream infection. It is possible that T-antigen expression is markedly higher in certain conditions *in vivo*, for example a throat micro-environment as pili are known to have a key-role in adhesion when infection is established in the pharynx (7, 37, 67). The recently adapted human-challenge model could provide a novel means to isolate and immediately measure T-antigen expression levels of GAS directly involved in throat colonisation during an active infection (6). Importantly, the controlled nature of the human challenge model would also mean the GAS samples used to generate infection could be measured for expression pre-infection for potential comparisons (6). Future research specifically on *emm*6 could take advantage of genetic manipulation to alter each strains T6-antigen expression levels. Alternatively, another option is research using GAS strains from the FCT-3 family of *tee* types, which naturally vary their pilus expression according to environmental influences like temperature and pH (67-69). Experimenting with these strains would provide control over T-antigen expression levels and could lead to more targeted outcomes in investigating the T6-antigen.

4.4 How M protein function influences targeted immune responses

The functional differences between the M1 and M6 proteins, and how they influence functional antibody responses are important to understand as this can shed fundamental new insight into how their functional characteristics may contribute to immune evasion.

4.4.1 M protein influences on functional capacity and vaccine assessments

The differences between the two M1 strains were significant. While both strains exhibited non-specific antibody binding, the clinical isolate M1:43 showed much higher non-specific binding than M1:SF370 (Figure 3-12). This result could be driven by the higher M1 expression levels of M1:43 which were measured as more than double M1:SF370 (Figure 3-11). Alternatively, the decreased non-specific binding by M1:SF370 could be related to its decreased virulence as this is a laboratory adapted strain. This highlights challenges of strain selection for vaccine research, as one showed high levels of killing

for T-antigen sera and the other showed none. Given these large differences in phenotype it maybe that multiple strains for each emm-type need to be assessed in future vaccine assessments.

4.4.2 The M6 protein lacks functional effects when expressed on live GAS

The M6 strain was selected in this project for its inability to bind host factor proteins via the M6 protein (32). This was confirmed during the serum characterisation in this project (both ELISAs and flow cytometry) and thus support the initial project design, which aimed to draw comparisons between the M1 and M6 OPKAs to discern if M protein functional differences influence killing, particularly using T-antigen targeted sera (29, 32, 65). Hence, an M protein with no functional capabilities (M6) provides a comparative tool against an M protein possessing a myriad of functional binding capabilities (M1) for future research (Table 1).

4.4.3 M protein function impacts GAS killing using rabbit antisera

All strains, regardless of their ability to bind IgG non-specifically were effectively killed by their homologous M protein sera. This suggests that the M1 proteins non-specific binding of IgG is unable to hinder an M1-targeted antibody response in high-titre rabbit sera. This contrasts with T-antigen specific killing. For M1 it appears that a high ratio of M protein to T-antigen blocks killing by T-antigen specific sera. Furthermore, for M6 strains, where T-antigen expression is low in liquid culture *in vitro*, there is a lack of T-antigen induced killing. While this meant the comparison of the functional impact of M proteins on T-antigen targeted killing between M1 and M6 strains was limited by the lack of T6 expression on the *emm*6 strains, it does highlight the importance of antigen expression and strain characterisation of GAS for vaccine research. GAS is a diverse bacterium for over 200 *emm*-types. This project focused on two *emm*-types and four strains, and even within this limited number of strains the functional antibody responses differed significantly. Future work assessing the protective capacity of M-protein and T-antigen based vaccines should carefully consider the strains selected and the limitations of working with strains *in vitro*. A balance between assessing a broad number of strains for coverage assessments, with practicality and data utility is also needed.

5 Conclusion

The project aimed to investigate how GAS virulence factor expression and function influenced an immune response, particularly an antibody response against the M protein and T-antigen. Specific rabbit antisera were utilised and binding characterised to their respective targets of the M1 protein, M6 protein, T1-antigen, or T6-antigen. Flow cytometry was used to measure the expression of these virulence factors on two *emm*1 strains and two *emm*6 strains, which were subsequently used in OPKAs to determine the killing capacity of the rabbit antisera against these strains. Results suggest that for M1, the M protein expression levels are impacting T-antigen targeted killing of GAS, with high M protein expression outcompeting T-antigen killing. However, *emm*6 strains displayed extremely low T6- antigen expression. While this limited the investigation into how the M1 and M6 functional differences influenced a T-antigen targeted immune response, they highlighted further challenges for assessing functional T-antigen antibody responses *in vitro*. Overall, this highlighted that characterisation of expression levels of the M protein and T-antigen are crucial when selecting strains for vaccine development.

References

1. Barnett TC, Bowen AC, Carapetis JR. The fall and rise of Group AStreptococcusdiseases. Epidemiology and Infection. 2019;147:1-6.
2. Carapetis JR, Steer AC, Mulholland EK, Weber M. The global burden of group A streptococcal diseases. Lancet Infect Dis. 2005;5(11):685-94.
3. Bennett J, Zhang J, Leung W, Jack S, Oliver J, Webb R, et al. Incidence of Acute Rheumatic Fever and Rheumatic Heart Disease among Ethnic Groups, New Zealand, 2000–2018. Emerging Infectious Diseases. 2021;27(1).
4. Watts V, Balasegaram S, Brown CS, Mathew S, Mearkle R, Ready D, et al. Increased Risk for Invasive Group AStreptococcusDisease for Household Contacts of Scarlet Fever Cases, England, 2011–2016. Emerging Infectious Diseases. 2019;25(3):529-37.
5. Cordery R, Purba AK, Begum L, Mills E, Mosavie M, Vieira A, et al. Frequency of transmission, asymptomatic shedding, and airborne spread of Streptococcus pyogenes in schoolchildren exposed to scarlet fever: a prospective, longitudinal, multicohort, molecular epidemiological, contact-tracing study in England, UK. The Lancet Microbe. 2022;3(5):e366-e75.
6. Osowicki J, Azzopardi KI, Fabri L, Frost HR, Rivera-Hernandez T, Neeland MR, et al. A controlled human infection model of Streptococcus pyogenes pharyngitis (CHIVAS-M75): an observational, dose-finding study. The Lancet Microbe. 2021;2(7):e291-e9.
7. Walker MJ, Barnett TC, McArthur JD, Cole JN, Gillen CM, Henningham A, et al. Disease Manifestations and Pathogenic Mechanisms of Group A Streptococcus. Clinical Microbiology Reviews. 2014;27(2):264-301.
8. Hurst JR, Brouwer S, Walker MJ, McCormick JK. Streptococcal superantigens and the return of scarlet fever. PLOS Pathogens. 2021;17(12):e1010097.
9. Lamagni T, Guy R, Chand M, Henderson KL, Chalker V, Lewis J, et al. Resurgence of scarlet fever in England, 2014–16: a population-based surveillance study. The Lancet Infectious Diseases. 2018;18(2):180-7.
10. Raynes JM, Young PG, Proft T, Williamson DA, Baker EN, Moreland NJ. Protein adhesins as vaccine antigens for Group A Streptococcus. Pathog Dis. 2018;76(2).
11. Moreland NJ, Waddington CS, Williamson DA, Sriskandan S, Smeesters PR, Proft T, et al. Working towards a Group A Streptococcal vaccine: Report of a collaborative Trans-Tasman workshop. Vaccine. 2014;32(30):3713-20.
12. Bennett J, Moreland NJ, Oliver J, Crane J, Williamson DA, Sika-Paotonu D, et al. Understanding group A streptococcal pharyngitis and skin infections as causes of rheumatic fever: protocol for a prospective disease incidence study. BMC Infectious Diseases. 2019;19(1).
13. Bessen DE, Smeesters PR, Beall BW. Molecular Epidemiology, Ecology, and Evolution of Group A Streptococci. Microbiology Spectrum. 2018;6(5).
14. Metzgar D, Zampolli A. The M protein of group A Streptococcus is a key virulence factor and a clinically relevant strain identification marker. Virulence. 2011;2(5):402-12.
15. Lynskey NN, Jauneikaite E, Li HK, Zhi X, Turner CE, Mosavie M, et al. Emergence of dominant toxigenic M1T1 Streptococcus pyogenes clone during increased scarlet fever activity in England: a population-based molecular epidemiological study. The Lancet Infectious Diseases. 2019;19(11):1209-18.
16. Cunningham MW. Pathogenesis of group A streptococcal infections and their sequelae. Adv Exp Med Biol. 2008;609:29-42.
17. Lee JL, Naguwa SM, Cheema GS, Gershwin ME. Acute rheumatic fever and its consequences: a persistent threat to developing nations in the 21st century. Autoimmun Rev. 2009;9(2):117-23.

18. Thomas S, Bennett J, Jack S, Oliver J, Purdie G, Upton A, et al. Descriptive analysis of group A Streptococcus in skin swabs and acute rheumatic fever, Auckland, New Zealand, 2010–2016. The Lancet Regional Health - Western Pacific. 2021;8:100101.
19. Cannon JW, Zhung J, Bennett J, Moreland NJ, Baker MG, Geelhoed E, et al. The economic and health burdens of diseases caused by group A Streptococcus in New Zealand. Int J Infect Dis. 2021;103:176-81.
20. Carapetis JR, Beaton A, Cunningham MW, Guilherme L, Karthikeyan G, Mayosi BM, et al. Acute rheumatic fever and rheumatic heart disease. Nat Rev Dis Primers. 2016;2:15084.
21. Global, regional, and national incidence, prevalence, and years lived with disability for 301 acute and chronic diseases and injuries in 188 countries, 1990-2013: a systematic analysis for the Global Burden of Disease Study 2013. Lancet. 2015;386(9995):743-800.
22. Dajani AS. Guidelines for the Diagnosis of Rheumatic Fever. JAMA. 1992;268(15):2069.
23. Hanson-Manful P, Whitcombe AL, Young PG, Atatoa Carr PE, Bell A, Didsbury A, et al. The novel Group A Streptococcus antigen SpnA combined with bead-based immunoassay technology improves streptococcal serology for the diagnosis of acute rheumatic fever. J Infect. 2018;76(4):361-8.
24. Whitcombe AL, Hanson-Manful P, Jack S, Upton A, Carr PA, Williamson DA, et al. Development and Evaluation of a New Triplex Immunoassay That Detects Group A Streptococcus Antibodies for the Diagnosis of Rheumatic Fever. J Clin Microbiol. 2020;58(9).
25. Whitcombe AL, McGregor R, Bennett J, Gurney JK, Williamson DA, Baker MG, et al. Increased Breadth of Group A Streptococcus Antibody Responses in Children With Acute Rheumatic Fever Compared to Precursor Pharyngitis and Skin Infections. J Infect Dis. 2022;226(1):167-76.
26. Sims Sanyahumbi A, Colquhoun S, Wyber R, Carapetis JR. Global Disease Burden of Group A Streptococcus. In: Ferretti JJ, Stevens DL, Fischetti VA, editors. Streptococcus pyogenes: Basic Biology to Clinical Manifestations. Oklahoma City (OK): University of Oklahoma Health Sciences Center© The University of Oklahoma Health Sciences Center.; 2016.
27. Smeesters PR, McMillan DJ, Sriprakash KS, Georgousakis MM. Differences among group A streptococcus epidemiological landscapes: consequences for M protein-based vaccines? Expert Review of Vaccines. 2009;8(12):1705-20.
28. Oliver J, Upton A, Jack SJ, Pierse N, Williamson DA, Baker MG. Distribution of Streptococcal Pharyngitis and Acute Rheumatic Fever, Auckland, New Zealand, 2010–2016. Emerging Infectious Diseases. 2020;26(6):1113-21.
29. Loh JMS, Rivera-Hernandez T, McGregor R, Khemlani AHJ, Tay ML, Cork AJ, et al. A multivalent T-antigen-based vaccine for Group A Streptococcus. Scientific Reports. 2021;11(1).
30. Brouwer S, Barnett TC, Rivera-Hernandez T, Rohde M, Walker MJ. *Streptococcus pyogenes* adhesion and colonization. FEBS Letters. 2016;590(21):3739-57.
31. Mora M, Bensi G, Capo S, Falugi F, Zingaretti C, Manetti AGO, et al. Group A Streptococcus produce pilus-like structures containing protective antigens and Lancefield T antigens. Proc Natl Acad Sci U S A. 2005;102(43):15641-6.
32. Sanderson-Smith M, De Oliveira DM, Guglielmini J, McMillan DJ, Vu T, Holien JK, et al. A systematic and functional classification of Streptococcus pyogenes that serves as a new tool for molecular typing and vaccine development. J Infect Dis. 2014;210(8):1325-38.
33. Smeesters PR, Botteaux A. The emm-Cluster Typing System. In: Springer US; 2020. p. 25-31.
34. Steemson JD, Moreland NJ, Williamson D, Morgan J, Carter PE, Proft T. Survey of the bp/tee genes from clinical group A streptococcus isolates in New Zealand – implications for vaccine development. Journal of Medical Microbiology. 2014;63(12):1670-8.
35. Young PG, Raynes JM, Loh JM, Proft T, Baker EN, Moreland NJ. Group A Streptococcus T Antigens Have a Highly Conserved Structure Concealed under a Heterogeneous Surface That Has Implications for Vaccine Design. Infection and Immunity. 2019;87(6).
36. Smeesters PR, McMillan DJ, Sriprakash KS. The streptococcal M protein: a highly versatile molecule. Trends Microbiol. 2010;18(6):275-82.

37. Tsai JC, Loh JM, Clow F, Lorenz N, Proft T. The Group A Streptococcus serotype M2 pilus plays a role in host cell adhesion and immune evasion. Mol Microbiol. 2017;103(2):282-98.
38. Smeesters PR, Mardulyn P, Vergison A, Leplae R, Van Melderen L. Genetic diversity of Group A Streptococcus M protein: implications for typing and vaccine development. Vaccine. 2008;26(46):5835-42.
39. Good MF, Pandey M, Batzloff MR, Tyrrell GJ. Strategic development of the conserved region of the M protein and other candidates as vaccines to prevent infection with group A streptococci. Expert Review of Vaccines. 2015;14(11):1459-70.
40. Steer AC, Carapetis JR, Dale JB, Fraser JD, Good MF, Guilherme L, et al. Status of research and development of vaccines for Streptococcus pyogenes. Vaccine. 2016;34(26):2953-8.
41. Påhlman LI, Olin AI, Darenberg J, Mörgelin M, Kotb M, Herwald H, et al. Soluble M1 protein of Streptococcus pyogenes triggers potent T cell activation. Cellular Microbiology. 2007;0(0):070928215112001.
42. Beall B, Facklam R, Thompson T. Sequencing emm-specific PCR products for routine and accurate typing of group A streptococci. Journal of Clinical Microbiology. 1996;34(4):953-8.
43. Williamson DA, Smeesters PR, Steer AC, Steemson JD, Ng ACH, Proft T, et al. M-Protein Analysis of Streptococcus pyogenes Isolates Associated with Acute Rheumatic Fever in New Zealand. Journal of Clinical Microbiology. 2015;53(11):3618-20.
44. McMillan DJ, Drèze PA, Vu T, Bessen DE, Guglielmini J, Steer AC, et al. Updated model of group A Streptococcus M proteins based on a comprehensive worldwide study. Clinical Microbiology and Infection. 2013;19(5):E222-E9.
45. McGregor KF, Spratt BG, Kalia A, Bennett A, Bilek N, Beall B, et al. Multilocus Sequence Typing of Streptococcus pyogenes Representing Most Known emm Types and Distinctions among Subpopulation Genetic Structures. Journal of Bacteriology. 2004;186(13):4285-94.
46. Syed S, Viazmina L, Mager R, Meri S, Haapasalo K. Streptococci and the complement system: interplay during infection, inflammation and autoimmunity. FEBS Letters. 2020;594(16):2570-85.
47. Fieber C, Kovarik P. Responses of innate immune cells to group A Streptococcus. Front Cell Infect Microbiol. 2014;4:140.
48. Falugi F, Zingaretti C, Pinto V, Mariani M, Amodeo L, Manetti AG, et al. Sequence variation in group A Streptococcus pili and association of pilus backbone types with lancefield T serotypes. J Infect Dis. 2008;198(12):1834-41.
49. Bennett J, Rentta N, Leung W, Anderson A, Oliver J, Wyber R, et al. Structured review of primary interventions to reduce group A streptococcal infections, acute rheumatic fever and rheumatic heart disease. J Paediatr Child Health. 2021;57(6):797-802.
50. Johnson D, Kaplan E, Sramek J, Bicova R, Havlicek J, Havlickova H, et al. Determination of T-protein agglutination patterns. Laboratory diagnosis of group A streptococcal infections World Health Organization, Geneva, Switzerland. 1996:37-41.
51. Jones S, Moreland NJ, Zancolli M, Raynes J, Loh JMS, Smeesters PR, et al. Development of an opsonophagocytic killing assay for group a streptococcus. Vaccine. 2018;36(26):3756-63.
52. Dale JB, Penfound TA, Chiang EY, Walton WJ. New 30-valent M protein-based vaccine evokes cross-opsonic antibodies against non-vaccine serotypes of group A streptococci. Vaccine. 2011;29(46):8175-8.
53. Frost HR, Laho D, Sanderson-Smith ML, Licciardi P, Donath S, Curtis N, et al. Immune Cross-Opsonization Within emm Clusters Following Group A Streptococcus Skin Infection: Broadening the Scope of Type-Specific Immunity. Clin Infect Dis. 2017;65(9):1523-31.
54. Wilson R, Cohen JM, Reglinski M, Jose RJ, Chan WY, Marshall H, et al. Naturally Acquired Human Immunity to Pneumococcus Is Dependent on Antibody to Protein Antigens. PLOS Pathogens. 2017;13(1):e1006137.
55. Bronze MS, Dale JB. Epitopes of streptococcal M proteins that evoke antibodies that cross-react with human brain. J Immunol. 1993;151(5):2820-8.
56. Massell BF. Rheumatic Fever Following Streptococcal Vaccination. JAMA. 1969;207(6):1115.

57. McNeil SA, Halperin SA, Langley JM, Smith B, Warren A, Sharratt GP, et al. Safety and Immunogenicity of 26-Valent Group A Streptococcus Vaccine in Healthy Adult Volunteers. Clinical Infectious Diseases. 2005;41(8):1114-22.
58. Pastural É, McNeil SA, MacKinnon-Cameron D, Ye L, Langley JM, Stewart R, et al. Safety and immunogenicity of a 30-valent M protein-based group a streptococcal vaccine in healthy adult volunteers: A randomized, controlled phase I study. Vaccine. 2020;38(6):1384-92.
59. Michael, Wendy, Mark, Zeng M, Pruksakorn S, Evelyn, et al. Protection against Group A Streptococcus by Immunization with J8 – Diphtheria Toxoid: Contribution of J8 - and Diphtheria Toxoid–Specific Antibodies to Protection. The Journal of Infectious Diseases. 2003;187(10):1598-608.
60. Pandey M, Langshaw E, Hartas J, Lam A, Batzloff MR, Good MF. A Synthetic M Protein Peptide Synergizes with a CXC Chemokine Protease To Induce Vaccine-Mediated Protection against Virulent Streptococcal Pyoderma and Bacteremia. The Journal of Immunology. 2015;194(12):5915-25.
61. Alhajj M, Farhana A. Enzyme Linked Immunosorbent Assay. In: StatPearls. Treasure Island (FL): StatPearls Publishing Copyright © 2022, StatPearls Publishing LLC.; 2022.
62. Russell H, Facklam RR, Edwards LR. Enzyme-linked immunosorbent assay for streptococcal M protein antibodies. J Clin Microbiol. 1976;3(5):501-5.
63. Galbusera L, Bellement-Theroue G, Urchueguia A, Julou T, van Nimwegen E. Using fluorescence flow cytometry data for single-cell gene expression analysis in bacteria. PLoS One. 2020;15(10):e0240233.
64. Lancefield RC. Differentiation of group A streptococci with a common R antigen into three serological types, with special reference to the bactericidal test. J Exp Med. 1957;106(4):525-44.
65. McGregor R, Jones S, Jeremy RM, Goldblatt D, Moreland NJ. An Opsonophagocytic Killing Assay for the Evaluation of Group A Streptococcus Vaccine Antisera. In: Springer US; 2020. p. 323-35.
66. Ferretti JJ, Stevens DL, Fischetti VA. spyogenes.
67. Nakata M, Kreikemeyer B. Genetics, Structure, and Function of Group A Streptococcal Pili. Frontiers in Microbiology. 2021;12.
68. Nakata M, Sumitomo T, Patenge N, Kreikemeyer B, Kawabata S. Thermosensitive pilus production by FCT type 3 Streptococcus pyogenes controlled by Nra regulator translational efficiency. Mol Microbiol. 2020;113(1):173-89.
69. Ichikawa M, Minami M, Isaka M, Tatsuno I, Hasegawa T. Analysis of two-component sensor proteins involved in the response to acid stimuli in Streptococcus pyogenes. Microbiology (Reading). 2011;157(Pt 11):3187-94.